UNIVERSITY OF CALIFORNIA
RIVERSIDE

Multi-Scale Analysis of Factors Influencing Urban Greenness, Temperature, and Vegetative Cooling

A Dissertation submitted in partial satisfaction
of the requirements for the degree of

Doctor of Philosophy

in

Plant Biology

by

Dion Carl Kucera

March 2024

Dissertation Committee:
Dr. G. Darrel Jenerette, Chairperson
Dr. Louis Santiago
Dr. Bai-Lian (Larry) Li

The Dissertation of Dion Carl Kucera is approved:

Committee Chairperson

University of California, Riverside

Acknowledgements

They say it takes a village to raise a child; in my case it took a team of mentors, advocates, and supporters to create a dissertation. First and foremost, I would like to thank my dissertation advisor, Dr. Darrel Jenerette, for his unwavering support and guidance through the years-long process of revise, revise, revise. I wanted to do a Ph.D. in urban ecology; I feel exceedingly fortunate that Dr. Jenerette not only gave me an opportunity to do so, but provided me with the support, mentorship, and resources for me to pursue my research interests. The guidance I have received on research design, hypotheses, scientific writing, and more, have been invaluable, and will indelibly improve my relationship with science over a lifetime of professional work. Particularly, I would like to thank Dr. Jenerette for his support in getting my first chapter published in Urban Climate in November 2023 as "Urban greenness and its cooling effects are influenced by changes in drought, physiography, and socio-demographics in Los Angeles, CA." Chapter 1 of this dissertation is a reprint of this publication. I would further like to extend my gratitude to the other members of my dissertation committee, Dr. Bai-Lian (Larry) Li and Dr. Louis Santiago. Their feedback, guidance, and support on my dissertation research were integral to my success as a Ph.D. student.

I would also like to thank the faculty members of my past committees, who provided guidance in support of my oral examination and improvement of this dissertation: Dr. Jeffrey Diez, Dr. Loralee Larios, Dr. Janet Franklin, and Dr. Francesca Hopkins. The support of my advisors, including Fidel Rivas, Dr. Amy Litt, and Dr. Laura McGeehan helped keep me on track. The administrative staff of Plant Biology including

Jessica Perez, Mariella Valdivia, and April Meinzer helped me navigate the financial and paperwork necessities of the department. The department chair of Plant Biology, Dr. Patricia Springer, fostered a department conducive to completing my research. I am grateful for the support, feedback, and camaraderie from my current and former fellow lab mates: Stephanie Piper, Stuart Schwab, Kristin Hamilton, Dr. Holly Andrews, and Dr. Julie Ripplinger. I would particularly like to thank Dr. Peter Ibsen, from who I learned how to core a tree, assess leaf water potential, and measure photosynthesis. Finally, I would like to thank my family: my parents, Dennis and Myriam Kucera, and my sister, Nicole Kucera, for their constant support over the many years it took to complete this dissertation.

Funding for this dissertation was provided from: the UC Riverside Chancellor's Distinguished Fellowship; the UCR Graduate Research Mentoring Program (GRMP); as a NASA/UCR Fellowships and Internships in Extremely Large Datasets (FIELDS) fellow; the Devirian Graduate Student Research Award from the UCR EDGE (Environmental Dynamics and GeoEcology) Institute; from EarthWatch; from the Urban Water Innovation Network; a grant from the Urban Ecology Section of the Ecological Society of America; and a fellowship from the Los Angeles Urban Center for Natural Resources Sustainability.

ABSTRACT OF THE DISSERTATION

Multi-Scale Analysis of Factors Influencing Urban Greenness, Temperature, and Vegetative Cooling

by

Dion Carl Kucera

Doctor of Philosophy, Graduate Program in Plant Biology
University of California, Riverside, March 2024
Dr. G. Darrel Jenerette, Chairperson

Urban ecosystems are defined by unique relationships between biological diversity and distribution, socio-demographics, and climate. These relationships occur in the context of a changing world: increasing temperatures, a shifting composition of urban residents, and rapid urbanization. It is likely that the relationships which structure the urban environment, such as that between temperature and income, or race-based exposure to heat and greenness, are not temporally stable. As urban temperatures and greenness have well known associations with morbidity, mortality, and mental health, non-stationarity of urban ecological relationships may pose significant challenges to the well-being of urban residents. I tested assumptions about non-stationarity by assessing the change through time of urban ecological relationships at three distinct spatial scales: the urban (single city) scale (chapter 1), at a continental scale (chapter 2), and at a global scale (chapter 3). At each spatial scale I used a multidecadal time series of satellite imagery, coupled with landcover and socio-demographic information, to assess how the

dynamics of urban greenness, temperature, and vegetative cooling evolved through time and what factors mediated any change. In chapter 1, where I used Los Angeles, CA as a case study, I found large intra-urban variability in how greenness, temperature, and vegetative cooling changed over time. The consequence of these changes was a weakening of the effectiveness of income as a mediator of urban greenness and temperature (the luxury effect). I corroborated the multidecadal decline in the luxury effect in chapter 2, a continental-scale assessment where I looked at 52 cities from the conterminous United States. In this chapter I additionally compared the biophysical dynamics in every city with a nearby non-urban reference site. Urbanization weakened the relationship between the weather and landcover and the biophysical environment, where the most arid cities were entirely decoupled from precipitation. In chapter 3, I looked at a subset of 266 global cities from 82 countries, finding that the evolving relationship between greenness and temperature led to declines in the cooling effectiveness of urban vegetation. Overall, this dissertation highlights the non-stationarity of urban dynamics, as well as the importance of climatic context in understanding these urban relationships.

Table of Contents

List of Tables

List of Figures

Chapter 1 **Page**

Chapter 3

Introduction

Urban ecosystems are characterized by novel relationships, particularly those between the urban socio-demographic and biophysical environments. Urban ecosystems are socio-ecological systems (SES) in which the social and biophysical urban systems are deeply integrated and interdependent (Frank 2017). The consequence of these novel relationships is that, compared to their non-urban counterparts, cities are typically hotter (Bartesaghi-Koc et al. 2020), have greater soil and air pollution (Baldauf and Nowak 2014), and may have conditions difficult for plants, leading to quicker tree mortality (Smith et al. 2019). However, factors such as irrigation may aid plant growth, minimizing losses in greenness from urbanization (Jia et al. 2018). As well, the built environment, whether designed by monetary constraints (Schwarz et al. 2015) or cultural preference (Clarke et al. 2014), also dictates what plants may grow and where. Despite the role of income or race on urban plants, the most species rich cities are those with higher minimum temperatures (Jenerette et al. 2016). As such, the distribution of plant cover and heat within cities is heavily informed by sociodemographics and the climate, leading to inequitable exposure for residents to urban heat and low plant cover. Understanding the nature of social-biophysical interactions within cities is crucial to informing the well-being of urban residents.

Research has shown that how green and how hot cities are directly affects morbidity, mortality, and mental well-being. In hot cities, all-cause mortality increases exponentially for females above 41.7 ℃ and for males above 38.9 ℃ (Harlan et al. 2014). Likewise, women living in neighborhoods with the highest greenness had 12%

lower all-cause mortality than those living in neighborhoods with the lowest greenness (James et al. 2016). Therefore, the urban biophysical environment can effectively mitigate some of the negative health consequences of urban living. For example, urban parks can be up to 3.8 °C cooler than their surrounding environment (Ren et al. 2013), where the cooling effect from parks can extend on average up to 179 meters into the city (Gao et al. 2023). Urban plants themselves can provide substantial urban cooling via both shade and from evaporative cooling via evapotranspiration (Konarska et al. 2016) in a phenomenon known as vegetative cooling. Trees can cool their local environment more than 10 °C (Pace et al. 2021, Wang et al. 2023), with plant cooling predominately driven by shading (Koyama et al. 2015, Tan et al. 2018). Yet, despite the many benefits received by people from urban plants, the distribution of these plants, and the delivery of their benefits, is inequitable.

The benefits that come from more greenness and cooler temperatures are inequitably distributed within and among cities. One of the most important determinants of urban tree canopy cover is income, where higher income neighborhoods consistently have greater tree canopy cover (Schwarz et al. 2015). Income is one the most important determinants of urban temperature and greenness. The luxury effect, first proposed by Hope et al. (2003), finds that the wealthiest regions of cities are also those with the lowest temperatures and greatest plant cover. The proximate reason for this is that wealthy neighborhoods have the financial resources to maintain and irrigate a higher quantity of plants. A luxury effect has been identified for many other urban biophysical metrics (Grove et al. 2014, Leong et al. 2018), and in cities around the world (Threlfall et al.

2022). Yet, despite the paramount importance of income in structuring the urban biophysical environment, it is not the only sociodemographic variable to do so. Temperature and greenness, at least in the United States, are race dependent, exhibiting spatial variability independent of income (Casey et al. 2017, Benz and Burney 2021, Hsu et al. 2021). Minority neighborhoods are less green and are hotter than their white counterparts, posing challenges for environmental equity as the benefits accruing from urban plant cover and lower temperatures are racially segregated. In urban SES, income and race lead to inequitable distributions of temperature and greenness within and among cities, however, non-sociodemographic drivers also influence the distribution of urban greenness and temperature.

Urban ecosystems, particularly those in arid environments and with adequate financial resources, may be characterized by extensive irrigation. The Los Angeles urban forest, perhaps the most diverse in the United States, contains over 100 and possibly more than 200 tree species (Gillespie et al. 2016, Jenerette et al. 2016), almost all of which are non-native and supported by irrigation. Irrigation may decouple urban greenness and temperature from precipitation, as has been observed in very arid cities (Buyantuyev and Wu 2012). Yet, precipitation, as an additional source of water, may supplement the water demands of urban trees even in irrigated landscapes (Bijoor et al. 2012), leading to uncertainties about the relationship between precipitation and urban greenness and temperature. At a global scale, low and lower-middle-income countries (LMIC) may not have the irrigation infrastructure to support a diverse urban forest in arid environments, leading to fundamentally different relationships between precipitation and urban

greenness and temperature than has been observed in North America or Europe. Relationships with precipitation may lead to substantial spatial variability in greenness and temperature in response to water availability.

Dynamics between greenness, temperature, and vegetative cooling are spatially dependent; race and income modify temperature and greenness at intra-urban scales, while gradients of aridity modify the urban biophysical environment at inter-urban scales. At a global scale, the spatial variability of urban biophysical characteristics may be dependent on a confluence of factors, particularly, the relationship between income and a city's climatic context. While it is likely that the urban biophysical dynamics in LMIC nations will be different from those found in the Global North, a paucity of urban ecological research from the Global South (du Toit et al. 2021) highlights important knowledge gaps in how urban ecological dynamics are structured more broadly. Yet, spatial heterogeneity in urban greenness and temperature in response to race, income, or the climate, suggests that greenness and temperature will change through time in response to changes in their spatial predictors. Despite the utility of understanding where the dynamics of urban ecosystems has changed through time, assessment of urban dynamics are often done at a single time point (Jenerette et al. 2006), or over a few years (Allen et al. 2021), leading to large uncertainties over how urban dynamics change across many cities at multidecadal scales.

Understanding how the dynamics of urban ecosystems are spatially determined and change through time can help further the field of urban ecology towards a science "of" cities (McPhearson et al. 2016, Pickett et al. 2017), particularly when multiple urban

ecosystems are compared. Comparative analysis of cities versus non-urban reference ecosystems can provide valuable insight in providing a baseline for the effect of urbanization (Kühn and Klotz 2006, Malkinson et al. 2018, Ruas et al. 2022), however, large unknowns in this comparison remain. Is the effect of urbanization context-specific, or is it driven by macro-scale processes? How do social systems interact with the effect of urbanization? Further, while there have been important multi-city ecological analyses, much urban ecological research has focused on single cities or small subsets of cities. Assessing the dynamics of urban ecosystems through the lens of macroecology by looking at urban dynamics over large spatial and temporal scales (Gaston 2004) can allow greater insight into the causes of urbanization and the determinants of the dynamics between social and biophysical systems in an urban SES (Kendal et al. 2018). Many ecological processes are known to be scale dependent (Schneider 2001, Chave 2013, Allen et al. 2014, Stein et al. 2014), and it is likely that processes guiding urban dynamics are similarly scale dependent, requiring a multi-scalar approach to better understand variability in urban ecosystem dynamics. Despite the potential value of urban macroecology, particularly in its ability to extend urban ecological theory on urban ecosystems as such, few studies have adopted this approach, and large uncertainties remain as to the relationship between urban ecosystems and the climate.

The goal of this dissertation is to better understand the dynamics of urban greenness, temperature, and vegetative cooling and their change through time, to better understand the factors influencing the effect of urbanization, and to assess how changing urban dynamics may lead to differences in environmental equity. To answer this goal, I

used satellite remote sensing, coupled with census, landcover, and climate data, at three distinct spatial scales: the single city (chapter 1), at a continental scale (chapter 2), and at a global scale assessing a subset of over 250 cities (chapter 3). This dissertation answers my primary goal by asking three similar questions related to urban dynamics. For chapter 1, where I used the Los Angeles urban region as a case study, I ask: How have urban surface temperatures and the distribution of vegetation changed over 1985-2021 in the greater Los Angeles region? In chapter 2, where I looked at urban dynamics at a multidecadal scale for 52 cities in the conterminous United States, I ask: How has urbanization affected urban greenness, land surface temperature, and vegetative cooling dynamics among cities throughout the United States and how do these differences affect urban equity in greenness and climate? Finally, in chapter 3, where I assessed changing urban dynamics in 266 cities from 82 countries across a 28-year timeseries, I ask: How does urban greenness, temperature, and vegetative cooling differ among cities at the global scale, and how have these variables changed over time?

References

Allen, C. R., D. G. Angeler, A. S. Garmestani, L. H. Gunderson, and C. S. Holling. 2014. Panarchy: Theory and Application. Ecosystems **17**:578-589.

Allen, M. A., D. A. Roberts, and J. P. McFadden. 2021. Reduced urban green cover and daytime cooling capacity during the 2012–2016 California drought. Urban Climate **36**.

Baldauf, R., and D. Nowak. 2014. Vegetation and Other Development Options for Mitigating Urban Air Pollution Impacts. Pages 479-485 Global Environmental Change.

Bartesaghi-Koc, C., P. Osmond, and A. Peters. 2020. Quantifying the seasonal cooling capacity of 'green infrastructure types' (GITs): An approach to assess and mitigate surface urban heat island in Sydney, Australia. Landscape and Urban Planning **203**.

Benz, S. A., and J. A. Burney. 2021. Widespread Race and Class Disparities in Surface Urban Heat Extremes Across the United States. Earth's Future **9**.

Bijoor, N. S., H. R. McCarthy, D. Zhang, and D. E. Pataki. 2012. Water sources of urban trees in the Los Angeles metropolitan area. Urban Ecosystems **15**:195-214.

Buyantuyev, A., and J. Wu. 2012. Urbanization diversifies land surface phenology in arid environments: Interactions among vegetation, climatic variation, and land use pattern in the Phoenix metropolitan region, USA. Landscape and Urban Planning **105**:149-159.

Casey, J. A., P. James, L. Cushing, B. M. Jesdale, and R. Morello-Frosch. 2017. Race, Ethnicity, Income Concentration and 10-Year Change in Urban Greenness in the United States. Int J Environ Res Public Health **14**.

Chave, J. 2013. The problem of pattern and scale in ecology: what have we learned in 20 years? Ecol Lett **16 Suppl 1**:4-16.

Clarke, L. W., L. Li, G. D. Jenerette, and Z. Yu. 2014. Drivers of plant biodiversity and ecosystem service production in home gardens across the Beijing Municipality of China. Urban Ecosystems **17**:741-760.

du Toit, M. J., C. M. Shackleton, S. S. Cilliers, and E. Davoren. 2021. Advancing Urban Ecology in the Global South: Emerging Themes and Future Research Directions. Pages 433-461 *in* C. M. Shackleton, S. S. Cilliers, E. Davoren, and M. J. du Toit, editors. Urban Ecology in the Global South. Springer.

Frank, B. 2017. Urban Systems: A Socio-Ecological System Perspective. Sociology International Journal **1**.

Gao, Y., H. Pan, and L. Tian. 2023. Analysis of the spillover characteristics of cooling effect in an urban park: A case study in Zhengzhou city. Frontiers in Earth Science **11**.

Gaston, K. J. 2004. Macroecology and people. Basic and Applied Ecology **5**:303-307.

Gillespie, T. W., J. de Goede, L. Aguilar, G. D. Jenerette, G. A. Fricker, M. L. Avolio, S. Pincetl, T. Johnston, L. W. Clarke, and D. E. Pataki. 2016. Predicting tree species richness in urban forests. Urban Ecosystems **20**:839-849.

Grove, J. M., D. H. Locke, and J. P. O'Neil-Dunne. 2014. An ecology of prestige in New York City: examining the relationships among population density, socio-economic status, group identity, and residential canopy cover. Environ Manage **54**:402-419.

Harlan, S. L., G. Chowell, S. Yang, D. B. Petitti, E. J. Morales Butler, B. L. Ruddell, and D. M. Ruddell. 2014. Heat-related deaths in hot cities: estimates of human tolerance to high temperature thresholds. Int J Environ Res Public Health **11**:3304-3326.

Hope, D., C. Gries, W. Zhu, W. F. Fagan, C. L. Redman, N. B. Grimm, A. L. Nelson, C. A. Martin, and A. Kinzig. 2003. Socioeconomics drive urban plant diversity. Proc Natl Acad Sci U S A **100**:8788-8792.

Hsu, A., G. Sheriff, T. Chakraborty, and D. Manya. 2021. Disproportionate exposure to urban heat island intensity across major US cities. Nat Commun **12**:2721.

James, P., J. E. Hart, R. F. Banay, and F. Laden. 2016. Exposure to Greenness and Mortality in a Nationwide Prospective Cohort Study of Women. Environ Health Perspect **124**:1344-1352.

Jenerette, G. D., L. W. Clarke, M. Avolio, D. Pataki, T. Gillespie, S. Pincetl, D. Nowak, L. R. Hutyra, M. McHale, J. P. McFadden, and M. Alonzo. 2016. Climate Tolerances and Trait choices shape continental patterns of urban tree biodiversity. Global Ecology and Biogeography **25**:1367-1376.

Jenerette, G. D., S. L. Harlan, A. Brazel, N. Jones, L. Larsen, and W. L. Stefanov. 2006. Regional relationships between surface temperature, vegetation, and human settlement in a rapidly urbanizing ecosystem. Landscape Ecology **22**:353-365.

Jia, W., S. Zhao, and S. Liu. 2018. Vegetation growth enhancement in urban environments of the Conterminous United States. Glob Chang Biol **24**:4084-4094.

Kendal, D., C. Dobbs, R. V. Gallagher, L. J. Beaumont, J. Baumann, N. S. G. Williams, S. J. Livesley, and A. Algar. 2018. A global comparison of the climatic niches of urban and native tree populations. Global Ecology and Biogeography **27**:629-637.

Konarska, J., J. Uddling, B. Holmer, M. Lutz, F. Lindberg, H. Pleijel, and S. Thorsson. 2016. Transpiration of urban trees and its cooling effect in a high latitude city. Int J Biometeorol **60**:159-172.

Koyama, T., M. Yoshinaga, K.-i. Maeda, and A. Yamauchi. 2015. Transpiration cooling effect of climber greenwall with an air gap on indoor thermal environment. Ecological Engineering **83**:343-353.

Kühn, I., and S. Klotz. 2006. Urbanization and homogenization – Comparing the floras of urban and rural areas in Germany. Biological Conservation **127**:292-300.

Leong, M., R. R. Dunn, and M. D. Trautwein. 2018. Biodiversity and socioeconomics in the city: a review of the luxury effect. Biol Lett **14**.

Malkinson, D., D. Kopel, and L. Wittenberg. 2018. From rural-urban gradients to patch – matrix frameworks: Plant diversity patterns in urban landscapes. Landscape and Urban Planning **169**:260-268.

McPhearson, T., S. T. A. Pickett, N. B. Grimm, J. Niemelä, M. Alberti, T. Elmqvist, C. Weber, D. Haase, J. Breuste, and S. Qureshi. 2016. Advancing Urban Ecology toward a Science of Cities. BioScience **66**:198-212.

Pace, R., F. De Fino, M. A. Rahman, S. Pauleit, D. J. Nowak, and R. Grote. 2021. A single tree model to consistently simulate cooling, shading, and pollution uptake of urban trees. Int J Biometeorol **65**:277-289.

Pickett, S. T. A., M. L. Cadenasso, D. L. Childers, M. J. McDonnell, and W. Zhou. 2017. Evolution and future of urban ecological science: ecology in, of, and for the city. Ecosystem Health and Sustainability **2**.

Ren, Z., X. He, H. Zheng, D. Zhang, X. Yu, G. Shen, and R. Guo. 2013. Estimation of the Relationship between Urban Park Characteristics and Park Cool Island Intensity by Remote Sensing Data and Field Measurement. Forests **4**:868-886.

Ruas, R. d. B., L. M. S. Costa, and F. Bered. 2022. Urbanization driving changes in plant species and communities – A global view. Global Ecology and Conservation **38**.

Schneider, D. C. 2001. The rise of the concept of scale in ecology. BioScience **51**:545-553.

Schwarz, K., M. Fragkias, C. G. Boone, W. Zhou, M. McHale, J. M. Grove, J. O'Neil-Dunne, J. P. McFadden, G. L. Buckley, D. Childers, L. Ogden, S. Pincetl, D. Pataki, A. Whitmer, and M. L. Cadenasso. 2015. Trees grow on money: urban tree canopy cover and environmental justice. PLoS One **10**:e0122051.

Smith, I. A., V. K. Dearborn, and L. R. Hutyra. 2019. Live fast, die young: Accelerated growth, mortality, and turnover in street trees. PLoS One **14**.

Stein, A., K. Gerstner, and H. Kreft. 2014. Environmental heterogeneity as a universal driver of species richness across taxa, biomes and spatial scales. Ecol Lett **17**:866-880.

Tan, P. Y., N. H. Wong, C. L. Tan, S. K. Jusuf, M. F. Chang, and Z. Q. Chiam. 2018. A method to partition the relative effects of evaporative cooling and shading on air temperature within vegetation canopy. Journal of Urban Ecology **4**.

Threlfall, C. G., L. D. Gunn, M. Davern, and D. Kendal. 2022. Beyond the luxury effect: Individual and structural drivers lead to 'urban forest inequity' in public street trees in Melbourne, Australia. Landscape and Urban Planning **218**.

Wang, C., Z. Ren, X. Chang, G. Wang, X. Hong, Y. Dong, Y. Guo, P. Zhang, Z. Ma, and W. Wang. 2023. Understanding the cooling capacity and its potential drivers in urban forests at the single tree and cluster scales. Sustainable Cities and Society **93**.

Chapter 1

Urban greenness and its cooling effects are influenced by changes in drought, physiography, and socio-demographics in Los Angeles, CA

Abstract

The multidecadal change in urban microclimate and greenness, particularly in response to drought and a warming climate, has implications for urban residents' well-being. Urban greenness, temperature, and vegetative cooling vary spatially. However, the dynamics of the relationships among these variables and their influencing factors are poorly characterized. Using the Los Angeles Urban Region, USA as a case study we evaluate the dynamics among urban vegetation and climate through an evaluation of satellite-based observations between 1985 and 2021. We hypothesize that microclimate changes are driven by water demand and aridity, with increasing aridity enhancing transpiration and vegetation-cooling, but that irrigation variation, assessed through proxy demographic variables of income modify water availability. Our results show that the L.A. region warmed by 0.13 °C/year, NDVI increased annually by 4.81 x 10-4, and vegetative cooling increased by 0.08 °C/NDVI/year. A consequence of these dynamics was that the luxury effect of income as a mediator of NDVI and LST declined 41% and 28%, respectively, between 1990 and 2020. The changes in urban microclimates over time and from drought are affected by social and physiographic variables associated with water availability and water demand and are increasingly leading to less racially equitable neighborhood distributions of heat.

Introduction

In arid and semi-arid cities, neighborhood temperature and vegetation distributions are generally coupled spatially, but these variables' dynamics are not well understood (Qi et al. 2022, Cheng et al. 2023). Urban environmental dynamics may reflect both responses to global climate changes (Varquez and Kanda 2018) as well as more local land management actions, notably tree planting and irrigation (Jin et al. 2019). Both climate changes and management decisions may interact in their effects on neighborhood greenness and temperature (Yuan and Bauer 2007, Jenerette et al. 2011, Ziter et al. 2019). The dynamics of urban environments lead to altered availability of both greenspace and heat risks. Further, variability in the effects of global and regional changes to urban microclimate conditions may be moderated by the built environment, physiography, and demographic distributions which may cause additional spatially varying trajectories of urban environments (Oke and Stewart 2012, Coseo and Larsen 2014) and likely will have consequences for societal equity. Thus, while urban neighborhood greenness and temperatures are likely changing, the magnitude, drivers, and impacts of urban variation in these changes are not well resolved.

Hydrologic changes in urban environments are directly tied to urban greenness and temperature dynamics (Qiu et al. 2013, Konarska et al. 2016, Litvak et al. 2017). Transpiration, dependent on both water availability and atmospheric demand, is a major component of neighborhood cooling by vegetation (Chen et al. 2019, Winbourne et al. 2020, Zhao et al. 2020). During drought, urban vegetative cooling may exhibit distinct shifts due to changes in the spatial availability of water and atmospheric evaporative

demand. This is particularly true in many arid and semi-arid cities where irrigation plays a pivotal role in the availability of water for the urban ecosystem (McCarthy and Pataki 2010, Pataki et al. 2011b, Liang et al. 2017). Irrigation modifies local temperatures, evaporative demand, and plant transpiration via an increase in water availability (Vahmani and Hogue 2015, Gao et al. 2020) and humidity (Broadbent et al. 2018, Mishra et al. 2020), potentially decoupling greenness and temperature dynamics from precipitation (Jenerette et al. 2013, Winbourne et al. 2020, Ibsen et al. 2023). Further, drought often co-occurs with hotter temperatures and higher vapor pressure deficit (VPD; (Grossiord et al. 2020), suggesting the variables that increase temperature or aridity may increase vegetative cooling during drought via increased evaporative demand. Although observations for individual droughts have noted the failure of urban irrigation to prevent greenness declines and temperature increases (Quesnel et al. 2019, Miller et al. 2020, Allen et al. 2021), these studies offer only a snapshot of an evolving temporal relationship between aridity, irrigation, and urban greenness-temperature dynamics. The urban water deficit hypothesis poses uncertainty about how urban ecosystems react to sustained aridity over time. While understanding the long-term impacts of urban aridity is outside the scope of individual drought analyses, the dynamics of greenness and temperature in response to aridity have not been assessed at a multidecadal scale.

Physiographic factors may also moderate the drivers in neighborhood greenness and temperature dynamics. Coastal regions are cooler and have a lower VPD than inland regions (representing a coast-to-inland maritime gradient), elevation is associated with decreased temperatures and VPD (Li et al. 2021), and impervious cover increases

sensible heat flux, increasing VPD (Zipper et al. 2017). However, VPD may not be the proximate driver of transpiration: VPD drives transpiration in water-limited sites, but solar radiation drives transpiration in energy-limited sites (Whitley et al. 2013). Therefore, the coastal marine layer, in decreasing photosynthetically active radiation (PAR), and impervious cover, in increasing temperature, may also have a role in mediating the relationship between vegetative cooling, plant greenness, and temperature. Beyond these physiographic factors, socioeconomic distributions may further modify the dynamics between urban greenness and temperature.

Social variables influence urban temperatures (Huang et al. 2011), water availability (Corral-Verdugo et al. 2003), and greenness (Schwarz et al. 2015). The luxury effect describes how wealthy regions of a city have greater greenness and are cooler than less affluent regions (Harlan et al. 2006, Leong et al. 2018, Wetherley et al. 2018, Barrera et al. 2019, Shih 2022). These demographic drivers may similarly influence the dynamics of neighborhood vegetation and temperature although how these effects occur is uncertain. While affluent neighborhoods might consume more water post-drought (Balling et al. 2008, House-Peters et al. 2010), strengthening the luxury effect, water restrictions could cause these areas to reduce irrigation, potentially weakening the effect. Through time greenness may have increased in response to municipal tree planting campaigns (Eisenman et al. 2021) such as MillionTreesNYC (McPhearson et al. 2010) and the Greening the Gateway Cities Program in Massachusetts (Breger et al. 2019). However, tree planting campaigns have been observed to increase tree cover in high tree-cover regions, perpetuating racial tree cover disparities (Krafft and Fryd 2016, Garrison

2017, 2018) and increasing the luxury effect. These patterns associated with wealth and demographics intersect with the luxury effect, emphasizing the importance of understanding how it may change through time.

The luxury effect itself may vary over time, potentially hindering individuals' ability to manage the urban heat and greenscape (Zhou et al. 2011). This instability may be compounded by race-specific characteristics that introduce additional complexity to the luxury effect's dynamics (Watkins and Gerrish 2018, Venter et al. 2020). For instance, even after controlling for income, racial minorities have been found to experience higher temperatures compared to their non-Hispanic White counterparts (Hoffman et al. 2020, Benz and Burney 2021). Furthermore, while affluence tends to promote increased greenness in predominantly White neighborhoods, Black and Asian neighborhoods demonstrate a different pattern, with low-income communities showing a greater likelihood of increased greenness (Huang et al. 2011). Increased affluence among minority communities can sometimes lead to a decrease in greenness, contradicting the trend observed in White neighborhoods and suggesting race-specific differences in how urban residents manage greenness (Casey et al. 2017). To better reflect the influence of race on mediating urban greenness and temperature (Jesdale et al. 2013, Locke and Grove 2014), the non-stationarity of race-dependent relationships should be assessed. The impact of race on greenness and temperature can vary over time and by race, potentially magnifying disparities in well-being (Clarke et al. 2014). This dynamic, race-mediated influence of income on greenness and temperature, may exacerbate disparities in well-

being across neighborhoods with predominantly different racial demographics (Morello-Frosch et al. 2011).

To address the uncertainties in the spatial and temporal distributions of urban greenness and temperature we evaluated their dynamics over 37 years throughout the semi-arid, irrigated Greater Los Angeles, USA urban region (LAUR). Using LAUR as a case study we ask: How have urban surface temperatures and the distribution of vegetation changed over 1985-2021 in the greater Los Angeles region? We answered our research question by evaluating the magnitude and possible drivers of changes in neighborhood greenness, temperature, and the effect of vegetation on temperatures throughout the LAUR between 1985 and 2021. We tested the prediction that urban greenness and temperature increased over time due to tree planting campaigns and climate change, respectively, and that vegetative cooling has increased due to global increases in temperature and aridity. We evaluated an urban water deficit hypothesis to identify whether long-term changes in greenness and temperature are associated with the relative distribution of water availability. We tested the prediction that greenness declines, temperature increases, and vegetative cooling increases with increasing drought. We also tested the prediction of large neighborhood variation in the dynamics of greenness and temperature and that this neighborhood variation would be related to both physiographic and income differences among neighborhoods. As an outcome of the dynamics in neighborhood greenness and temperature, we evaluated the dynamics of their social equity throughout the region to assess the changing availability of greenness and heat throughout the region. By quantifying the change in urban greenness,

temperatures, and vegetative cooling over a multidecadal timescale we describe how physiographic and social variables modify urban vegetation dynamics in a model city.

Methods

2.1 *Study Area*

All data were averaged to the census tract before analysis, other than the Standardized Precipitation Evapotranspiration Index, which has one data point per month for the study area. The census tract was chosen as the scale of analysis consistent with census-provided data and is sufficiently large to provide robust demographic data (Wong and Sun 2013). Over the temporal span of this study, the study area had a mean NDVI of 0.25, a mean LST of 35 °C, and an average of 34.8 cm rain year^{-1}. LAUR has unique characteristics making it a useful model city for this study. The LAUR is one of two megacities in the United States, located on the southwestern coast with a Mediterranean climate (Köppen Csa and Csb). Within the LAUR neighborhood per capita median income varies from $9,000 to over $250,000 per year, while racial diversity is one of the greatest in the nation. LAUR's socio-economic diversity contributes to inequities in the distribution of heat and urban greenness (Schwarz et al. 2015, Tayyebi and Jenerette 2016, Yin et al. 2023). To partially rectify this, Los Angeles planted 69,776 trees between 2007 and 2014 as part of the Million Trees L.A. initiative, focusing new plantings in regions with non-white residents (Garrison 2018). As almost all of LAUR's urban trees are non-native (Gillespie et al. 2016, Jenerette et al. 2016), they require extensive management. Further, the region's physiography is unique for large cities in the United

States, where temperature and aridity increase along a maritime climate gradient from the coast to the San Gabriel Mountains ~48 km inland. LAUR also experiences frequent drought both annually (due to the Mediterranean semi-arid weather) and inter-annually. Regionally, patterns of urban greenness are closely associated with rates of evaporation, highlighting the importance of irrigation in a region where summertime rainfall accounts for only 13% of evapotranspiration (Pataki et al. 2011a, Bijoor et al. 2012, Liang et al. 2017). Urban trees in the LAUR can use a large amount of water for transpiration (Pataki et al. 2011a), which may make LAUR's urban forest susceptible to drought as trees in the LAUR, particularly those that are shallowly rooted, may supplement their water needs with rainfall (Bijoor et al. 2012). During the 2012-2016 California megadrought, urban green cover mediated drought-induced heat waves via vegetative cooling, albeit reduced from pre-drought levels (Allen et al. 2021).

Our study area covers 3,474 km^2 of urbanized land cover in the Greater Los Angeles, California urban region (LAUR [Fig. 1]). Most of the area is within Los Angeles County, however, about a quarter of the urban extent is within Orange and San Bernardino Counties. We defined the extent of the study region by 2010 census tract boundaries that overlay non-mountain populated areas of the greater Los Angeles region. Census tracts in the mountains (e.g., Santa Monica, San Gabriel) or that otherwise contained less than ~50% urbanized land cover were removed, as were tracts with no or very little population (such as around the airport or industrial centers). We used all populated, non-mountain census tracts within the boundaries of the Landsat tile centered over Los Angeles, yielding 2,794 tracts. In 1990, the first year of census data utilized, the

LAUR had a population of 10,880,125 and an average density of 4,150 people km^{-2}. By the end of the time series at the 2020 census the LAUR's population had increased 15% percent to 12,498,697 whereas density increased 23% percent to 5,098 people km^{-2}.

2.2 *Changes in Urban Greenness and Land Surface Temperature*

We assessed the distribution of vegetated cover and land surface temperature using the Landsat 4, 5, 7, and 8 satellites collected from all months from 1985 through the end of 2021. The Landsat satellites pass over the LAUR in the morning between approximately 16:00 and 18:00 GMT (8:00-10:00 PST). The individual Landsat satellites have a 16-day return interval, however, subsequent satellites (e.g., Landsat 7 vs. Landsat 8) are in an eight-day offset orbit, providing greater temporal fidelity. Landsat is provided at 30 m^2 resolution as captured natively (visible bands) or via resampling (thermal bands). Landsat has the longest publicly-available satellite record of Earth observation (Loveland and Dwyer 2012) and has been used for urban research for decades, including to estimate urban vegetative cover, microclimate, and their relationships (Buyantuyev et al. 2007). We relied on the Collection-2 Analysis Ready Data (ARD) product, provided by the United States Geological Survey (USGS) and accessed from Earth Explorer (Dwyer et al. 2018). The ARD product is atmospherically corrected and radiometrically calibrated by the USGS using a standardized approach to make the data from the different Landsat satellites directly comparable to one another, facilitating comparative analyses (Banskota et al. 2014, Zhu 2019) and making it suitable for time series analysis (Zhu 2019).

All data were pre-processed in MATLAB r2021b and ArcGIS Pro 2.9. To ensure the highest quality data we only downloaded Landsat tiles that contained less than 10% cloud cover. Further, we did not use Landsat 7 after May 31st, 2003, following the failure of the satellite's scan line corrector. The subsequent striping of Landsat 7 imagery, coupled with cloud masking, yielded a limited number of usable pixels and produced unreliable results. Therefore, we have no data from December 2011 - March 2013, representing the gap between Landsat 5 and Landsat 8. All non-clear pixels (clouds, water, aerosols, etc.) were masked in MATLAB to take advantage of parallel processing. Images that were not usable following cloud masking (e.g., contained too few pixels) were manually discarded following visual inspection yielding a final stack of 215 images. The masked TIFF files were then imported to ArcGIS Pro where they were clipped to the study extent (Fig. 1). The data were then averaged at the census tract scale using 1990, 2000, 2010, and 2020 census tract boundaries. The TIFF imagery was finally re-uploaded to MATLAB where the data were averaged to the monthly scale, generating a data product consistent with the monthly scale of the weather and drought datasets.

From the Collection-2 ARD dataset, we derived the Normalized Difference Vegetation Index (NDVI), a commonly used proxy for vegetation cover (Carlson and Ripley 1997) or biomass (Borowik et al. 2013). NDVI, which ranges from -1 to +1, takes advantage of chlorophyll's reflectivity in the near-infrared but absorption in the red portion of the electromagnetic spectrum, where values closer to +1 indicate greater vegetated cover and values less than zero are unvegetated (Pettorelli et al. 2011, Esau et al. 2016, Huang et al. 2020). For the LAUR we found that pixels with a Landsat NDVI of

0.1 have 1% green cover. We derived this value by randomly selecting images from across the time series, randomly identifying individual pixels within those images, and then demarcating the vegetated area of those pixels using the sub-meter World Imagery from ArcGIS. To remove unvegetated pixels we excluded all pixels with an NDVI<0.1 before analysis, consistent with previous studies using locally assessed thresholds (Esau et al. 2016, Liu et al. 2018). Few pixels transitioned between the 0.1 threshold over the time series: between the start and end of the time series the number of "vegetated" pixels with an NDVI>0.1 increased by 1.52%. The LST dataset was not similarly modified.

To assess the change in land surface temperature we used the Surface Temperature product from the Collection-2 ARD dataset. ARD LST is derived using the single-channel algorithm based on the thermal band while accounting for both atmospheric effects and surface emissivity, although Landsat 8-9 utilizes the LaSRC algorithm (USGS 2021b) whereas Landsat 4-7 utilize the LEDAPS algorithm (USGS 2021a). These algorithms use the radiative transfer equation, incorporating emissivity corrections based on NDVI values to account for the distinct emissivity of vegetation compared to other surfaces. USGS processes the ARD LST by applying atmospheric compensation to the thermal bands, which adjusts for the effects of water vapor and other atmospheric gases, ensuring accurate ground temperature readings. The resolution of surface temperature varies by satellite: Landsat 4-5 are at 120 m^2, Landsat 7 is at 60 m^2, and Landsat 8 is at 100 m^2, however, all data were resampled by USGS to 30 m^2. The thermal images are collected at the same time as the visible bands that go into the derivation of NDVI, making the stack of LST and NDVI images the same size. The ARD

Surface Temperature product, provided in Kelvin, is similarly comparable between satellites in the Landsat series (Cook et al. 2014); the standardization of the LST ARD processing makes it appropriate for time series analysis.

2.3 *Changes in LST-NDVI*

Using our 215-image dataset allowed us to quantify variability in LST-NDVI. Vegetative cooling, defined as the slope of the LST-NDVI relationship, is used as a proxy for drought in non-urban landscapes in indices such as the Vegetation Temperature Condition Index (VTCI; (Wan et al. 2004), the Vegetation Supply Water Index (VSWI; (Cunha et al. 2015), and the modified Temperature Vegetation Drought Index (mTVDI; (Zhao et al. 2017). To determine the temporal change in the cooling provided by urban plants we linearly regressed average monthly NDVI against average monthly LST, where the slope represents the cooling provided by plants in °C/NDVI and the intercept represents the bare-soil surface temperature. We evaluated this regression for each date in the time series to create a new array showing the change in LST-NDVI through time.

2.4 *Weather Datasets and the Standardized Precipitation Evapotranspiration Index (SPEI)*

We used weather data from TerraClimate, a ~4 km^2 global multidecadal weather dataset (Abatzoglou et al. 2018). From TerraClimate we acquired actual evapotranspiration, climate water deficit, potential evapotranspiration, precipitation accumulation, solar radiation, minimum temperature, maximum temperature, vapor pressure, and vapor pressure deficit. We accessed TerraClimate

(IDAHO_EPSCOR/TERRACLIMATE) using Google Earth Engine (GEE), a cloud-based petabyte-scale GIS (Gorelick et al. 2017). We downloaded weather data from GEE for the LAUR from 1984 through the end of the time series, allowing us to derive new variables of 1-12 months of cumulative precipitation for each month. As with the Landsat imagery, we averaged the TerraClimate data in ArcGIS Pro to our 2010 census tract boundaries before uploading the averaged data to MATLAB for analysis. In addition to TerraClimate, the climatic water balance was an important variable in our study.

We quantified drought using the Standardized Precipitation Evapotranspiration Index (SPEI), as provided by SPEIbase v2.7 (Vicente-Serrano et al. 2010). The SPEI, initially proposed by Vicente-Serrano et al. (2010), considers both precipitation and temperature-derived potential evapotranspiration, making it notably sensitive to climatic changes. This approach provides a series where negative values signify drought conditions and positive ones indicate wetter-than-average periods. The SPEI is commonly used in ecological research as a measure of drought, overcoming limitations of the similarly derived standardized precipitation index in its inclusion of both temperature and potential evapotranspiration (Vicente-Serrano et al. 2010). SPEI values further from zero indicate increasingly wet (positive) or dry (negative) periods relative to the long-term average. A unique feature of the SPEI relative to other drought indices is that data are aggregated at monthly scales. For instance, a 3-month SPEI of 0.64 for June indicates that the June of interest is 0.64 standard deviations wetter than the average of all April-June periods in the time series used to generate the SPEI. At intra-annual scales, monthly aggregations help to overcome the effect of seasonality in rainfall. Inter-annual

aggregations are useful to quantify the effects of long-term drought. We used all monthly aggregations provided by SPEIbase from SPEI-1 through SPEI-48.

Drought is defined by SPEI values ≤-0.5 (mild drought), while wet periods have an SPEI ≥0.5 (Feng et al. 2020). The more negative the value, the greater the deficit in precipitation/potential evapotranspiration. For this study, we defined drought as having an SPEI ≤-1 (moderate drought), with wet periods having an SPEI ≥+1. The standardization of SPEI ensures that its values are directly comparable both across different locations and over various time periods. This makes SPEI an ideal tool for time series analysis, especially when incorporating seasonal variations (Vicente-Serrano et al. 2010). Using the monthly indices of when "dry" and "wet" periods occur, we created mean "dry" and "wet" variables for NDVI, LST, and LST-NDVI for each SPEI monthly aggregation.

2.5 *Socio-demographic and physiographic variables*

Census-tract level socio-economic data were obtained for each decennial census from 1990 to 2020. To minimize information loss when comparing relationships across time we used the census tract boundaries consistent with that year's data. When assessing mean change in our variables in response to SPEI we used the 2010 census tract boundaries, as this is the only census tract year with associated tree canopy cover data. We derived population density by dividing the population of each census tract by that census tract's area. We also determined the racial composition of each census tract by dividing the population of White, Hispanic, Black, and Asian persons per census tract by

the census tract's total population. The distribution of races within the LAUR is spatially heterogeneous, but there are race-specific agglomerations (Fig. 2). Other census variables we used were percent graduate degree holders per census tract, median household income, per-capita income, and income by race. We categorized census tracts by racial population using census datasets which denote the census-tract population of a given race as well as providing race-based income metrics; race-based census tract data utilized in this study were provided directly from the United States Census Bureau. These census datasets allowed us to use the percent of a given racial population per census tract as a dependent variable in regression analysis. Census data for 2000, 2010, and 2020 were obtained from data.census.gov. Data for 2000 is derived from the decennial census, while data for 2010 and 2020 are derived from the decennial census and the American Community Survey 5-year Estimates. Relevant tract-level census data for 1990 was found hosted by the Centers for Disease Control at https://www2.cdc.gov/nceh/lead/census90/house11/download.htm. Boundaries of census tracts for all years were obtained from https://www.census.gov/geographies/mapping-files.html. Census tract boundaries were used to manipulate the predictor variables.

The physiographic variables we evaluated included distance from the coast, elevation, percent impervious cover per tract, and percent tree canopy cover per tract. We created the distance from the coast variable in ArcGIS Pro by finding the distance from the Pacific Ocean to the centroid of the respective 1990-2020 census tract boundary. Visual inspection ensured irregularly shaped tracts did not lead to more than one centroid per tract. Elevation, acquired using GEE, came from the Shuttle Radar Topography

Mission (SRTM) provided at a spatial resolution of 1-arc-second and a vertical accuracy of ±6.87 m (Elkhrachy 2018). It is important to note that in the LAUR "high elevation" connotes a few hundred meters; the median elevation is 80 meters. Low elevation regions $\leq 25^{th}$ percentile range from sea level up to 34 meters, whereas high elevation regions $\geq 75^{th}$ percentile are ≥ 204 meters. Both percent impervious cover and percent tree canopy cover came from the National Land Cover Database (NLCD). We used NLCD impervious cover for 2001 (to match the 2000 census), 2011 (2010 census), and 2021 (2020 census). We used only one data point for tree canopy cover, tying the 2011 NLCD tree canopy cover with the 2010 census. Finally, we also used the change in NDVI (either through time or during drought) as an independent variable to explain the change in LST. All datasets used in this study are described in Table 1.

To assess the effect these variables had on the change in NDVI and LST during drought we used bivariate linear regression in MATLAB, where ΔNDVI and ΔLST (wet-dry) were the dependent variables. Further, to assess the change in these variables through time we ran a pixel-by-pixel temporal linear regression of NDVI and LST in MATLAB. Our approach to determining the NDVI-Precipitation slope followed the same structure. For this temporal regression, we isolated the slope coefficient and used this term as a dependent variable in a new regression designed to explain the spatial variability of the NDVI and LST trends.

We explained the spatial variability of the per-pixel NDVI and LST trends through time by using structural equation modeling (SEM). SEM is a statistical approach

used to test hypotheses about the relationships among observed and unobserved variables. SEM allows for the exploration of complex relationships, including those that are direct, indirect, and reciprocal (Wu et al. 2021, Manavvi and Rajasekar 2023). In multiple regression, nearly all explanatory variables significantly explain variation in the dependent variables due to a large sample size of census tracts leading to p-values lower than 0.05 (Lantz 2013). We only kept variables that had a partial r^2 of at least 0.05 in multiple regression.

Results

3.1 *Spatiotemporal Dynamics of NDVI, LST, and LST-NDVI*

Initial analyses confirmed the expectation that the average NDVI and LST across the time series are well correlated spatially (pearson's $r=-0.80$, $p<0.001$), such that the hottest urban regions are also those which are least vegetated (Fig. 1). Spatial variation in the long-term average for NDVI and LST is itself associated with income and the built environment. In multiple regression, impervious cover and tree canopy cover explained 87% of the spatial variability of NDVI, where the effect of impervious cover on NDVI was 63% greater than that of tree cover (supplemental Fig. 1). Every 10% increase in impervious cover was associated with a decrease in NDVI by 0.041 (p-value<0.001), while every 10% increase in tree cover was associated with an increase in NDVI of 0.0047 (p-value<0.001). Similarly, impervious cover and income explained 69% of the spatial variability of LST (supplemental Fig. 2), with these variables increasing and decreasing LST, respectively. Impervious cover had an effect 59% greater on the spatial variation of LST than income. Every 10% increase in impervious cover led to an

additional 0.80 °C of warming (p-value<0.001), while median household income led to an average cooling benefit of 0.349 °C/$10,000 (p-value<0.001).

In the context of these long-term spatial distributions, greenness and temperatures also exhibited temporal variability and trends during the time series (Fig. 3). Between 1985 and 2021 land surface temperature increased 0.13 °C/year (p=0.041) and NDVI increased 5.05 x 10^{-4} per year between 1985 and 2021 (p<0.001). However, the change in NDVI through time was uneven, so that the rate of increase in greenness is different when assessed from different years. Starting in 1992 NDVI increased 6.21 x 10^{-4} per year (p<0.001), while from 2007 to the end of the time series NDVI increased 0.002 per year (p<0.001). The increase in LST through time was evenly distributed throughout the year, increasing slightly more during the summer months (June-August) at 0.18 °C/year (p=0.02) than the winter months (December-February) at 0.15 °C/year (p=0.002), although the difference in slopes between seasons was not significant (p=0.17). Partially mitigating this increased heat, vegetative cooling increased 0.08 °C/year (p=0.0497). Between 1985 and 2021 urban plants provided an additional 2.96 °C/NDVI of cooling. The changes in vegetation and temperature also occurred in the context of a decrease in precipitation of 1.9 mm/year (p=0.009).

Weather plays a significant role in the temporal variability of NDVI and LST at the whole LAUR spatial scale (Fig. 4). The dynamics of urban greenness at the whole city scale was coupled with precipitation and increased 0.007 NDVI per 100 mm of three-months cumulative precipitation (p-value<0.001). Precipitation explained 20% of the temporal variability in NDVI. Urban NDVI was most responsive to precipitation with

three months of cumulative rainfall; the fit declined with additional months of rain until nine months of cumulative precipitation when there was no relationship between greenness and precipitation (p-value=0.47). The weather variables most responsible for the temporal variability in LST were solar radiation and air temperature, which together explained 87% of the variance in LST. Every 1 w/m^2 increase in solar radiation increased LST 0.13 °C, while every 1 °C increase in minimum air temperature increased LST 2.3 °C (p-value<0.001). Solar radiation was the only variable with a partial r^2 of at least 0.05 to significantly modify the temporal variability of vegetative cooling. Vegetative cooling increased with solar radiation at a rate of 0.077 °C/NDVI per 1 w/m^2, with solar radiation explaining 62% of the temporal variability (p-value <0.001). The temporal variability of NDVI, LST, and vegetative cooling was substantially influenced by the weather, highlighting the key role of weather in shaping urban greenness and temperature dynamics over time.

The temporal trends of greenness and temperature exhibited wide spatial variability in their rates of change within the LAUR (Fig. 5). At both the pixel and census tract scales the median increase in LST was 0.16 °C/year with a standard deviation of 0.03 °C/year at the pixel scale and of 0.02 °C/year at the census tract scale. No pixels exhibited cooling. Pixels at the 5^{th} percentile warmed 0.13 °C/year, while pixels at the 95^{th} percentile warmed 0.20 °C/year. Aggregated to the census tract scale, only six census tracts warmed greater than 0.20 °C/year while only one census tract warmed less than 0.1 °C/year. The median increase in NDVI was 3.01×10^{-4} /year at the pixel scale with a standard deviation of 0.003, while at the census tract scale, the median increase in NDVI

was 2.62 x 10^{-4} /year with a standard deviation of 5.91 x 10^{-4}. The 5th percentile of pixels lost 3.6 x 10^{-3} NDVI/year, while the 95th percentile of pixels gained 4.7 x 10^{-3} NDVI/year. Pixels with non-significant LST trends overlap downtown Los Angeles and regions with high commercial activity and impervious cover. When averaging the significant per-pixel trends through time to the census tract scale, 2,372 (86%) tracts warmed and 386 (14%) tracts had no change through time. No tracts exhibited cooling. In contrast, 1,801 (65%) census tracts significantly increased greenness while 592 (21%) browned. Overall, the pixels that warmed the most warmed over 1.5x as fast as the coolest pixels, while the greenest pixels greened at a rate similar to the pixels that lost the most greenness. We sought to explain this spatial variability in the rate of change for NDVI and LST.

3.2 *Variability in the NDVI and LST trends*

The per-pixel changes through time in NDVI and LST, when aggregated to the census-tract scale, were most strongly influenced by 2010 per-capita income, while the change in LST was also strongly responsive to the change through time in NDVI (Fig. 6). Every $10,000 increase in per-capita income increased the NDVI trend 1.32 x 10^{-4} per year (p-value<0.001) while the same increase in income reduced the LST trend by 0.015 °C/year (p-value<0.001). The change in greenness had a large effect on the change in temperature; every 0.01 NDVI/year increase in greenness was associated with less warming of 0.12 °C/year (p<0.001). We also tested physiographic variables to explain the NDVI and LST trends. Impervious cover had a weak effect on increasing LST, while the distance from the coast had the same effect size on decreasing NDVI. Per-capita income and distance from the coast explain 19% of the spatial variability in the NDVI trend,

while per-capita income, impervious cover, and the NDVI trend explain 39% of the spatial variability in the LST trend.

3.3 *The NDVI and LST drought response*

The effect of drought on NDVI and LST temperature trends was spatially variable (Fig. 7). We assessed the drought response at SPEI-6, as this was the SPEI aggregation that led to the largest change in both NDVI and LST. During drought NDVI decreased on average 0.023, while LST increased 4.41 °C. Vegetative cooling increased 0.08 °C/NDVI during drought. Regions that saw the largest decrease in NDVI (a loss of NDVI of ≥0.09) visually overlap large urban parks and hilly terrain, however, we did not include fine-scale variability in land cover in our dataset to test this explicitly. Surprisingly, our results indicate that NDVI increased during drought in a minority (13%) of pixels. Aggregated to the census tract scale, no tracts greened during drought. In contrast, the LST drought response exhibited a clear coast-to-inland gradient. During drought inland regions warmed ~8 °C, whereas regions right on the coast warmed ~2-3 °C. The benefit of the coast in moderating drought temperatures dissipated approximately 5-10 km from the coast. The consistent decrease in greenness and increase in temperature during drought indicates that NDVI and LST may be directly associated with SPEI. Testing this directly, across all dates NDVI increased 0.007 per unit increase in SPEI-6 (p-value<0.001), representing an increase in greenness with a more positive water balance. There was no relationship between SPEI-6 and LST across all dates, however, the relationship between SPEI and LST was seasonally dependent. In the spring (March-June), LST decreased 0.88 °C with every 0.5 unit increase in SPEI. There was no change through time in the

severity or frequency of drought at SPEI-6, although drought at inter-annual SPEI aggregations was becoming more severe and more frequent. Similarly, greenness was responsive to changes in SPEI with greenness increasing during periods of more positive water balance, showcasing the sensitivity of urban vegetation to climatological water availability.

We sought to explain the spatial variability in NDVI and LST during drought at SPEI-6 (Fig. 8). Using multiple regression, we identified all variables explaining the change in NDVI and LST which had a partial r^2 of at least 0.05. The change in NDVI during drought was only influenced by impervious cover (r^2=0.35, p-value<0.001), where every 10% decrease in impervious cover led to a greater loss in NDVI of 0.004. As drought predominately led to a decline in NDVI, greater impervious cover led to smaller losses in greenness. The change in LST during drought was more readily explained than that of NDVI. The increase in LST during drought was greatest in regions that lost NDVI (r^2=0.24, p-value<0.001) and which were further inland (r^2=0.44, p-value<0.001). These two variables explained 61% of the variance in the change in LST during drought. The change in NDVI during drought had an effect 74% larger on the change in LST than that of distance from the coast despite the distance from the coast having a larger effect in univariate regression. LST increased 0.05 °C/km distance from the coast (p-value<0.001) and 0.29 °C per 0.01 loss in NDVI (p-value<0.001). The large spatial and temporal variability in the change in NDVI and LST through time and during drought may have socio-economic and racial consequences.

3.4 *The Luxury Effect becomes weaker through time and stronger during drought*

We found that income had a significantly lower effect on greenness (p-value<0.001) and temperature (p-value<0.001) in 2020 than it did in 1990 (Fig. 9). In 1990, every $10,000 increase in median household income provided 0.4 °C of cooling and an increase of 0.0202 NDVI. In 2020, the same increase in income provided 0.29 °C of cooling and a 0.0119 increase in NDVI. Income became weaker as a mediator of LST by 0.1 °C/$10,000 (p-value<0.001), an effect 58% as strong in 2020 as it was in 1990, while the effect of income on NDVI declined by 0.008 NDVI/$10,000 (p-value<0.001), an effect 74% as strong in 2020 as it was in 1990. The decline in the effect of income is concomitant with an increase in the effect of impervious cover on increasing temperature and decreasing greenness. In 2020 every 10% increase in impervious cover led to an additional 0.15 °C of warming compared to 1990 (a 24% increase from 0.61 °C to 0.76 °C; p-value<0.001) and an additional loss of 0.007 NDVI (a 20% decrease from -0.0034 to -0.0042 NDVI; p-value<0.001). In contrast to the weakening of the effect of income through time, the income effect became stronger for LST but not for NDVI during drought (Fig. 10). At an intra-annual scale with SPEI aggregations up to SPEI-10, the effect of income increased, on average, 0.071 °C/$10,000 (p-value<0.001) during dry periods. Notably, droughts of longer duration were associated with increasingly stronger relationships between income and temperature, up until SPEI-11 when the luxury effect became weaker during drought. However, this increase in the effect of income on cooling was not necessarily associated with cooler temperatures at the whole-city scale. Vegetative cooling increased during drought at short timescales (SPEI-2 through SPEI-5) on average 0.99 °C/NDVI (p-value<0.001), while for longer term drought (at SPEI-7

through SPEI-12) vegetative cooling decreased during drought by 1.15 °C/NDVI (p-value<0.001) despite an average increase in the effect of income on cooling of 0.064 °C/$10,000 between SPEI-7 and SPEI-10 (p-value<0.001). Income-NDVI did not change between wet (SPEI>+1) and dry periods (SPEI<-1), but income-LST became stronger during dry periods. The decline in the effect of income as a mediator of NDVI and LST may have important equity-based consequences.

The non-stationarity of the socio-economic relationships mediating urban greenness and temperatures was also associated with increasingly marginalized minority populations. Throughout the time series, areas with higher Hispanic populations were consistently found to have increased LST and reduced greenness. Over time, the association between Hispanic-dominated neighborhoods and increased LST significantly strengthened. Compared to 1990, by 2020 LST warming associated with Hispanic-dominated neighborhoods increased 63%; in 1990 every 10% increase in a census tract's Hispanic population increased LST 0.22 °C while the same increase in Hispanic populations increased LST 0.35 °C in 2020. Likewise, the association between Hispanic-dominated neighborhoods and reduced greenness strengthened through time, although this change was not significant. Compared to 1990, by 2020 every 10% increase in a census tract's Hispanic population led to an additional 8% loss in greenness, but this additional decline in greenness was not significant. White-dominated neighborhoods did not experience similar trajectories. In 1990 every 10% increase in the census tract White population led to an increase in NDVI of 0.01 and a decrease in LST of 0.19 °C. In 2020 the same increase in the White population led to the same 0.01 increase in NDVI and a

significant 58% increase in cooling to 0.30 °C. Whereas the experience of Hispanic populations with regards to greenness and temperature is unchanged and significantly worse, respectively, the experience of White populations with regards to greenness and temperature is unchanged and significantly better, respectively. This dichotomy is not reflective of the race-specific changes in the effect of income (Fig. 11); the effect of income on both NDVI and LST declined proportionally similar amounts between White and Hispanic populations. Between 2000 (the first year we had race-specific income data) and 2020, the effect of income declined across White, Hispanic, Black, and Asian communities, with the decline most strongly driven by a decline in the effectiveness of income in White and Hispanic communities. The effect of income was always greatest in White populations and always lowest in Black and Asian populations. In 2000, income in White communities provided 2.42x as much greening and 2.68x as much cooling as the same income in Black communities, declining to an effect 2.12x and 2.31x greater by the 2020 census.

Discussion

In the Los Angeles urban region over the past 36 years, urban greenness, land surface temperatures, and the cooling effectiveness of vegetation have all increased. These trajectories were related to changes in weather patterns, exhibited extensive spatial heterogeneity associated with physiographic and demographic distributions, and were associated with changing patterns of equity in access to greenspace and heat risks. Droughts were consistently associated with increased temperature and decreased greenness. However, land cover distributions moderated the drought response, consistent

with our hypothesis on the importance of physiography. The temporal increases in LST and NDVI are consistent with climate changes and tree-planting campaigns. The increase in LST through time was at least partially mitigated by an increase in vegetative cooling. The modification of the NDVI and LST trends in response to income, distance from the coast, and impervious cover supports our hypothesis about the importance of water availability. At the monthly scale, weather explains temporal variability in NDVI, LST, and vegetative cooling, and the spatial variability across the urban extent is explained by land cover and income alone. These results suggest the capacity to manage the dynamics of NDVI and LST has declined through time with the decline of the luxury effect. Despite the decline in the effectiveness of income, the changing urban dynamics led to the increasing marginalization of predominantly Hispanic communities but an improvement in conditions for predominantly White communities. Overall, our results show the multidecadal dynamics of NDVI, LST, and vegetative cooling are multifactorial and have important race-based equity implications.

From 1985-2021, NDVI, LST, and vegetative cooling increased in the context of decreasing annual precipitation (Fig. 3). Vegetative cooling (°C LST/NDVI), standardized on a per-unit NDVI basis, suggests that the urban vegetation within LAUR is becoming more effective over time. Increased cooling may be due to increased transpiration from warming-induced evaporative demand (Kirschbaum 2004, Drake et al. 2018). The multidecadal increase in greenness and temperature are consistent with tree planting campaigns and climate change, respectively. The average city-wide increase in LST of 0.13 °C/year is consistent with other cities such as Atlanta, USA (Fu and Weng

2016), Ahmedabad, India (Siddiqui et al. 2021), and Marseille, France (Polydoros et al. 2018). Temporal variability in NDVI, LST, and vegetative cooling was unaffected by anthropogenic variables, as variables such as income and land cover may minimally change on a month-to-month basis. NDVI, LST, and vegetative cooling increased through time; we sought to explain the spatial variability in these trends.

The dynamics of NDVI, LST, and vegetative cooling were well correlated with the weather (Fig. 4). Precipitation, temperature, and solar radiation were key drivers of monthly temporal variability. Despite the LAUR being a heavily irrigated semi-arid city, NDVI was sensitive to cumulative rainfall, increasing the most in response to three months of cumulative precipitation. The overall sensitivity of LAUR urban greenness to precipitation contrasts with the finding from Phoenix, AZ where urbanization completely decoupled urban greenness from precipitation (Buyantuyev and Wu 2012). However, Phoenix is in a desert climate that receives 57% of the annual rainfall of the LAUR, a semi-arid city. The finding that urbanization does not decouple greenness from precipitation in a Mediterranean city like the LAUR is consistent with Jenerette et al. (2013) and suggests that the decoupling of urban greenness from precipitation occurs along a gradient of precipitation where decoupling occurs only in the most arid cities. Further, during the 2011-2016 California megadrought, the most severe in over a millennium (Griffin and Anchukaitis 2014), we observed a decrease in NDVI in the LAUR, consistent with findings from another California city where urban greenness decreased despite little change in irrigation (Quesnel et al. 2019). This hint of an underlying water deficit despite anthropogenic input (Bijoor et al. 2012) suggests an

urban water deficit hypothesis, where neighborhood greenness and temperature are modified by the difference between irrigation and evaporative demand yet where anthropogenic inputs do not fully satisfy plant water demands. In contrast to the importance of weather for temporal variability, tree canopy cover and income were the only determinants of the spatial variability of NDVI and LST (Supplemental Figs. 1 & 2); in the LAUR anthropogenic drivers overrode any effect natural drivers have on the spatial variability of NDVI and LST. The pre-eminence of anthropogenic drivers may be related to the composition of the LAUR's urban forest. This sensitivity of the spatial variability of NDVI and LST to anthropogenic factors is suggestive that NDVI and LST are sensitive to water availability and water demand, supporting our urban water deficit hypothesis. We suspect the dominance of anthropogenic variables in explaining spatial variability may be particularly important for the LAUR as it exists in a semi-arid environment, making the dynamics of urban greenness and temperature more sensitive to urban tree cover and irrigation. The spatial and temporal variability of NDVI, LST, and vegetative cooling were dependent on water availability and water demand.

Compared to hotter and drier inland semi-arid cities, the LAUR experiences a milder thermal environment due to its coastal location which moderates temperatures via sea breezes. For example, the daytime land surface temperature in the LAUR averaged 35 °C annually, while inland semi-arid cities like Jaipur, India experienced much higher average summer land surface temperatures exceeding 50 °C (Shahfahad et al. 2023). The relatively mild summer temperatures in coastal Mediterranean climates like Los Angeles allow urban vegetation to thrive and provide substantial local cooling through

evapotranspiration and shading, though in a climatically similar coastal Mediterranean city vegetative cooling was greatest in the spring and summer (Dronova et al. 2018). For instance, Los Angeles parks generate 4.73°C of local cooling with a cooling distance of 165 meters (Gao et al. 2022), compared to summertime cooling from parks in more inland semi-arid cities such as Tehran of 0.8 °C for up to 68 meters (Jamali et al. 2021). In contrast, (Li et al. 2015) found that in the inland semi-arid city of Beijing, differences in latent heat fluxes between urban and rural areas lead to heat wave intensification of urban heat islands, constraining the cooling capacity of vegetation. Overall, the relatively mild climate of the LAUR enables urban greenery to more effectively mitigate urban heat compared to drier and hotter inland semi-arid cities. This greater mitigation capacity is reflected in the long-term increasing trend in vegetative cooling in the LAUR.

At the pixel scale there was wide spatial variability in the NDVI and LST trends (Fig. 5). While trends of NDVI and LST have been conducted at a city-wide scale (Voogt and Oke 2003, Imhoff et al. 2010, Ren et al. 2021, Yang et al. 2021), several studies have shown substantial heterogeneity of the intraurban environment (Liu et al. 2021, Jombo et al. 2022, Lemoine-Rodriguez et al. 2022, Purio et al. 2022). In the LAUR, temperature increased the most in low-income communities that lost greenness, suggesting that the dynamics of NDVI and LST have been inequitably distributed and that inequity is increasing through time. Spatial inequities in urban heat (Reid et al. 2009, Harlan et al. 2013) and greenness (Boone et al. 2009, Jennings et al. 2012) are therefore being propagated through time in the LAUR. The multidecadal change in greenness and temperature was spatially variable, and via income was partially associated with

anthropogenic inputs of water (Fig. 6). To explain this variability we looked at drought, being a natural extreme of both water availability and, via aridity, water demand, as a possible determinant of the dynamics of urban NDVI, LST, and vegetative cooling.

The urban water deficit hypothesis suggests that, during drought, changes in NDVI, LST, or vegetative cooling would be closely associated with variables that modify water availability or demand (Fig. 7). We found partial support for this hypothesis. Greenness decreased the most in regions with low impervious cover, which was the only variable we identified to modify this relationship (Fig. 8). The increase in greenness in a minority of pixels at SPEI-06 may also be due to impervious cover, as many, but not all, of the pixels which greened overlap with impervious surfaces like roads and business centers. We interpret the importance of impervious cover in determining the change in NDVI during drought to suggest two things: first, that census tracts with greater open space (e.g., large urban parks), may have vegetation that is less actively managed than vegetation in highly impervious landscapes (e.g., street trees or vegetation at a residential property). Second, the decline in greenness during drought with increasing pervious cover suggests that drought negatively affects all vegetation and that in regions with a greater potential amount of vegetated cover, via less impervious cover, more greenness can potentially be lost during drought. Increasing distance from the coast is associated with increased evaporative demand (Vasey et al. 2014, Tayyebi and Jenerette 2016), supporting our urban water deficit hypothesis that the change in LST would be greater in regions with a larger difference between water availability and water demand (Fig. 8). In this context, water availability is the total amount of water available for plants, whether

from irrigation or rain. Water demand refers to the water requirements of plants, and here would be driven by atmospheric aridity and temperature. Within a few kilometers of the coast the maritime environment, which includes cooler, cloudier conditions, appears to have mitigated the increase in temperature associated with drought. The regions furthest inland, in contrast, warmed the most during drought; this was driven by a decrease in vegetative greenness which subsequently decreased vegetative cooling. The loss of greenness was the most important variable to increase temperature during drought, consistent with our finding of the strong relationship between temperature and greenness over multidecadal periods. Although the coast-to-inland gradient for the change in temperature during drought was more pronounced from west to east than from south to north, this likely occurred because the minimal Landsat imagery on the coast for the southern region of the study area was unable to capture the coastal phenomena, which is only present within a few kilometers of the coast. Finally, drought increased vegetative cooling, suggesting that increased aridity increased transpiration (Fig. 10). Contrary to Allen et al. (2021) who observed a decrease in urban cooling capacity during drought, our study found drought to increase vegetative cooling; this discrepancy likely stems from the differing conceptualizations of 'drought' across studies, underlining the necessity to interpret drought effects on urban greenness and temperature in the context of their specific definitions and parameters (Slette et al. 2019). Drought led to consistent decreases in greenness and temperature increases that were able to be explained via potential plantable space and the urban water deficit hypothesis. The resulting spatial

heterogeneity of the dynamics of NDVI and LST appears to have important equity implications.

As a consequence of changes in greenness and heat, our results suggest the luxury effect, an important driver of the spatial heterogeneity of urban greenness and temperature, is becoming weaker through time (Fig. 9) but stronger during drought (Fig. 10). Between 1990-2020 the effect of income on temperature declined 41% while the effect on greenness declined 28%. The decline of the luxury effect through time despite the LAUR's increasing aridity is counter to our hypothesis that the effect of income on mediating temperature and greenness would increase with greater aridity. The non-stationarity of income in its relationship with NDVI and LST underscores the dynamic and complex influence of socioeconomic factors on urban ecological patterns (Romolini et al. 2013, Fan et al. 2019), warranting further investigation into the mechanisms behind this temporal variability. The luxury effect may have declined due to wealthy residents actively reducing greenness as they transitioned to drought-tolerant landscaping. Los Angeles and surrounding communities have been aggressively replacing water-intense landscaping with xeriscaping, a practice known to raise urban temperatures 1.8 °C in arid cities (Dialesandro et al. 2019). In 2014 Los Angeles replaced 9.8 million m^2 of turfgrass (Pincetl et al. 2019), however, affluent residents may have a greater capacity to install drought-tolerant landscaping (Larson and Brumand 2014). During drought between SPEI-01 and SPEI-10 the luxury effect increased for income-LST but not for income-NDVI, partially supporting our hypothesis that higher-income neighborhoods use more water during drought. Income, via the luxury effect, may become more important with

aridity due to the increased demand for water at a higher VPD (Chamberlain et al. 2020). Higher-income neighborhoods have been associated with more water consumption following droughts (Balling et al. 2008, House-Peters et al. 2010), potentially enhancing the luxury effect during drought. This may explain the strengthening of the luxury effect with droughts of increasing duration up to SPEI-11. However, the increase in the importance of income on mediating urban temperature during drought did not always lead to greater cooling overall. The increase in vegetative cooling during droughts from SPEI-2 to SPEI-5 suggests that existing water reserves and irrigation unrestricted by water limitations served to increase cooling under conditions of greater atmospheric aridity. The trend reversed at SPEI-7 and above, suggesting that for droughts longer than half a year, irrigation restrictions as well as depleted soil water reserves were insufficient to meet vegetative transpiration water demands. This likely also explains the inverted relationship of income with LST at SPEI-11, where the luxury effect becomes weaker during drought. However, the increased importance of income in mediating temperature during drought between SPEI-01 and SPEI-10 suggests that wealthy regions are somewhat insulated from increased temperatures during drought. The changing magnitude of the luxury effect highlights how variables that modify urban greenness and temperature are not stable across time. We found these changing relationships were also dissimilar by race.

The decline in the luxury effect across time is primarily driven by a reduction in the correlation between income in White and Hispanic communities. The decline in the luxury effect was at least partially responsible for the increasing marginalization of

Hispanic populations but did not explain the improvement of conditions for White populations. The multidecadal increase in temperature associated with Hispanic census tracts, despite White census tracts being associated with greater cooling through time, points to an increasingly inequitable pattern of urban warming where Hispanic residents are bearing the brunt of rising urban heat compared to historically White areas (Fig. 9). This increasing inequity may be associated with green investment preferentially targeted to wealthy neighborhoods (Locke and Grove 2014, Shokry et al. 2020), whereas green investment in low-income neighborhoods may lead to gentrification and displacement (Anguelovski et al. 2017, Keenan et al. 2018). The disparity in the experience of White and Hispanic populations in their ability to mediate temperature is not reflective of race-based changes in the luxury effect, which proportionally declined a similar amount between White and Hispanic populations (Fig. 11). The different trajectories of how White and Hispanic communities experience greenness and temperature suggests a mediating variable other than income is rising in importance as the effect of income declines. For instance, communities of color are characterized by greater impervious cover (Fossa et al. 2023), which is known to increase urban heat (Tian et al. 2021, Yang et al. 2021). Further, these decoupled trajectories may be explained by increasing urban wealth; although the effect of income is declining, there is more income over time, and there is more income overall in White communities versus Hispanic ones (Flippen 2016). Inequitable urban warming linked to racial and socioeconomic disparities in vegetation has been widely documented and poses dangers to public health (Jesdale et al. 2013, Oudin Åström et al. 2013). Communities of color, independent of income, are

disproportionately exposed to high urban heat (Benz and Burney 2021, Hsu et al. 2021) and their negative health effects on morbidity and mortality (Harlan et al. 2014, James et al. 2016, Son et al. 2016, Murage et al. 2020). The observed decline in the luxury effect reflects a narrowing equity gap as the effect of income converges towards a minimum income effectiveness among all races, leading to risk for people already living in hot/unvegetated neighborhoods. The complex relationship between urban temperatures, race, and income poses challenges for urban land managers striving to improve environmental justice for increasingly marginalized minority populations. Addressing greenspace inequity is a key step towards mitigating the intensifying heat impacts experienced by these communities (Jennings et al. 2019, Kephart 2022).

Conclusion

The world is warming, urban drought is increasing, and the atmosphere is drying, increasing the importance of understanding how urban ecosystems will respond. Our 36-year longitudinal study of the Los Angeles urban region reveals notable racial inequities: Hispanic communities faced disproportionate warming when compared to their White counterparts. Over the whole LA region, average land surface temperature (LST) increased by 0.13°C per annum, while the mean NDVI (Normalized Difference Vegetation Index) increased by 0.0009 each year. Interestingly, we observed an increase in vegetative cooling through time of 0.08 °C/year, suggesting urban vegetation became more effective at cooling. Vegetative cooling is strongly related to income; however, we observed a decline of 28% and 41% in the luxury effect for income-NDVI and income-LST relationships, respectively. As cities like Los Angeles grapple with intensifying heat

and dryness, urban planners and land managers need better resources to forecast how urban ecosystems will respond. However, the non-stationarity observed in NDVI, LST, and vegetative cooling dynamics suggest that past patterns may not reliably predict future dynamics. However, this study wasn't without its limitations. While the spatial granularity of our Landsat satellite data provided valuable insights into broad urban trends, the resolution might not capture finer neighborhood-level nuances. Employing higher-resolution data and integrated modeling could help elucidate these micro-scale patterns and strengthen the links between environmental factors and social dimensions. Future research could bridge these gaps by employing higher-resolution imagery, collecting in-situ demographic data, and using integrated models that utilize climate, hydrology, social aspects, and land use. The observed increasing marginalization of Hispanic communities compared to White communities emphasizes the importance of environmental justice initiatives; the entrenchment of these spatial inequities through time is likely exhibited in other cities. Recognizing the non-stationarity of urban relationships underscores the necessity for continuous re-evaluation in urban ecological research, as the dynamics we currently observe may evolve, challenging our existing understanding and management of urban ecosystems.

References

Abatzoglou, J. T., S. Z. Dobrowski, S. A. Parks, and K. C. Hegewisch. 2018. TerraClimate, a high-resolution global dataset of monthly climate and climatic water balance from 1958-2015. Sci Data **5**:170191.

Allen, M. A., D. A. Roberts, and J. P. McFadden. 2021. Reduced urban green cover and daytime cooling capacity during the 2012–2016 California drought. Urban Climate **36**.

Anguelovski, I., J. J. T. Connolly, L. Masip, and H. Pearsall. 2017. Assessing green gentrification in historically disenfranchised neighborhoods: a longitudinal and spatial analysis of Barcelona. Urban Geography **39**:458-491.

Balling, R. C., P. Gober, and N. Jones. 2008. Sensitivity of residential water consumption to variations in climate: An intraurban analysis of Phoenix, Arizona. Water Resources Research **44**.

Banskota, A., N. Kayastha, M. J. Falkowski, M. A. Wulder, R. E. Froese, and J. C. White. 2014. Forest Monitoring Using Landsat Time Series Data: A Review. Canadian Journal of Remote Sensing **40**:362-384.

Barrera, F. d. l., C. Henriquez, V. Ruiz, and L. Inostroza. 2019. Urban Parks and Social Inequalities in the Access to Ecosystem Services in Santiago, Chile. IOP Conference Series: Materials Science and Engineering **471**.

Benz, S. A., and J. A. Burney. 2021. Widespread Race and Class Disparities in Surface Urban Heat Extremes Across the United States. Earth's Future **9**.

Bijoor, N. S., H. R. McCarthy, D. Zhang, and D. E. Pataki. 2012. Water sources of urban trees in the Los Angeles metropolitan area. Urban Ecosystems **15**:195-214.

Boone, C. G., G. L. Buckley, J. M. Grove, and C. Sister. 2009. Parks and People: An Environmental Justice Inquiry in Baltimore, Maryland. Annals of the Association of American Geographers **99**:767-787.

Borowik, T., N. Pettorelli, L. Sönnichsen, and B. Jędrzejewska. 2013. Normalized difference vegetation index (NDVI) as a predictor of forage availability for ungulates in forest and field habitats. European Journal of Wildlife Research **59**:675-682.

Breger, B. S., T. S. Eisenman, M. E. Kremer, L. A. Roman, D. G. Martin, and J. Rogan. 2019. Urban tree survival and stewardship in a state-managed planting initiative: A case study in Holyoke, Massachusetts. Urban Forestry & Urban Greening **43**.

Broadbent, A. M., A. M. Coutts, N. J. Tapper, and M. Demuzere. 2018. The cooling effect of irrigation on urban microclimate during heatwave conditions. Urban Climate **23**:309-329.

Buyantuyev, A., and J. Wu. 2012. Urbanization diversifies land surface phenology in arid environments: Interactions among vegetation, climatic variation, and land use pattern in the Phoenix metropolitan region, USA. Landscape and Urban Planning **105**:149-159.

Buyantuyev, A., J. Wu, and C. Gries. 2007. Estimating vegetation cover in an urban environment based on Landsat ETM+ imagery: A case study in Phoenix, USA. International Journal of Remote Sensing **28**:269-291.

Carlson, T. N., and D. A. Ripley. 1997. On the relation between NDVI, fractional vegetation cover, and leaf area index. Remote Sensing of Environment **62**:241-252.

Casey, J. A., P. James, L. Cushing, B. M. Jesdale, and R. Morello-Frosch. 2017. Race, Ethnicity, Income Concentration and 10-Year Change in Urban Greenness in the United States. Int J Environ Res Public Health **14**.

Chamberlain, D., C. Reynolds, A. Amar, D. Henry, E. Caprio, P. Batáry, and B. McGill. 2020. Wealth, water and wildlife: Landscape aridity intensifies the urban luxury effect. Global Ecology and Biogeography **29**:1595-1605.

Chen, X., P. Zhao, Y. Hu, L. Ouyang, L. Zhu, and G. Ni. 2019. Canopy transpiration and its cooling effect of three urban tree species in a subtropical city- Guangzhou, China. Urban Forestry & Urban Greening **43**.

Cheng, X., Y. Liu, J. Dong, J. Corcoran, and J. Peng. 2023. Opposite climate impacts on urban green spaces' cooling efficiency around their coverage change thresholds in major African cities. Sustainable Cities and Society **88**.

Clarke, P., J. Morenoff, M. Debbink, E. Golberstein, M. R. Elliott, and P. M. Lantz. 2014. Cumulative exposure to neighborhood context: consequences for health transitions over the adult life course. Res Aging **36**:115-142.

Cook, M., J. Schott, J. Mandel, and N. Raqueno. 2014. Development of an Operational Calibration Methodology for the Landsat Thermal Data Archive and Initial Testing of the Atmospheric Compensation Component of a Land Surface Temperature (LST) Product from the Archive. Remote Sensing **6**:11244-11266.

Corral-Verdugo, V. c., R. B. Bechtel, and B. Fraijo-Sing. 2003. Environmental beliefs and water conservation: An empirical study. Journal of Environmental Psychology **23**:247-257.

Coseo, P., and L. Larsen. 2014. How factors of land use/land cover, building configuration, and adjacent heat sources and sinks explain Urban Heat Islands in Chicago. Landscape and Urban Planning **125**:117-129.

Cunha, A. P. M., R. C. Alvalá, C. A. Nobre, and M. A. Carvalho. 2015. Monitoring vegetative drought dynamics in the Brazilian semiarid region. Agricultural and Forest Meteorology **214-215**:494-505.

Dialesandro, J. M., S. M. Wheeler, and Y. Abunnasr. 2019. Urban heat island behaviors in dryland regions. Environmental Research Communications **1**.

Drake, J. E., M. G. Tjoelker, A. Varhammar, B. E. Medlyn, P. B. Reich, A. Leigh, S. Pfautsch, C. J. Blackman, R. Lopez, M. J. Aspinwall, K. Y. Crous, R. A. Duursma, D. Kumarathunge, M. G. De Kauwe, M. Jiang, A. B. Nicotra, D. T. Tissue, B. Choat, O. K. Atkin, and C. V. M. Barton. 2018. Trees tolerate an extreme heatwave via sustained transpirational cooling and increased leaf thermal tolerance. Glob Chang Biol **24**:2390-2402.

Dronova, I., M. Friedman, I. McRae, F. Kong, and H. Yin. 2018. Spatio-temporal non-uniformity of urban park greenness and thermal characteristics in a semi-arid region. Urban Forestry & Urban Greening **34**:44-54.

Dwyer, J. L., D. P. Roy, B. Sauer, C. B. Jenkerson, H. K. Zhang, and L. Lymburner. 2018. Analysis Ready Data: Enabling Analysis of the Landsat Archive. Remote Sensing **10**.

Eisenman, T. S., T. Flanders, R. W. Harper, R. J. Hauer, and K. Lieberknecht. 2021. Traits of a bloom: a nationwide survey of U.S. urban tree planting initiatives (TPIs). Urban Forestry & Urban Greening **61**.

Elkhrachy, I. 2018. Vertical assessment for SRTM and ASTER Digital Elevation Models: A case study of Najran city, Saudi Arabia. Ain Shams Engineering Journal **9**:1807-1817.

Esau, I., V. V. Miles, R. Davy, M. W. Miles, and A. Kurchatova. 2016. Trends in normalized difference vegetation index (NDVI) associated with urban development in northern West Siberia. Atmospheric Chemistry and Physics **16**:9563-9577.

Fan, C., M. Johnston, L. Darling, L. Scott, and F. H. Liao. 2019. Land use and socio-economic determinants of urban forest structure and diversity. Landscape and Urban Planning **181**:10-21.

Feng, W., H. Lu, T. Yao, and Q. Yu. 2020. Drought characteristics and its elevation dependence in the Qinghai-Tibet plateau during the last half-century. Sci Rep **10**:14323.

Flippen, C. A. 2016. Racial and Ethnic Inequality in Homeownership and Housing Equity. The Sociological Quarterly **42**:121-149.

Fossa, A. J., J. Zelner, R. Bergmans, K. Zivin, and S. D. Adar. 2023. Sociodemographic correlates of greenness within public parks in three U.S. cities. Wellbeing, Space and Society **5**.

Fu., P., and Q. Weng. A time series analysis of urbanization induced land use and land cover change and its impact on land surface temperature with Landsat imagery. Remote Sensing of Environment **175**:205-214.

Gao, K., M. Santamouris, and J. Feng. 2020. On the cooling potential of irrigation to mitigate urban heat island. Sci Total Environ **740**:139754.

Gao, Z., B. F. Zaitchik, Y. Hou, and W. Chen. 2022. Toward park design optimization to mitigate the urban heat Island: Assessment of the cooling effect in five U.S. cities. Sustainable Cities and Society **81**.

Garrison, J. D. 2017. Seeing the park for the trees: New York's "Million Trees" campaign vs. the deep roots of environmental inequality. Environment and Planning B: Urban Analytics and City Science **46**:914-930.

Garrison, J. D. 2018. Environmental Justice in Theory and Practice: Measuring the Equity Outcomes of Los Angeles and New York's "Million Trees" Campaigns. Journal of Planning Education and Research **41**:6-17.

Gillespie, T. W., J. de Goede, L. Aguilar, G. D. Jenerette, G. A. Fricker, M. L. Avolio, S. Pincetl, T. Johnston, L. W. Clarke, and D. E. Pataki. 2016. Predicting tree species richness in urban forests. Urban Ecosystems **20**:839-849.

Gorelick, N., M. Hancher, M. Dixon, S. Ilyushchenko, D. Thau, and R. Moore. 2017. Google Earth Engine: Planetary-scale geospatial analysis for everyone. Remote Sensing of Environment **202**:18-27.

Griffin, D., and K. J. Anchukaitis. 2014. How unusual is the 2012-2014 California drought? Geophysical Research Letters **41**:9017-9023.

Grossiord, C., T. N. Buckley, L. A. Cernusak, K. A. Novick, B. Poulter, R. T. W. Siegwolf, J. S. Sperry, and N. G. McDowell. 2020. Plant responses to rising vapor pressure deficit. New Phytol **226**:1550-1566.

Harlan, S. L., A. J. Brazel, L. Prashad, W. L. Stefanov, and L. Larsen. 2006. Neighborhood microclimates and vulnerability to heat stress. Soc Sci Med **63**:2847-2863.

Harlan, S. L., G. Chowell, S. Yang, D. B. Petitti, E. J. Morales Butler, B. L. Ruddell, and D. M. Ruddell. 2014. Heat-related deaths in hot cities: estimates of human tolerance to high temperature thresholds. Int J Environ Res Public Health **11**:3304-3326.

Harlan, S. L., J. H. Declet-Barreto, W. L. Stefanov, and D. B. Petitti. 2013. Neighborhood effects on heat deaths: social and environmental predictors of vulnerability in Maricopa County, Arizona. Environ Health Perspect **121**:197-204.

Hoffman, J. S., V. Shandas, and N. Pendleton. 2020. The Effects of Historical Housing Policies on Resident Exposure to Intra-Urban Heat: A Study of 108 US Urban Areas. Climate **8**.

House-Peters, L., B. Pratt, and H. Chang. 2010. Effects of urban spatial structure, sociodemographics, and climate on residential water consumption in Hillsboro, Oregon. Journal of the American Water Resources Association **46**:461-472.

Hsu, A., G. Sheriff, T. Chakraborty, and D. Manya. 2021. Disproportionate exposure to urban heat island intensity across major US cities. Nat Commun **12**:2721.

Huang, G., W. Zhou, and M. L. Cadenasso. 2011. Is everyone hot in the city? Spatial pattern of land surface temperatures, land cover and neighborhood socioeconomic characteristics in Baltimore, MD. J Environ Manage **92**:1753-1759.

Huang, S., L. Tang, J. P. Hupy, Y. Wang, and G. Shao. 2020. A commentary review on the use of normalized difference vegetation index (NDVI) in the era of popular remote sensing. Journal of Forestry Research **32**:1-6.

Ibsen, P. C., L. S. Santiago, S. A. Shiflett, M. Chandler, and G. D. Jenerette. 2023. Irrigated urban trees exhibit greater functional trait plasticity compared to natural stands. Biol Lett **19**:20220448.

Imhoff, M. L., P. Zhang, R. E. Wolfe, and L. Bounoua. 2010. Remote sensing of the urban heat island effect across biomes in the continental USA. Remote Sensing of Environment **114**:504-513.

Jamali, F. S., S. Khaledi, and M. T. Razavian. 2021. Seasonal impact of urban parks on land surface temperature (LST) in semi-arid city of Tehran. International Journal of Urban Sustainable Development **13**:248-264.

James, P., J. E. Hart, R. F. Banay, and F. Laden. 2016. Exposure to Greenness and Mortality in a Nationwide Prospective Cohort Study of Women. Environ Health Perspect **124**:1344-1352.

Jenerette, G. D., L. W. Clarke, M. L. Avolio, D. E. Pataki, T. W. Gillespie, S. Pincetl, D. J. Nowak, L. R. Hutyra, M. McHale, J. P. McFadden, and M. Alonzo. 2016. Climate tolerances and trait choices shape continental patterns of urban tree biodiversity. Global Ecology and Biogeography **25**:1367-1376.

Jenerette, G. D., S. L. Harlan, W. L. Stefanov, and C. A. Martin. 2011. Ecosystem services and urban heat riskscape moderation: water, green spaces, and social inequality in Phoenix, USA. Ecological Applications **21**:2637-2651.

Jenerette, G. D., G. Miller, A. Buyantuev, D. E. Pataki, T. W. Gillespie, and S. Pincetl. 2013. Urban vegetation and income segregation in drylands: a synthesis of seven metropolitan regions in the southwestern United States. Environmental Research Letters **8**.

Jennings, V., M. H. E. M. Browning, and A. Rigolon. 2019. Urban Green Space at the Nexus of Environmental Justice and Health Equity. Pages 47-69 Urban Green Spaces.

Jennings, V., C. Johnson Gaither, and R. S. Gragg. 2012. Promoting Environmental Justice Through Urban Green Space Access: A Synopsis. Environmental Justice **5**:1-7.

Jesdale, B. M., R. Morello-Frosch, and L. Cushing. 2013. The racial/ethnic distribution of heat risk-related land cover in relation to residential segregation. Environ Health Perspect **121**:811-817.

Jin, J., S. E. Gergel, Y. Lu, N. C. Coops, and C. Wang. 2019. Asian Cities are Greening While Some North American Cities are Browning: Long-Term Greenspace Patterns in 16 Cities of the Pan-Pacific Region. Ecosystems **23**:383-399.

Jombo, S., E. Adam, M. J. Byrne, and S. W. Newete. 2022. Assessing the intraurban differences in vegetation coverage and surface climate in a heterogeneous area. Transactions of the Royal Society of South Africa **77**:1-10.

Keenan, J. M., T. Hill, and A. Gumber. 2018. Climate gentrification: from theory to empiricism in Miami-Dade County, Florida. Environmental Research Letters **13**.

Kephart, L. 2022. How Racial Residential Segregation Structures Access and Exposure to Greenness and Green Space: A Review. Environmental Justice **15**:204-213.

Kirschbaum, M. U. 2004. Direct and indirect climate change effects on photosynthesis and transpiration. Plant Biol (Stuttg) **6**:242-253.

Konarska, J., J. Uddling, B. Holmer, M. Lutz, F. Lindberg, H. Pleijel, and S. Thorsson. 2016. Transpiration of urban trees and its cooling effect in a high latitude city. Int J Biometeorol **60**:159-172.

Krafft, J., and O. Fryd. 2016. Spatiotemporal patterns of tree canopy cover and socioeconomics in Melbourne. Urban Forestry & Urban Greening **15**:45-52.

Lantz, B. 2013. The large sample size fallacy. Scand J Caring Sci **27**:487-492.

Larson, K. L., and J. Brumand. 2014. Paradoxes in Landscape Management and Water Conservation: Examining Neighborhood Norms and Instititional Forces. Cities and the Environment (CATE) **7**.

Lemoine-Rodriguez, R., L. Inostroza, and H. Zepp. 2022. Does urban climate follow urban form? Analysing intraurban LST trajectories versus urban form trends in 3 cities with different background climates. Sci Total Environ **830**:154570.

Leong, M., R. R. Dunn, and M. D. Trautwein. 2018. Biodiversity and socioeconomics in the city: a review of the luxury effect. Biol Lett **14**.

Li, D., T. Sun, M. Liu, L. Yang, L. Wang, and Z. Gao. 2015. Contrasting responses of urban and rural surface energy budgets to heat waves explain synergies between urban heat islands and heat waves. Environmental Research Letters **10**.

Li, M., J. Yao, J. Guan, and J. Zheng. 2021. Observed changes in vapor pressure deficit suggest a systematic drying of the atmosphere in Xinjiang of China. Atmospheric Research **248**.

Liang, L. L., R. G. Anderson, S. A. Shiflett, and G. D. Jenerette. 2017. Urban outdoor water use and response to drought assessed through mobile energy balance and vegetation greenness measurements. Environmental Research Letters **12**.

Litvak, E., K. F. Manago, T. S. Hogue, and D. E. Pataki. 2017. Evapotranspiration of urban landscapes in Los Angeles, California at the municipal scale. Water Resources Research **53**:4236-4252.

Liu, H., B. Huang, S. Gao, J. Wang, C. Yang, and R. Li. 2021. Impacts of the evolving urban development on intra-urban surface thermal environment: Evidence from 323 Chinese cities. Sci Total Environ **771**:144810.

Liu, Y., J. Peng, and Y. Wang. 2018. Efficiency of landscape metrics characterizing urban land surface temperature. Landscape and Urban Planning **180**:36-53.

Locke, D. H., and J. M. Grove. 2014. Doing the Hard Work Where it's Easiest? Examining the Relationships Between Urban Greening Programs and Social and Ecological Characteristics. Applied Spatial Analysis and Policy **9**:77-96.

Loveland, T. R., and J. L. Dwyer. 2012. Landsat: Building a strong future. Remote Sensing of Environment **122**:22-29.

Manavvi, S., and E. Rajasekar. 2023. Assessing thermal comfort in urban squares in humid subtropical climate: A structural equation modelling approach. Building and Environment **229**.

McCarthy, H. R., and D. E. Pataki. 2010. Drivers of variability in water use of native and non-native urban trees in the greater Los Angeles area. Urban Ecosystems **13**:393-414.

McPhearson, T., M. Feller, A. Felson, R. Karty, and J. W. T. Lu. 2010. Assessing the effects of the urban forest restoration effort of MillionTreesNYC on the structure and functioning of New York City ecosystems. Cities and the Environment (CATE) **3**.

Miller, D. L., M. Alonzo, D. A. Roberts, C. L. Tague, and J. P. McFadden. 2020. Drought response of urban trees and turfgrass using airborne imaging spectroscopy. Remote Sensing of Environment **240**.

Mishra, V., A. K. Ambika, A. Asoka, S. Aadhar, J. Buzan, R. Kumar, and M. Huber. 2020. Moist heat stress extremes in India enhanced by irrigation. Nature Geoscience **13**:722-728.

Morello-Frosch, R., M. Zuk, M. Jerrett, B. Shamasunder, and A. D. Kyle. 2011. Understanding the cumulative impacts of inequalities in environmental health: implications for policy. Health Aff (Millwood) **30**:879-887.

Murage, P., S. Kovats, C. Sarran, J. Taylor, R. McInnes, and S. Hajat. 2020. What individual and neighbourhood-level factors increase the risk of heat-related mortality? A case-crossover study of over 185,000 deaths in London using high-resolution climate datasets. Environ Int **134**:105292.

Oke, T. R., and I. D. Stewart. 2012. Local Climate Zones for Urban Temperature Studies. Bulletin of the American Meteorological Society **93**:1879-1900.

Oudin Åström, D., B. Forsberg, K. L. Ebi, and J. Rocklöv. 2013. Attributing mortality from extreme temperatures to climate change in Stockholm, Sweden. Nature Climate Change **3**:1050-1054.

Pataki, D., H. R. McCarthy, E. Litvak, and S. Pincetl. 2011a. Transpiration of urban forests in the Los Angeles metropolitan area. Ecological Applications **21**:661-677.

Pataki, D. E., C. G. Boone, T. S. Hogue, G. D. Jenerette, J. P. McFadden, and S. Pincetl. 2011b. Socio-ecohydrology and the urban water challenge. Ecohydrology **4**:341-347.

Pettorelli, N., S. Ryan, T. Mueller, N. Bunnefeld, B. Jedrzejewska, M. Lima, and K. Kausrud. 2011. The Normalized Difference Vegetation Index (NDVI): unforeseen successes in animal ecology. Climate Research **46**:15-27.

Pincetl, S., T. W. Gillespie, D. E. Pataki, E. Porse, S. Jia, E. Kidera, N. Nobles, J. Rodriguez, and D.-a. Choi. 2019. Evaluating the effects of turf-replacement programs in Los Angeles. Landscape and Urban Planning **185**:210-221.

Polydoros, A., T. Mavrakou, and C. Cartalis. 2018. Quantifying the Trends in Land Surface Temperature and Surface Urban Heat Island Intensity in Mediterranean Cities in View of Smart Urbanization. Urban Science **2**.

Purio, M. A., T. Yoshitake, and M. Cho. 2022. Assessment of Intra-Urban Heat Island in a Densely Populated City Using Remote Sensing: A Case Study for Manila City. Remote Sensing **14**.

Qi, Y., H. Li, Z. Pang, W. Gao, and C. Liu. 2022. A Case Study of the Relationship Between Vegetation Coverage and Urban Heat Island in a Coastal City by Applying Digital Twins. Front Plant Sci **13**:861768.

Qiu, G.-y., H.-y. Li, Q.-t. Zhang, W. Chen, X.-j. Liang, and X.-z. Li. 2013. Effects of Evapotranspiration on Mitigation of Urban Temperature by Vegetation and Urban Agriculture. Journal of Integrative Agriculture **12**:1307-1315.

Quesnel, K. J., N. Ajami, and A. Marx. 2019. Shifting landscapes: decoupled urban irrigation and greenness patterns during severe drought. Environmental Research Letters **14**.

Reid, C. E., M. S. O'Neill, C. J. Gronlund, S. J. Brines, D. G. Brown, A. V. Diez-Roux, and J. Schwartz. 2009. Mapping community determinants of heat vulnerability. Environ Health Perspect **117**:1730-1736.

Ren, T., W. Zhou, and J. Wang. 2021. Beyond intensity of urban heat island effect: A continental scale analysis on land surface temperature in major Chinese cities. Sci Total Environ **791**:148334.

Romolini, M., J. M. Grove, and D. H. Locke. 2013. Assessing and comparing relationships between urban environmental stewardship networks and land cover in Baltimore and Seattle. Landscape and Urban Planning **120**:190-207.

Schwarz, K., M. Fragkias, C. G. Boone, W. Zhou, M. McHale, J. M. Grove, J. O'Neil-Dunne, J. P. McFadden, G. L. Buckley, D. Childers, L. Ogden, S. Pincetl, D. Pataki, A. Whitmer, and M. L. Cadenasso. 2015. Trees grow on money: urban tree canopy cover and environmental justice. PLoS One **10**:e0122051.

Shahfahad, A. A. Bindajam, M. W. Naikoo, J. P. Horo, J. Mallick, M. Rihan, M. D. Malcoti, S. Talukdar, R. Rahman, and A. Rahman. 2023. Response of soil moisture and vegetation conditions in seasonal variation of land surface temperature and surface urban heat island intensity in sub-tropical semi-arid cities. Theoretical and Applied Climatology **153**:367-395.

Shih, W.-Y. 2022. Socio-ecological inequality in heat: The role of green infrastructure in a subtropical city context. Landscape and Urban Planning **226**.

Shokry, G., J. J. T. Connolly, and I. Anguelovski. 2020. Understanding climate gentrification and shifting landscapes of protection and vulnerability in green resilient Philadelphia. Urban Climate **31**.

Siddiqui, A., G. Kushwaha, B. Nikam, S. K. Srivastav, A. Shelar, and P. Kumar. 2021. Analysing the day/night seasonal and annual changes and trends in land surface temperature and surface urban heat island intensity (SUHII) for Indian cities. Sustainable Cities and Society **75**.

Slette, I. J., A. K. Post, M. Awad, T. Even, A. Punzalan, S. Williams, M. D. Smith, and A. K. Knapp. 2019. How ecologists define drought, and why we should do better. Glob Chang Biol **25**:3193-3200.

Son, J. Y., K. J. Lane, J. T. Lee, and M. L. Bell. 2016. Urban vegetation and heat-related mortality in Seoul, Korea. Environ Res **151**:728-733.

Tayyebi, A., and G. D. Jenerette. 2016. Increases in the climate change adaption effectiveness and availability of vegetation across a coastal to desert climate gradient in metropolitan Los Angeles, CA, USA. Sci Total Environ **548-549**:60-71.

Tian, P., J. Li, L. Cao, R. Pu, Z. Wang, H. Zhang, H. Chen, and H. Gong. 2021. Assessing spatiotemporal characteristics of urban heat islands from the perspective of an urban expansion and green infrastructure. Sustainable Cities and Society **74**.

USGS, U. S. G. S. 2021a. Landsat 4-7 Collection 2 (C2) Level 2 Science Product (L2SP) Guide. LSDS-1618, Sioux Falls, South Dakota.

USGS, U. S. G. S. 2021b. Landsat 8-9 Calibration and Validation (Cal/Val) Algorithm Description Document (ADD). LSDS-1747, Sioux Falls, South Dakota.

Vahmani, P., and T. S. Hogue. 2015. Urban irrigation effects on WRF-UCM summertime forecast skill over the Los Angeles metropolitan area. Journal of Geophysical Research: Atmospheres **120**:9869-9881.

Varquez, A. C. G., and M. Kanda. 2018. Global urban climatology: a meta-analysis of air temperature trends (1960–2009). npj Climate and Atmospheric Science **1**.

Vasey, M. C., V. T. Parker, K. D. Holl, M. E. Loik, and S. Hiatt. 2014. Maritime climate influence on chaparral composition and diversity in the coast range of central California. Ecol Evol **4**:3662-3674.

Venter, Z. S., C. M. Shackleton, F. Van Staden, O. Selomane, and V. A. Masterson. 2020. Green Apartheid: Urban green infrastructure remains unequally distributed across income and race geographies in South Africa. Landscape and Urban Planning **203**.

Vicente-Serrano, S. M., S. Beguería, and J. I. López-Moreno. 2010. A Multiscalar Drought Index Sensitive to Global Warming: The Standardized Precipitation Evapotranspiration Index. Journal of Climate **23**:1696-1718.

Voogt, J. A., and T. R. Oke. 2003. Thermal remote sensing of urban climates. Remote Sensing of Environment **86**:370-384.

Wan, Z., P. Wang, and X. Li. 2004. Using MODIS Land Surface Temperature and Normalized Difference Vegetation Index products for monitoring drought in the southern Great Plains, USA. International Journal of Remote Sensing **25**:61-72.

Watkins, S. L., and E. Gerrish. 2018. The relationship between urban forests and race: A meta-analysis. J Environ Manage **209**:152-168.

Wetherley, E. B., J. P. McFadden, and D. A. Roberts. 2018. Megacity-scale analysis of urban vegetation temperatures. Remote Sensing of Environment **213**:18-33.

Whitley, R., D. Taylor, C. Macinnis-Ng, M. Zeppel, I. Yunusa, A. O'Grady, R. Froend, B. Medlyn, and D. Eamus. 2013. Developing an empirical model of canopy water flux describing the common response of transpiration to solar radiation and VPD across five contrasting woodlands and forests. Hydrological Processes **27**:1133-1146.

Winbourne, J. B., T. S. Jones, S. M. Garvey, J. L. Harrison, L. Wang, D. Li, P. H. Templer, and L. R. Hutyra. 2020. Tree Transpiration and Urban Temperatures: Current Understanding, Implications, and Future Research Directions. BioScience **70**:576-588.

Wong, D. W., and M. Sun. 2013. Handling Data Quality Information of Survey Data in GIS: A Case of Using the American Community Survey Data. Spatial Demography **1**:3-16.

Wu, W., L. Li, and C. Li. 2021. Seasonal variation in the effects of urban environmental factors on land surface temperature in a winter city. Journal of Cleaner Production **299**.

Yang, Q., X. Huang, J. Yang, and Y. Liu. 2021. The relationship between land surface temperature and artificial impervious surface fraction in 682 global cities: spatiotemporal variations and drivers. Environmental Research Letters **16**.

Yin, Y., L. He, P. O. Wennberg, and C. Frankenberg. 2023. Unequal exposure to heatwaves in Los Angeles: Impact of uneven green spaces. Science Advances **9**.

Yuan, F., and M. E. Bauer. 2007. Comparison of impervious surface area and normalized difference vegetation index as indicators of surface urban heat island effects in Landsat imagery. Remote Sensing of Environment **106**:375-386.

Zhao, D., Q. Lei, Y. Shi, M. Wang, S. Chen, K. Shah, and W. Ji. 2020. Role of Species and Planting Configuration on Transpiration and Microclimate for Urban Trees. Forests **11**.

Zhao, S., D. Cong, K. He, H. Yang, and Z. Qin. 2017. Spatial-Temporal Variation of Drought in China from 1982 to 2010 Based on a modified Temperature Vegetation Drought Index (mTVDI). Sci Rep **7**:17473.

Zhou, W., G. Huang, and M. L. Cadenasso. 2011. Does spatial configuration matter? Understanding the effects of land cover pattern on land surface temperature in urban landscapes. Landscape and Urban Planning **102**:54-63.

Zhu, Z. 2019. Science of Landsat Analysis Ready Data. Remote Sensing **11**.

Zipper, S. C., J. Schatz, C. J. Kucharik, and S. P. Loheide. 2017. Urban heat island-induced increases in evapotranspirative demand. Geophysical Research Letters **44**:873-881.

Ziter, C. D., E. J. Pedersen, C. J. Kucharik, and M. G. Turner. 2019. Scale-dependent interactions between tree canopy cover and impervious surfaces reduce daytime urban heat during summer. Proc Natl Acad Sci U S A **116**:7575-7580.

Tables and Figures

Table 1.1 Descriptive characteristics of all datasets used in the study. Census datasets are from 2010 for reference, but census data from 1990, 2000, 2010, and 2020 were utilized.

Dataset	Data Utilized	Provider	Spatial Resolution	Temporal Resolution
Landsat Analysis Ready Data	NDVI and LST	USGS Earth Explorer	30-120m^2	8-16 days
TerraClimate	All Weather Variables	University of California, Merced	1/24th degree (~4km)	Monthly
Shuttle Radar Topography Mission (SRTM)	Elevation	NASA/USGS/JPL-Caltech	1 arc second (~30m^2) with <7m vertical accuracy	
SPEIbase	Standardized Precipitation Evapotranspiration Index	Global SPEI Database v2.7	0.5° (~46 km for LAUR)	Monthly
National Landcover Data Base	Tree Cover, Impervious Cover	Multi-Resolution Land Characteristics consortium	30m^2	Decadal
P1, P9 (2010)	Demographic variables of race and population	United States Census Bureau	Census Tract	Decadal
S1901, S1903, S1501, B19301 (2010)	Social Variables of income and education	United States Census Bureau	Census Tract	Decadal
TIGER/Line® Shapefiles	Census Tract Boundaries	United States Census Bureau	Census Tract	

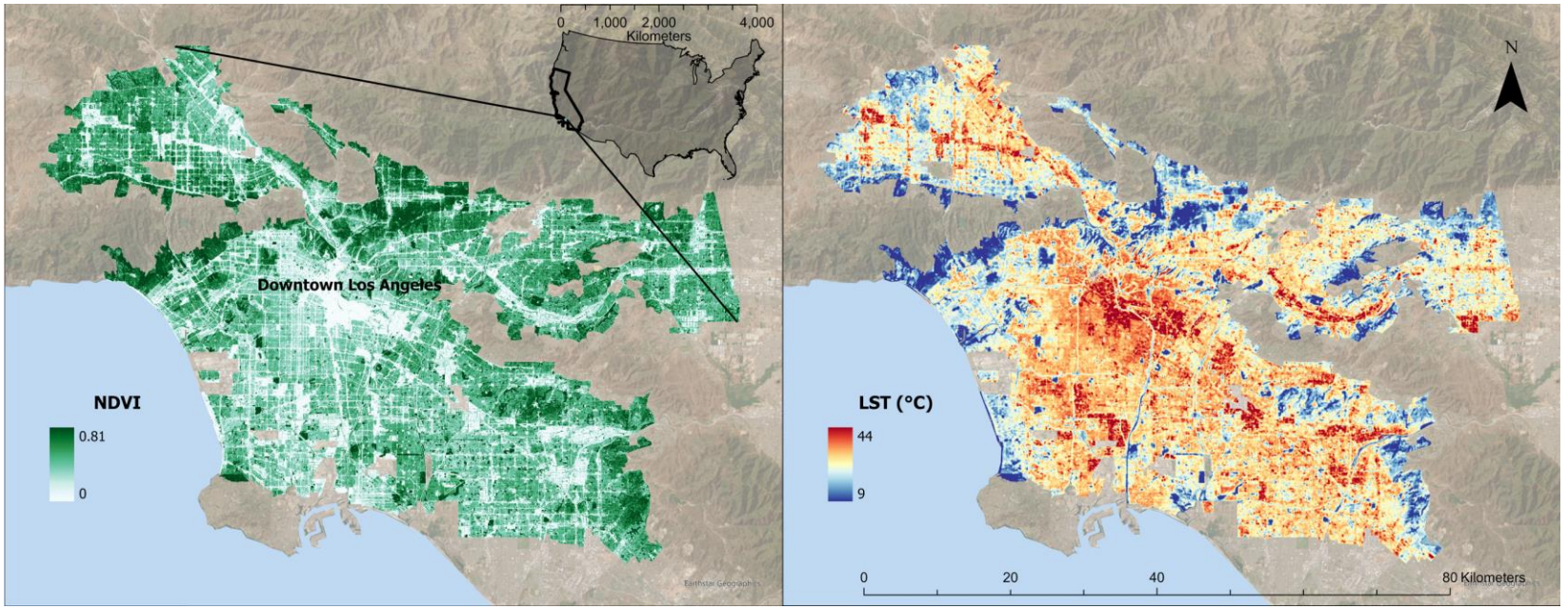

Figure 1.1 The study area encompassed the Greater Los Angeles, California urban region (LAUR). Using a long-term mean of Landsat imagery from 1985-2021, the hottest regions were those that had the lowest plant greenness.

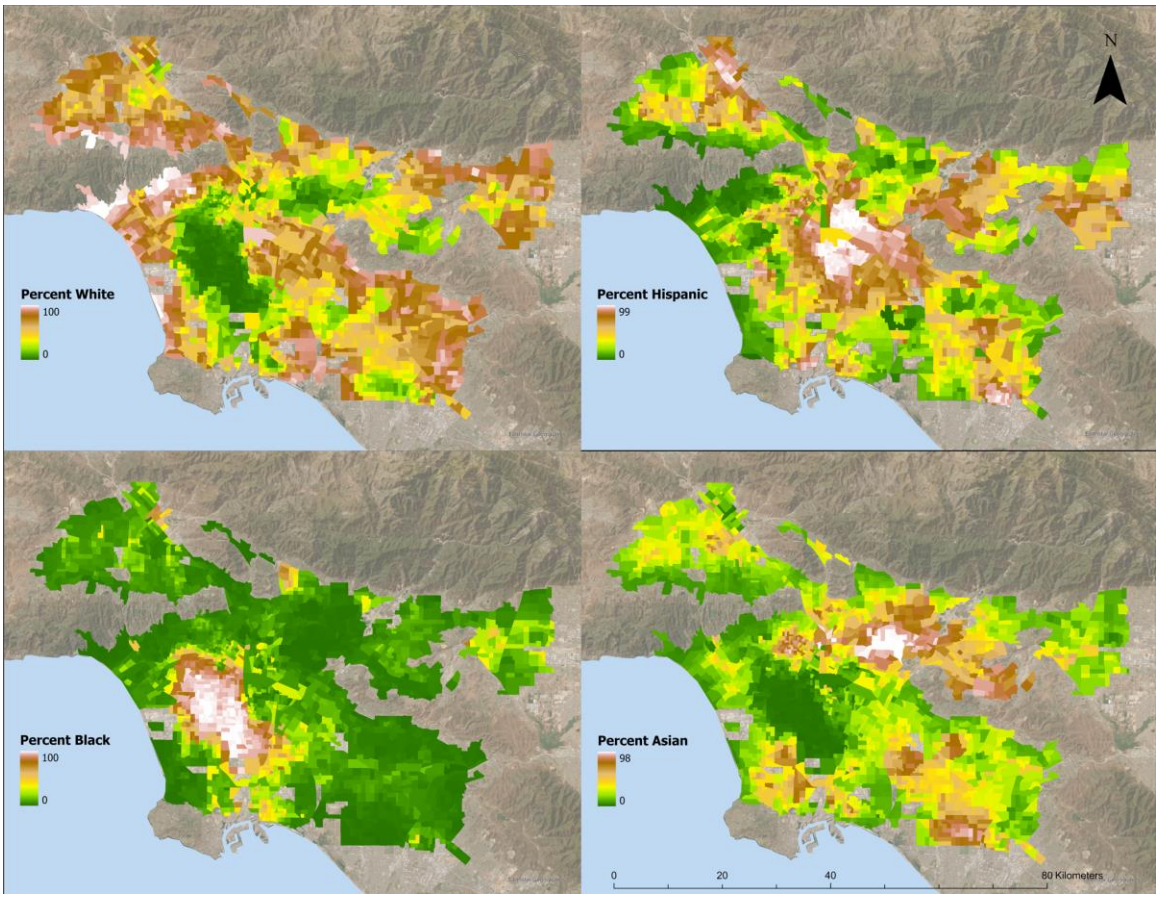

Figure 1.2 The census tract distribution by race is heterogeneous, with per-race agglomerations. White communities are most common along the foothills, Hispanic communities are predominantly found around downtown Los Angeles, Black communities are west of downtown L.A., and Asian communities are found north of downtown near the city of Industry. Data are based on the 2010 census.

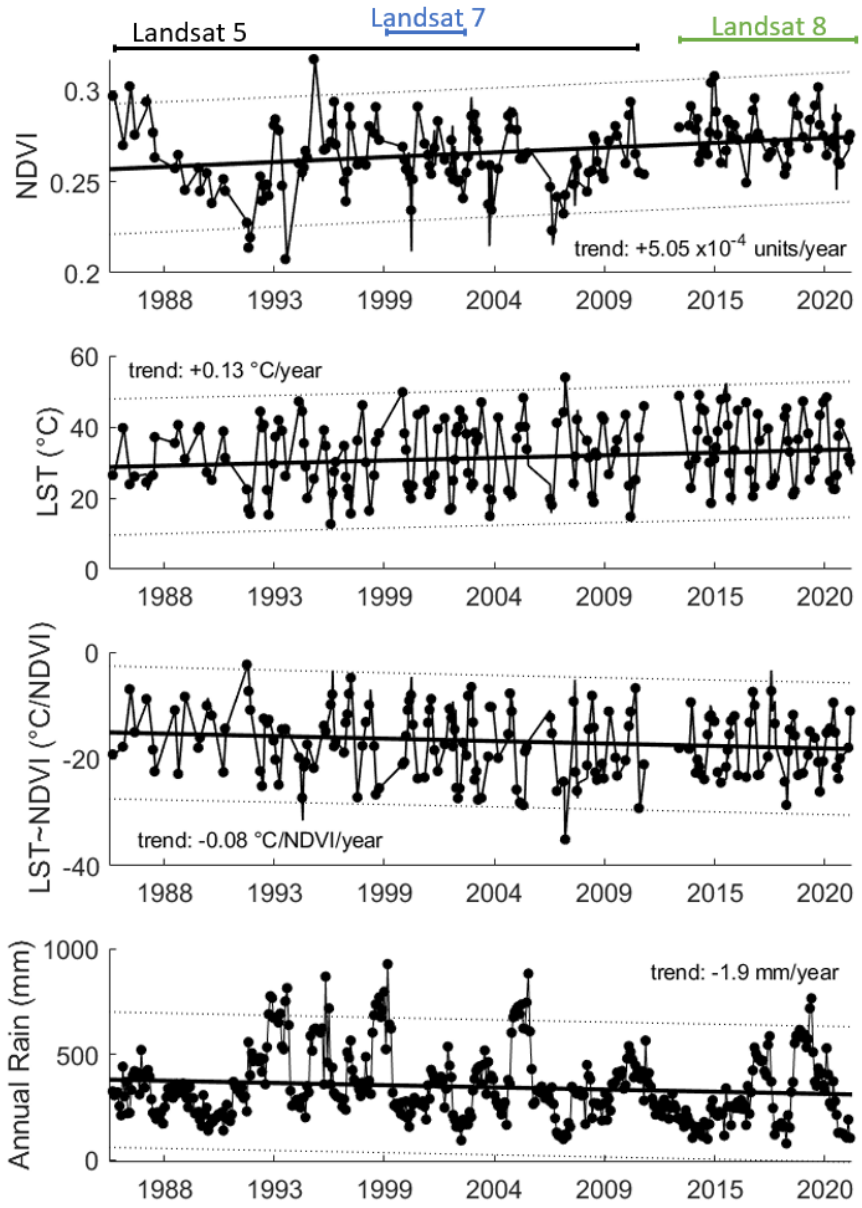

Figure 1.3 Between 1985 and 2021 the LST-NDVI slope became significantly more negative, reflecting vegetation that is becoming more efficient at cooling, while urban greenness and temperature both significantly increased through time. A gap in data between December 2011 and March 2013 reflects the period between the end of Landsat 5 and the launch of Landsat 8; Landsat 7 was not used during this period due to the failure of the scan line corrector. These changing NDVI and LST dynamics occurred in the context of increasing aridity, with annual rainfall declining 1.9 mm/year.

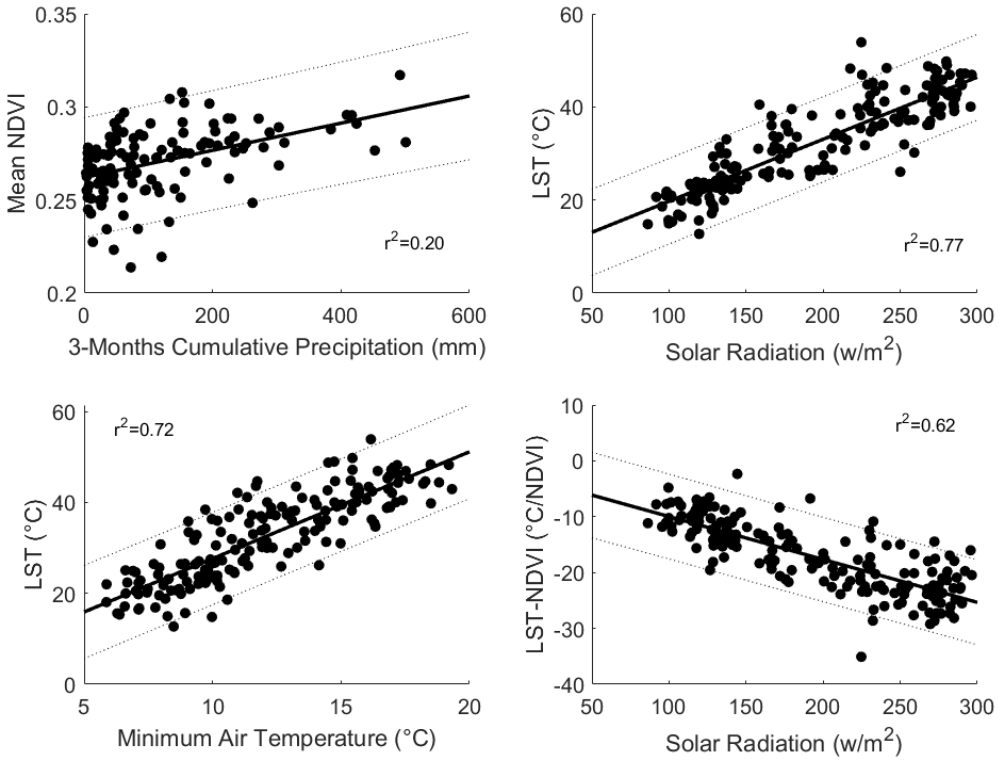

Figure 1.4 Urban NDVI, LST, and vegetative cooling responded to changes in the weather; each dot represents a mean monthly value. Despite the LAUR being heavily irrigated, NDVI was still coupled with precipitation with this relationship strongest at a 3-month lag. Solar radiation and air temperature jointly explained 87% of the temporal variability in LST, while vegetative cooling increased with solar radiation.

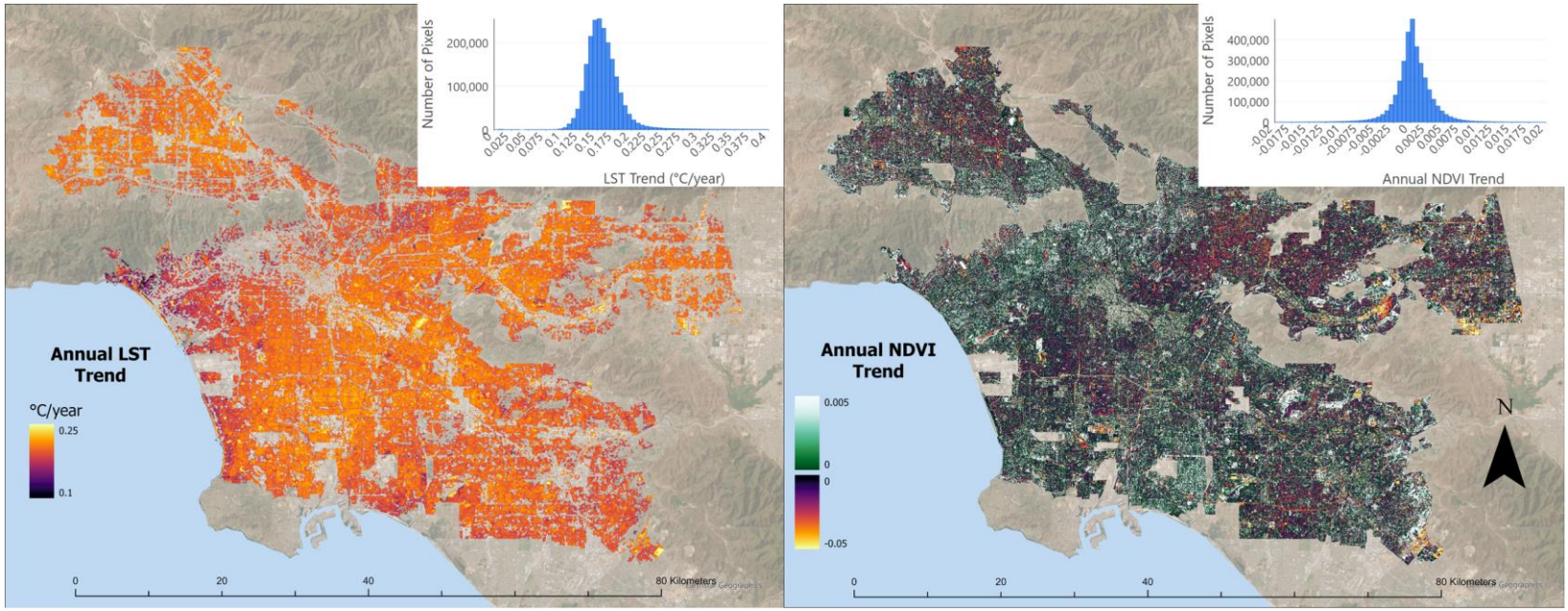

Figure 1.5 Between 1985 and 2021 the LAUR warmed everywhere but unevenly; no pixel got significantly cooler. Some regions (in orange and yellow) warmed much faster than the 0.16 °C/year per-pixel average. The only region in the lowest tier of cooling (≤0.1 °C/year) was along the coast. The regions that got the hottest through time were also spatially related to regions that lost the most greenness. Missing pixels represent regions where the temporal regression was not significant ($p \geq 0.05$).

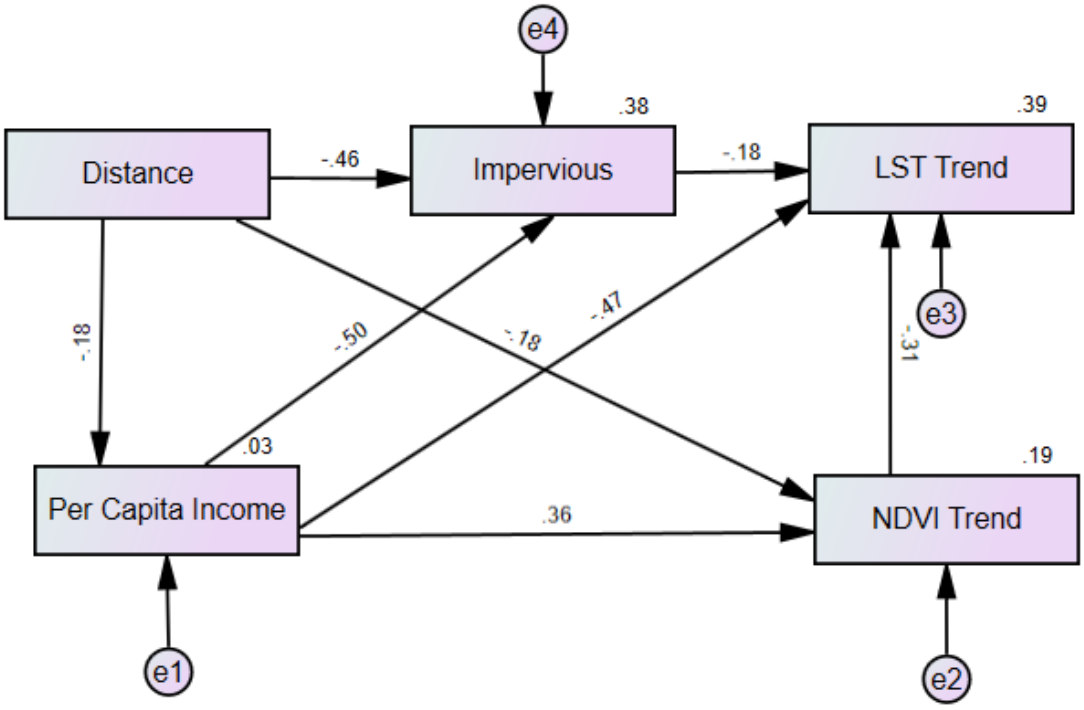

Figure 1.6 The change through time of temperature and greenness was best explained by variability in income, as well as in impervious cover and distance from the coast. The wealthiest urban regions saw the slowest rate of warming as well as the greatest increase in greenness. The increase in temperature also increased the slowest in census tracts that saw the most greening.

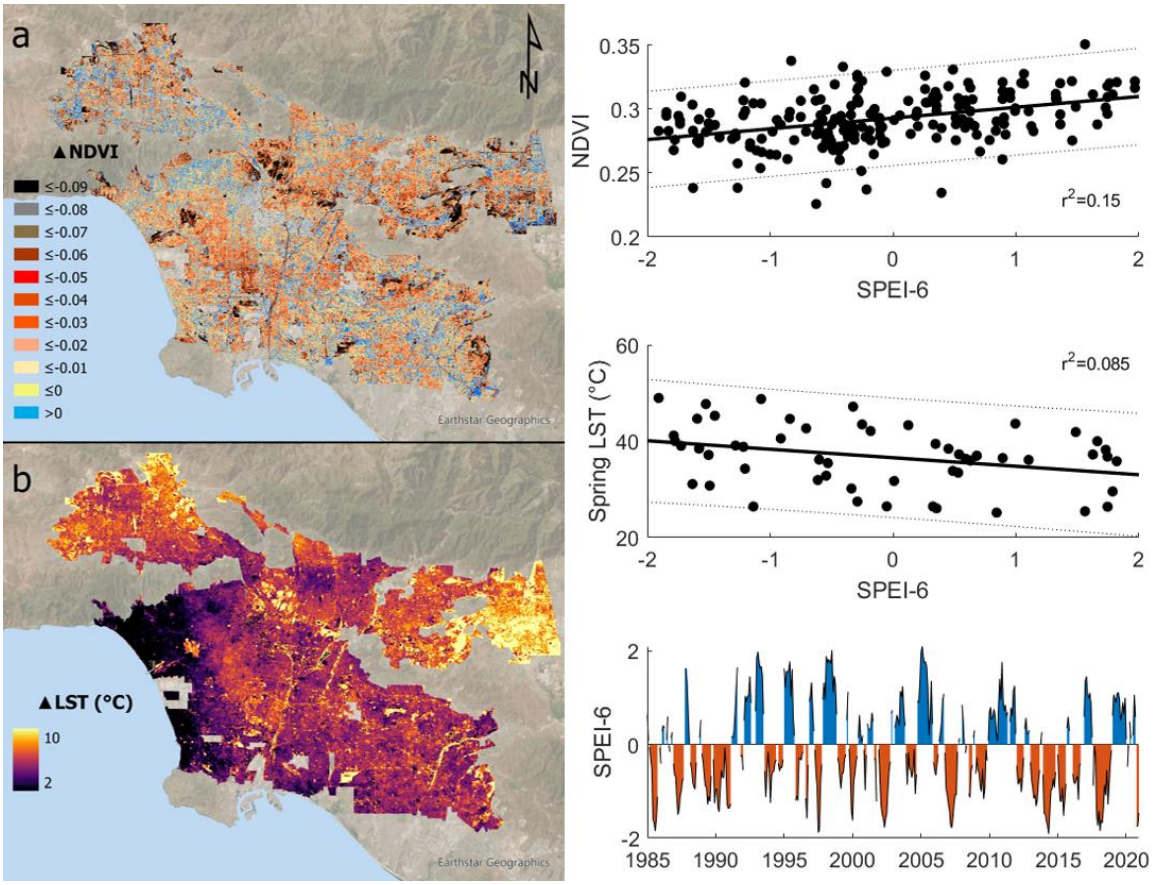

Figure 1.7 During drought NDVI and LST exhibited overall trends but also wide spatial variation in their response. When comparing wet versus dry periods at SPEI-6, NDVI decreased on average 0.023, and LST increased on average 4.41 °C. The NDVI response was more spatially heterogeneous, while the LST response exhibited a clear coastal to inland gradient. When regressing all days in the time series against SPEI-6, only NDVI had a significant relationship, increasing by 0.004 with every 0.5 unit increase in SPEI-6. In contrast, the relationship between LST and SPEI-6 was seasonally dependent, with the greatest declines in LST in response to a positive water balance occurring in the spring.

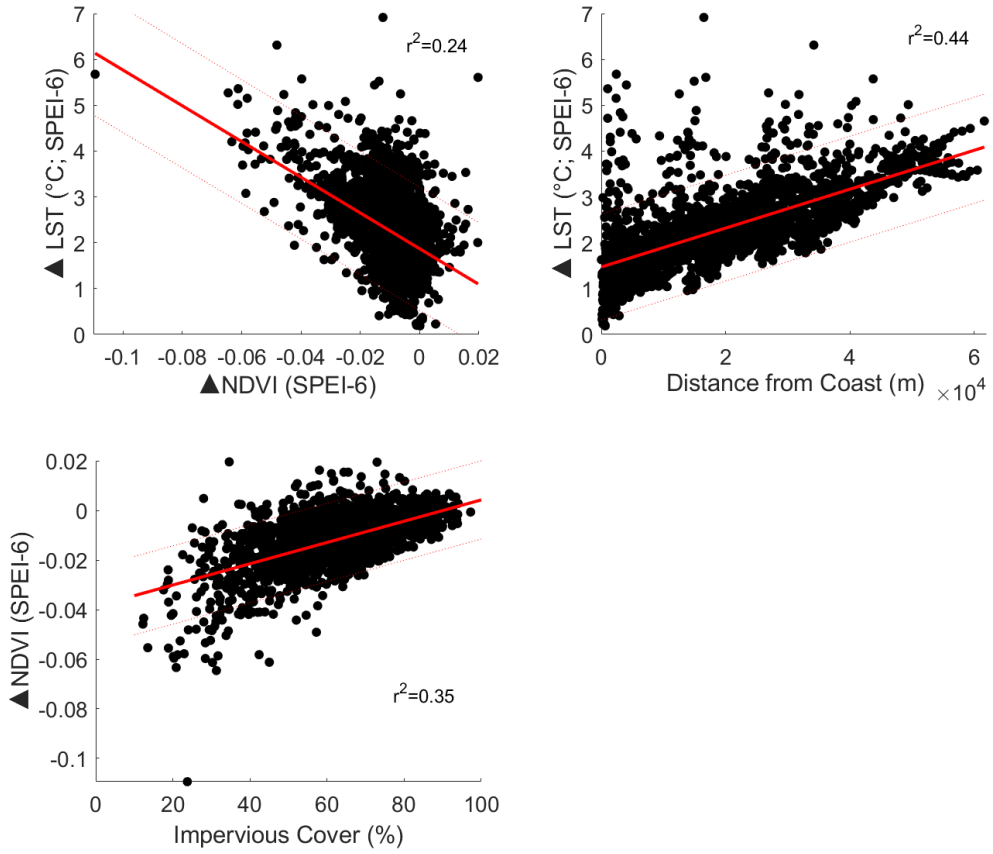

Figure 1.8 During drought, LST increased the most in census tracts which lost the most NDVI and which were furthest inland from the coast. From multiple regression, these two variables explained 61% of the variability in the LST drought response. Impervious cover was the only variable identified from multiple regression to modify the NDVI drought response. Greater impervious cover was associated with less change in NDVI during drought, where each point represents one census tract.

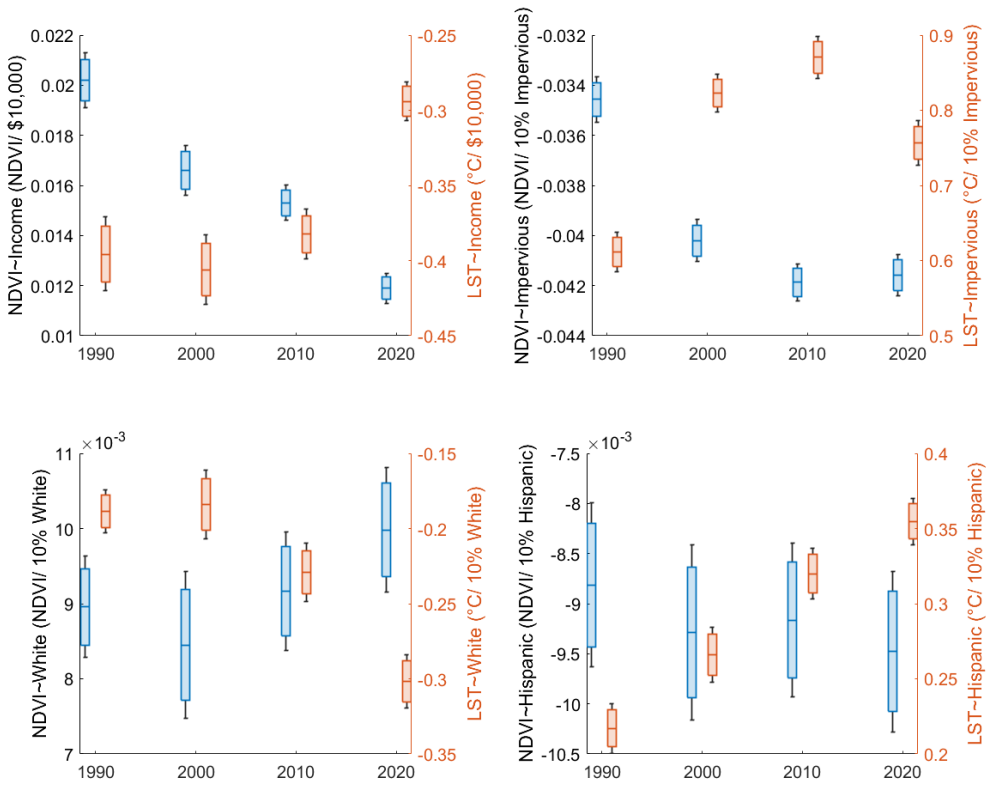

Figure 1.9 Between 1990 and 2020 the effect of income on increasing greenness and decreasing temperatures significantly declined. As the LAUR has gotten hotter the luxury effect has gotten weaker. In 1990 $10,000 of income led to a 0.4 °C decrease in LST, whereas in 2020 the same increase in income led to a 0.29 °C decrease. In conjunction with the weakening of the luxury effect, the effect of impervious cover on decreasing greenness and increasing temperatures increased through time. These differences were race specific. Despite the weakening effect of income, Hispanic communities experienced greater heat through time while White communities did not. Blue boxplots refer to the left y-axis, representing the relationship between NDVI and either income, impervious cover, percent White population, or percent Hispanic population. Orange boxplots refer to the right y-axis and represent the relationship between LST and the same variables.

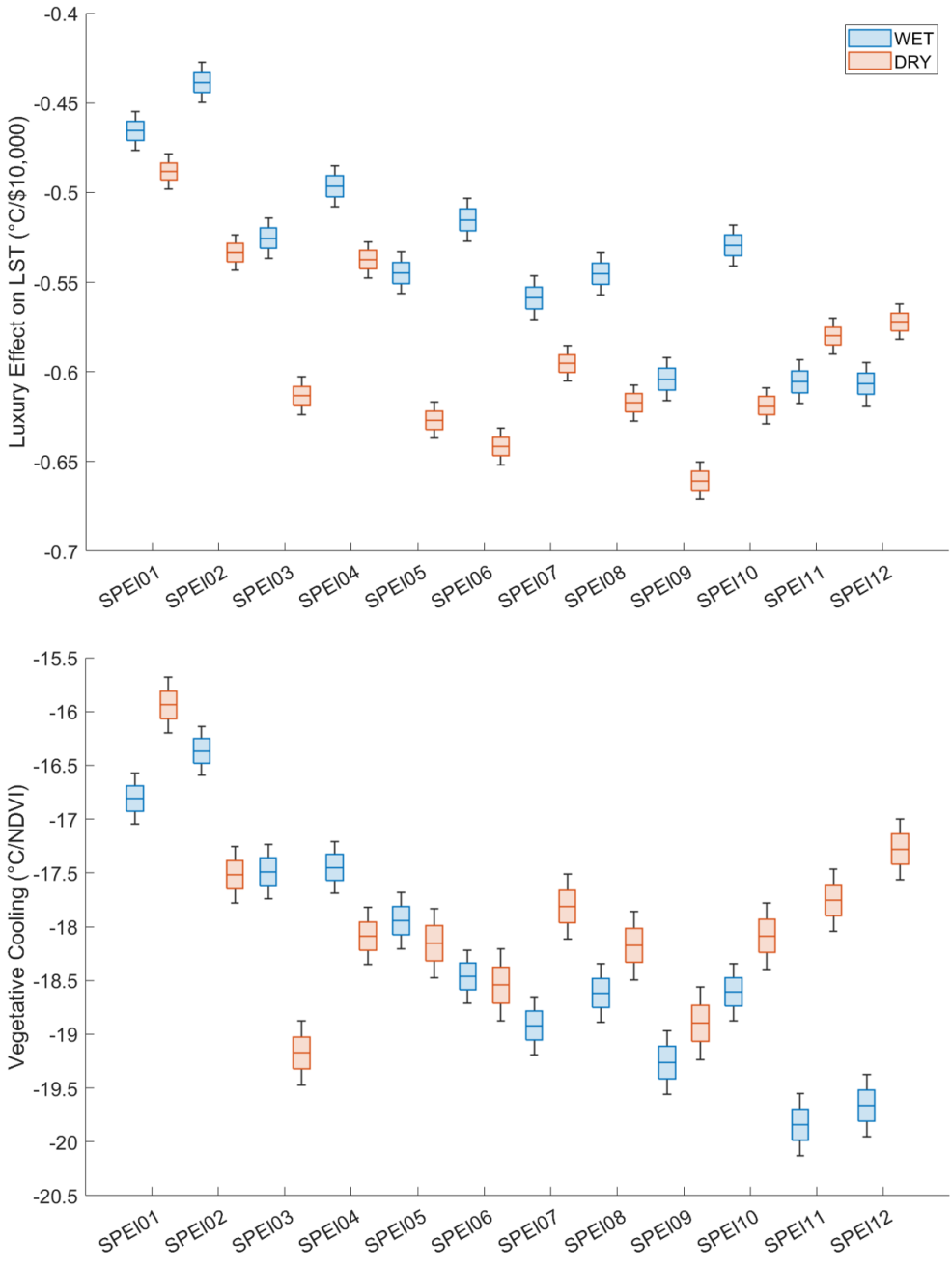

Figure 1.10 At most intra-annual SPEI aggregations the effect of income on LST becomes stronger. Only at SPEI-11 and at SPEI-12 does the luxury effect on temperature become weaker during drought. This increase in the luxury effect is not necessarily reflected in increased vegetative cooling; drought may slightly increase vegetative cooling for sub-6-month SPEI aggregations, but from SPEI-7 and up vegetative cooling declines during drought.

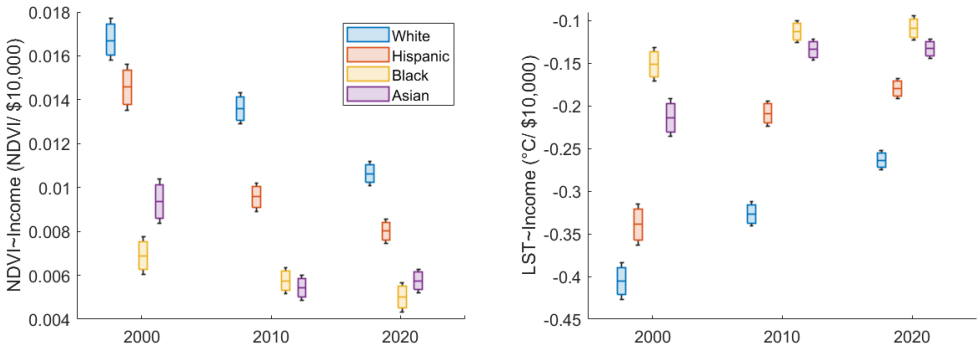

Figure 1.11 The decrease in the luxury effect was primarily due to a reduction in the relationships between income and both LST and NDVI in white communities, with similar declines in Hispanic and Asian communities. The influence of income was not uniform across races. As per the 2000 census data, the same amount of income in white communities led to 2.68 times as much cooling and 2.42 times as much greening compared to Asian and black communities. Over time, the impact of income on cooling and greening has become more equitable across races due to city-wide declines in the effectiveness of income.

Supplementary Figures

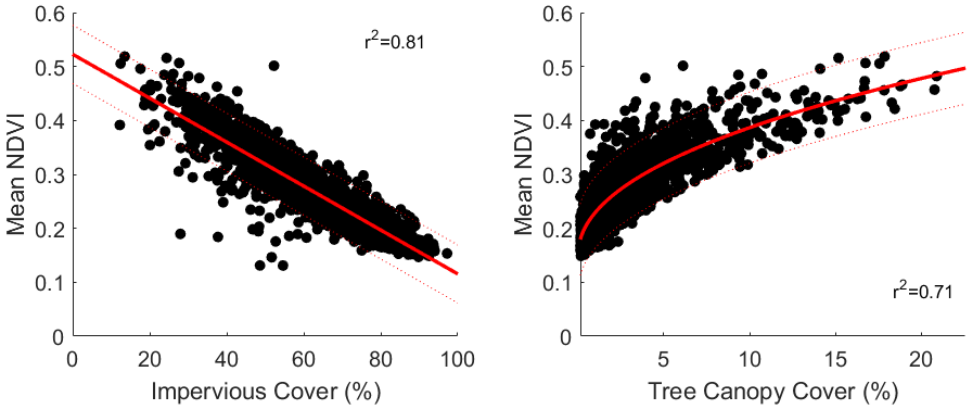

Figure 1.S1 Between 1985 and 2021, mean urban NDVI increased in census tracts with the highest tree canopy cover and decreased in census tracts with high impervious cover. From multiple regression, these two variables explained 87% of the spatial variability of NDVI in the LAUR.

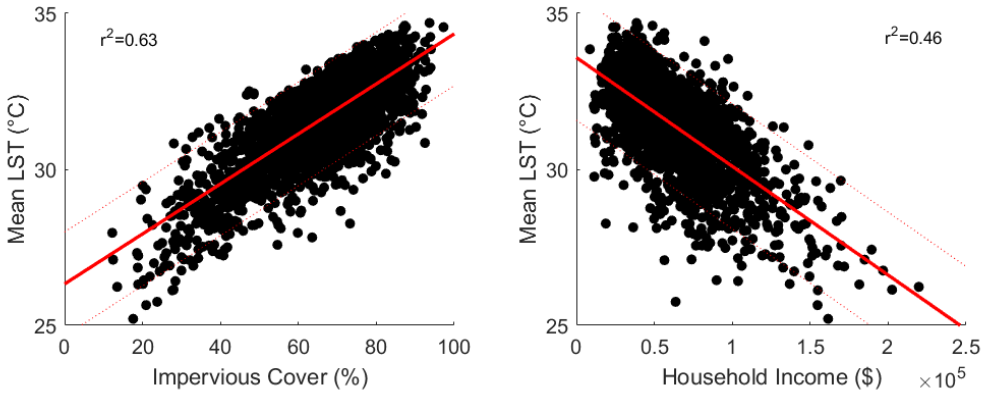

Figure 1.S2 Between 1985 and 2021, mean urban LST increased in response to impervious cover and decreased in response to income. These two variables explained 69% of the spatial variability of LST in the LAUR.

Chapter 2

The Changing Effect of Urbanization on Greenness and Temperature at a Continental, Multidecadal Scale Has Implications for Environmental Equity

Abstract

Urbanization profoundly reshapes the interconnected dynamics of vegetation greenness, land surface temperature, and their relationship, termed vegetative cooling; using satellite imagery we can quantify urbanization's continental-scale impacts on these biophysical dynamics. However, there are large uncertainties in how the effect of urbanization alters these dynamics from a non-urban reference. Using a subset of 52 cities from across the conterminous United States we assessed the spatial and temporal dynamics of urban greenness, temperature, and vegetative cooling and in how urbanization alters these relationships. Using satellite imagery coupled with landcover, climate, and census records between 2000 and 2022, we hypothesize that precipitation, by greening and cooling the local environment, drives inter-urban variability in urban biophysical dynamics, as well as differences between urban and nearby non-urban ecosystems. Our results show that, at the continental scale, urban temperatures increased 0.16 °C/year, while NDVI and vegetative cooling had variable trends. These changing dynamics led to an average reduction in the effect of income as a mediator of temperature and greenness by 53% and 62% across all cities between 2000 and 2020. Water availability from precipitation drives inter-urban variability in biophysical dynamics, whose change through time has led to a significant continental-scale decline in the luxury effect.

Introduction

Urbanization significantly influences the landscape distributions and dynamics of vegetation and climate. It typically increases temperature through the urban heat island (UHI) effect (Yang et al. 2016) and reduces greenness (Yang et al. 2020, Cheng et al. 2023b), while also altering the greenness-temperature relationship in a context-dependent manner (Zhao et al. 2014, Yu et al. 2018). However, there are notable exceptions, such as the oasis effect where some urban areas may be cooler than their surroundings (Potchter et al. 2008, Fan et al. 2017, Zhao et al. 2017). On a continental scale, urbanization has been shown to homogenize environmental conditions (Kühn and Klotz 2006, McKinney 2006, Gong et al. 2013, Groffman et al. 2014, Polsky et al. 2014, Pearse et al. 2018) but this variation has primarily been studied through limited city comparisons over short timeframes. Over multidecadal periods, changing urban landcover, socio-demographics, and climate suggest evolving dynamics in greenness and temperature due to urbanization. These changes are linked to demographic distributions, as human activity can modify vegetation distribution and consequently, neighborhood climate conditions. Within cities, studies have consistently found hotter neighborhoods with lower vegetation, typically inhabited by lower-income and non-white residents (Harlan et al. 2006, Jesdale et al. 2013, Casey et al. 2017). However, these patterns vary geographically and temporally. Therefore, understanding the variation in the interplay of urban vegetation, climate, and demographics is crucial for advancing urban ecosystem theories and developing climate adaptation tools amidst global warming. Thus, the intra-city distribution of greenness and temperature is likely dissimilar among cities, the inter-urban relationship between

greenness and temperature are likely changing through time, yet large uncertainties remain as to the effect of urbanization on these dynamics (Estoque et al. 2017, Zhang et al. 2017, Guo et al. 2022, Liu et al. 2022).

In characterizing how urbanization affects vegetation and climate distributions, the role of water balance may be a useful starting point. In non-urban ecosystems, sensitivity of greenness to precipitation declines with increasing mean annual precipitation (MAP) in non-limited environments due in part to soil saturation (Huxman et al. 2004, Chamaillé-Jammes and Fritz 2009). Urbanization, via land cover modifications and irrigation, may decouple greenness and temperature from precipitation, particularly in response to increasing aridity due to a greater reliance on irrigation for plant water demands (Buyantuyev and Wu 2012, Jenerette et al. 2013, Lazzarini et al. 2015). Importantly, vegetation is known to decrease surface temperatures due to an increase in evaporative cooling (Trenberth and Shea 2005, Zhu et al. 2023).

Within cities, the relationships among vegetation, temperature, and demographics also vary at continental scales and are likely changing. Increased temperatures and aridity may also strengthen the interaction between greenness and temperature (Ibsen et al. 2021), commonly characterized as the slope between greenness and temperature, or vegetative cooling. Further, as aridity is increasing globally (Chai et al. 2021) in the context of a warming planet. These trends suggest that the effect of urbanization will increase in arid cities, which are becoming more arid, but will decrease in cold cities, which are becoming warmer, and that precipitation, which modifies aridity, will mediate the effect of urbanization. Variables associated with irrigation, such as income (Reyes-

Paecke et al. 2019), or which may alter the distribution of plants such as race (Das and Ramaswami 2022) may further alter distributions of greenness and temperature. We propose an inter-urban water deficit hypothesis, where urban biophysical dynamics, and the difference in those dynamics between a city and its non-urban reference, are predicated on the availability of and demand of water for plants.

Income and race are well-known to moderate intra-urban greenness and temperature, with the luxury effect—the ability for median household income to increase urban greenness and decrease temperature—playing a significant role in urban dynamics (Hope et al. 2003, Grove et al. 2014, Threlfall et al. 2022). For instance, the distribution of the urban forest exhibits income-dependence (Schwarz et al. 2015). However, the effect of income on moderating greenness is highly variable; in China, the decoupling of urban greenness from urban wealth was partially related to precipitation (Cheng et al. 2023a), while extreme aridity decouples urban greenness from precipitation (Buyantuyev and Wu 2012). Home ownership may similarly affect urban temperature and greenness, as it is strongly associated with income and race (Gyourko et al. 1999, Bostic and Surette 2001, McCabe 2018) as well as plant greenness (Ossola et al. 2018). Further, race modifies urban greenness even after controlling for the climate and income (Casey et al. 2017); non-white neighborhoods are warmer and less green than white neighborhoods (Benz and Burney 2021) due in part to historic legacies of redlining and disinvestment (Wilson 2020, Nardone et al. 2021). Therefore, the effects of race and income on greenness and temperature are inextricably linked, while the greenest and coolest neighborhoods are both those which are the wealthiest and which have smaller minority populations. Long-

term changes in urban vegetation and socio-demographics, such as the loss of 36 million urban trees per year in the United States between 2009-2014 (Nowak and Greenfield 2012, 2018), suggests that the intra-urban relationships between greenness and temperature and socio-demographics likely changes over multidecadal scales. If long-term relationships are changing, then neighborhood-scale losses in environmental equity may also occur, particularly if these changing relationships diminish the effectiveness of income to moderate greenness and temperature. At intra-urban scales socio-demographics interact with greenness and temperature; understanding if, and how, these neighborhood-scale relationships change among cities could highlight broader patterns of urban ecological change and environmental justice.

In seeking to understand urban vegetation dynamics, we ask: How has urbanization affected urban greenness, land surface temperature, and vegetative cooling dynamics among cities throughout the United States and how do these differences affect urban equity in greenness and climate? We answered our research question by assessing the change in urban greenness, temperature, and vegetative cooling at the inter-city scale from intra-urban dynamics among 52 cities and their non-urban reference sites representing gradients of aridity and sociodemographics for the summer months between 2000-2022. Assessing the effect of urbanization may be done via a comparison with non-urban reference dynamics (Kondratyeva et al. 2020), however, few studies have assessed how the effect of urbanization has changed at a continental, multi-decadal scale. Therefore, large uncertainties remain as to the effect of urbanization on the sensitivity of greenness and temperature to precipitation at inter-urban scales. We tested the prediction

that the effect of urbanization on greenness and temperature decreases and increases, respectively in response to precipitation. We tested an inter-urban water deficit hypothesis positing precipitation as a major driver of inter-urban greenness and temperature dynamics; with increasing mean annual precipitation greenness increases, temperature decreases, and the relationship between greenness and temperature becomes weaker. Over multidecadal scales we predict greenness decreases, while temperature, and the interaction between greenness and temperature increase, due, respectively, to losses in urban tree cover, increasing global temperatures, and increasing global aridity. At inter-urban scales, we predict variation in landcover and sociodemographics modify greenness and temperature dynamics, while we predict that the effect of urbanization on these dynamics is due to gradients of precipitation and temperature. The predictions that the income-greenness and income-temperature relationships are not temporally stable suggest possible declines in environmental equity. Through a multidecadal, multi-scale, inter-urban, continental-scale analysis which assesses the effect of urbanization via comparison with non-urban reference sites, we evaluate how the vegetation ecology of cities is sensitive to landcover, climatic and social variables.

Methods

2.1 *Study Sites*

We collected data for 52 cities from across the conterminous United States representing 28 states. Cities were chosen to reflect a diversity of sociodemographics and climate; median household income ranged from a low of $28,675 (Kansas City, MO) to

$86,141 (Thousand Oaks, CA) while mean annual precipitation ranged from 85 mm/year in Yuma, AZ to 1,616 mm/year in New Orleans, LA (Fig. 1). Selected cities exhibited wide variability in NDVI, land surface temperature, and in vegetative cooling (Fig. 1). City extents were manually delimited in ArcGIS Pro 2.9 based on 1995 boundaries using the average of the 1995 RGB Landsat imagery as acquired on Google Earth Engine. Urban extents included impervious landcover and urban parks but did not include airports, natural reserves, or agricultural land. Using the 1995 boundaries for a study beginning in 2000 allowed us to focus solely on the urban core rather than on effects of urban growth and land use change. Each city was paired with a non-urban reference site such that there were 104 total study sites. Reference sites were chosen to represent the non-urban ecosystem the city replaced as closely as possible. Reference sites may include regional or state parks, a national forest, a wildlife refuge, or another parcel of undeveloped non-agricultural land near the city. Data on urban/reference greenness and urban/reference temperatures were acquired via satellite remote sensing.

2.2 *Landsat Analysis Ready Data, Greenness, and Temperature*

To determine the change through time of vegetative greenness and land surface temperature (LST) we utilized data from the Collection-2 Landsat U.S. Analysis Ready Data (ARD) product as acquired from EarthExplorer (https://earthexplorer.usgs.gov). Analysis Ready Data is atmospherically corrected and radiometrically calibrated by the United States Geological Survey (USGS) (Dwyer 2018), making the different Landsat satellite data products directly comparable to one another (Zhu 2019) and preventing the need for time-consuming inter-satellite calibration (Banskota et al. 2014). The

consistency between satellites makes Analysis Ready Data ideal for timeseries analysis (Qiu et al. 2018, Zhu 2019). We utilized Landsat 5, 7, 8, and 9 ARD imagery spanning from May to September and from 2000 through 2022. The selection of warm-season months was to ensure deciduous vegetation had leaf cover.

Landsat 5 was launched on March 1st, 1984 and collected imagery through January 6th, 2013 before the USGS began the process of decommissioning the satellite on January 15th, 2013. Landsat 5 became the longest-serving Earth observing satellite (Roy et al. 2020). Landsat 7 was launched on April 15th, 1999, with decommissioning beginning on April 6th, 2022. However, on May 31st, 2003, the satellite's Scan Line Corrector failed, resulting in wedges of missing pixels ranging from no missing pixels in the center of an image to 14 missing pixels on the periphery of an image (Markham et al. 2004). As such, we elected to not use Landsat 7 imagery following the failure of the Scan Line Corrector. Landsat 8 was launched on February 11th, 2013, and is still collecting data as of 2023. Landsat 9, the most recent Landsat satellite, launched on September 27th, 2021 and began collecting imagery on October 31, 2021. The next Landsat satellite, Landsat Next, is not expected to launch until 2030. Each of these satellites collect visible imagery at 30 m^2 spatial resolution. The native resolution of the thermal imagery varies by satellite: for Landsat 5 it is at 120 m^2, for Landsat 7 it is at 60 m^2, and Landsat 8 and 9 are both collected at 100 m^2, however, all imagery are resampled by USGS to 30 m^2. Upon downloading the imagery for our cities and reference sites from Earth Explorer we masked out clouds, water, and aerosols in MATLAB 2022b using the associated Quality Assessment band. In MATLAB we then eliminated any image missing more than 10% of

pixels within the boundary of the city or reference site based on the maximum number of pixels identified within that boundary over the timeseries. Excessive cloudiness may be associated with cooler temperatures due to increased albedo and reduced solar insolation, or warmer temperatures due to longwave re-radiation (Sun et al. 2000). We assessed greenness using the Normalized Difference Vegetation Index (NDVI), a commonly used metric for plant productivity (Pettorelli et al. 2011) which is sensitive to the chlorophyll of all plants which are photosynthesizing (Ibsen et al. 2021). We derived NDVI in MATLAB using the following:

$$NDVI = (NIR - Red)/(NIR + Red) \quad (1)$$

where NIR is the near infrared band and red is the red band. Land surface temperature (LST) was acquired directly from the Analysis Ready Data Surface Temperature product. We made no modifications to the Surface Temperature product, following cloud masking, other than to rescale the data from Kelvin (°K) to Celsius (°C).

2.3 *Climate, Landcover, and Social data*

We acquired climate data from TerraClimate. Terraclimate is a monthly ~4 km^2 global climate dataset valid from January 1958 through December 2021 (Abatzoglou et al. 2018). We acquired TerraClimate beginning in May 1999 for every month through September 2021. We accessed TerraClimate (IDAHO_EPSCOR/TERRACLIMATE) and clipped TerraClimate imagery to all our study sites using Google Earth Engine (GEE). Google Earth Engine is a cloud-based petabyte-scale GIS (Gorelick et al. 2017) which allows for the seamless manipulation of large quantities of spatial or temporal GIS imagery using JavaScript. From TerraClimate we acquired data on actual

evapotranspiration, climate water deficit, potential evapotranspiration, precipitation accumulation, solar radiation, minimum temperature, maximum temperature, vapor pressure, and vapor pressure deficit. We modified the precipitation dataset in Matlab to produce new datasets of 1-12 months cumulative precipitation for each month in the timeseries.

We additionally used GEE to acquire variables representing landscape heterogeneity. To assess the change in greenness in response to changing urban water availability we used data from the Soil Moisture Active Passive (SMAP) instrument, which provides soil moisture at a high global accuracy of <0.04 m3 m-3 (Abdelkader et al. 2022). SMAP (NASA_USDA/HSL/SMAP10KM_soil_moisture) was attached to the International Space Station in 2015; we accessed all SMAP data from May 2015-May 2022. From SMAP we acquired both surface soil moisture and subsurface soil moisture. The surface soil moisture product measures the water content in the top 5 cm of soil; subsurface soil moisture is not directly measured by SMAP but is modeled at up to 1-meter depth based on surface soil moisture measurements (Entekhabi et al. 2010). We obtained tree canopy cover for both urban and reference sites and percent impervious cover for urban sites only from the 2016 release of the 2011 National Landcover Dataset (USGS/NLCD_RELEASES/2016_REL). We sought to assess a city's geographic and climatic context on its biophysical dynamics and on the effect of urbanization. We did so by utilizing a global map of biomes (OpenLandMap/PNV/PNV_BIOME-TYPE_BIOME00K_C/v01) to assess ecological organization at 1 km^2 spatial resolution (Hengl 2018) as well as the Köppen-Geiger classification map for 1991-2020 to assess

climatic context (Beck et al. 2023). Finally, we acquired elevation from the Shuttle Radar Topography Mission digital elevation map (USGS/SRTMGL1_00).

To assess the sensitivity of urban NDVI, LST, or vegetative cooling to inter-city social variability we acquired a selection of social variables from the 2010 American Community Survey 5-year Estimates at the census tract scale. We derived the racial composition of each city by determining the mean percentage of White, Asian, Black (table B02001), and Hispanic (table B03003) residents. We derived the population density of all urban residents and the population density of the non-Hispanic population using the racial composition tables. Finally, we characterized income by acquiring data for median household income (table S1903) and per-capita income (table B19301).

2.4 *Assessment of the precipitation-NDVI relationship*

For each city and reference site we assessed the relationship between precipitation and NDVI using TerraClimate precipitation. For each site we used the following regression:

$$NDVI = \beta_0 + \beta_1 Precipitation_{1-12} + \varepsilon \quad (2)$$

We then isolated the β_1 coefficient for each site. We were unsure at what temporal lag best described precipitation-NDVI at the continental scale and so acquired β_1 at 1-12 months cumulative precipitationfall. Further, our preliminary data suggested that urban precipitation-NDVI may be well approximated by a power function. Therefore, we also conducted a non-linear regression of the form:

$$NDVI = \alpha + Precipitation^{b}_{1-12} + \varepsilon \quad (3)$$

To compare the nonlinear relationship among sites we used the b exponent.

For each site we assessed the long-term trend (2000-2022) in NDVI, LST, and vegetative cooling (°C/NDVI), precipitation and its sensitivity to NDVI, assessed the mean of these variables, and compared the difference in these values between paired urban and reference sites. We assessed significant differences between paired urban and reference sites using a 2-sample t-test. In all cases the delta (▲) term between urban and reference sites was derived as *urban-reference*. Values close to zero denote no difference between a paired urban and reference site, whereas positive values indicate the urban site has a greater value relative to the reference site.

2.5 *Assessing Change in the Luxury Effect through Time*

To assess the change in the luxury effect through time at the national scale we compared the regression slope for income~NDVI and income~LST between 2000 and 2020 for all 52 cities using 2000, 2010, and 2020 census data. Median household income for 2000 came from census table HCT036 variable HCT036001. Median household income for 2010 and 2020 came from census table S1901 variable S1901_C01_012E. All regressions were conducted at the tract level, which is a large enough unit of analysis to provide reliable socio-demographic information (Wong and Sun 2013). NDVI and LST for the three time points were characterized by the median image from May-September between 1999-2001, 2009-2011, and 2019-2021, respectively. Assessment of median NDVI and LST were done exclusively in GEE and did not utilize the ARD dataset.

The NDVI and LST datasets for the luxury effect analysis were derived using GEE. This was done to allow us to take advantage of GEE and the ease it provides in quickly manipulating large quantities of geospatial imagery. NDVI was harmonized from

Landsat Collection-2 Level-2 imagery for Landsat 5 (LANDSAT/LT05/C02/T1_L2), Landsat 7 (LANDSAT/LE07/C02/T1_L2), and Landsat 8 (LANDSAT/LC08/C02/T1_L2) using the scaling coefficients published in Roy et al. (2016). To derive the scaling coefficients Landsat 8/OLI was linearly transformed via ordinary least squares regression to be consistent with Landsat 5/TM and Landsat 7/ETM+. Land surface temperature was derived from Landsat Collection-2 Level-2 imagery using the open-source GEE code published by Ermida et al. (2020). The LST derived from this code maintains high agreement with in-situ measurements with a difference of no more than 0.5 °C. Following data acquisition NDVI and LST were cloud masked and clipped to the city boundaries using GEE. These data were then transferred to ArcGIS Pro 3.0.3 where we projected all data to USA Contiguous Albers Equal Area Conic USGS, and then aggregated NDVI and LST to their median value per census tract. All data were finally exported to Matlab r2022b to assess the Luxury Effect.

To assess factors influencing the variability of the luxury effect at a continental scale, we determined the mean luxury effect per city. We did so by averaging the income-NDVI and income-LST slopes for each city for 2000, 2010, and 2020. This regression takes the form of:

$$NDVI = \beta_0 + \beta_1 * income + \varepsilon \quad (4)$$

where β_1 represents the effect of income on modifying NDVI or LST. We used the average of the β_1 slope coefficients as a new dependent variable in multiple regression to assess how the luxury effect varied among cities.

We determined the change through time of the luxury effect and whether this change was significant for a given city using multiple regression. To set up each city's regression we created single variables of NDVI, LST, and median household income using 2000, 2010, and 2020 data. We added a categorical variable "year", demarcating the data by which year the data came from. The interaction term represents the product of the independent variable (income) and the categorical variable (year). The form of the regression for the effect of income on NDVI (Eq. 5) is the same as it is for LST except for the different dependent variable.

$$NDVI = \beta_0 + \beta_1 * income + \beta_2 * year + \beta_3 * interaction + \varepsilon \quad (5)$$

Ultimately, we ran three regressions, comparing the change in the luxury effect between 2000 and 2010, between 2010 and 2020, and between 2000 and 2020. For a given city a significant interaction term indicates that the regression coefficient of income on NDVI is significantly different between any two years, such as 2000 and 2020, while the interaction coefficient represents the magnitude of that change. We used the coefficient of the interaction term (β_3) as a dependent variable in a new multiple regression where we sought to explain the variability of the multidecadal change in the effect of income on NDVI and LST. The β_1 coefficient represents the income-NDVI relationship in the baseline year (e.g., if comparing 2000 to 2020, then income-NDVI in 2000), and β_2 represents the difference in NDVI through time. However, we did not use either coefficient from this equation for our analysis. We did not use β_1 from equation 5 to assess the mean luxury effect, as this regression coefficient is estimated with the effects of the year and interaction terms partialled out. Further, the additional terms may change

ε by altering how much variance is captured in NDVI. We felt assessing the mean luxury effect via Eq. 4 was the most straightforward, easily interpretable approach.

Results

3.1 *Urbanization weakens urban biophysical relationships*

At the continental scale urban NDVI and LST exhibited strong relationships with the climate, although urbanization weakened these relationships compared to a non-urban reference (Fig. 2). Testing with ANCOVA confirmed that the urban and reference site relationships between NDVI and LST against precipitation, climate water deficit, and tree canopy cover were significantly different ($p<0.001$). In increasingly mesic environments cities became less green than and hotter than their reference site. However, in the environments with the lowest rainfall cities were greener than their reference site, although temperatures were not different. Urban NDVI and LST exhibited a weaker response to climate water deficit than non-urban reference sites, however, in environments with a very high climate water deficit cities were both greener and cooler than their reference. Urbanization also affected how NDVI and LST respond to landcover. Tree canopy cover decreased LST and increased NDVI non-linearly more slowly in cities than in non-urban reference sites. Mean annual precipitation, climate water deficit, and tree canopy cover explained, respectively, 81% and 74% of the continental-scale variability in mean urban NDVI and LST.

Across all 52 cities, representing more than a magnitude difference in 12-months cumulative precipitation, urban NDVI increased with precipitation according to the power function:

$$NDVI = 0.04064 * x^{0.3433} \quad (5)$$

where x is the 12-months cumulative precipitation. Likewise, precipitation reduced urban LST according to the power function:

$$LST = 425.1 * x^{-0.7245} + 34.27 \quad (6)$$

The effect of climate on NDVI and LST was mediated by urbanization, with the most arid cities being greener than and cooler than their reference. A primary driver of change in NDVI and LST between reference sites and cities was a gradient of precipitation, necessitating a clearer understanding of under what conditions precipitation acts as a mediating variable.

3.2 *Aridity decouples urban greenness from precipitation*

The sensitivity of NDVI and LST to precipitation was mediated by precipitation (Fig. 3). In cities and reference sites, NDVI-Precipitation was assessed using breakpoint regression. The sensitivity of urban and reference site NDVI peaked at intermediate levels of rainfall, occurring in cities with 358 mm of 6-months cumulative precipitation, and in reference sites with 340 mm of 6-months cumulative precipitation. The sensitivity of urban NDVI was distinct from that in reference sites in extremely arid and extremely mesic environments. Under extreme aridity the urban NDVI-precipitation relationship dropped to zero, indicating a complete decoupling of urban greenness from precipitation not observed in the most arid reference sites. Conversely, in the wettest environments, reference site NDVI became non-responsive to precipitation, while urban NDVI still maintained a positive relationship.

6-months cumulative rain was chosen as the monthly aggregation due to the reference site having the highest correlation between NDVI and precipitation at 6 months cumulative precipitation (pearson's r= -0.63, p-value<0.001). The highest correlation between urban NDVI and precipitation occurred at 10-months cumulative precipitation (pearson's r= -0.86, p-value<0.001), however, the urban relationship at 6 months was not much different (pearson's r= -0.78, p-value<0.001). Assessing both the urban and reference site NDVI-Precipitation relationship at 6-months cumulative precipitation therefore allowed for direct comparison between urban and reference sites.

Notably, although we assessed the variability in NDVI-precipitation for all 52 cities and reference sites, 16 of 52 cities (31%) and 19 of 52 reference sites (37%) had no significant relationship between NDVI and precipitation at 6-months cumulative precipitation. A generalized linear model was able to explain 43% of the variance in whether a city had a significant NDVI-precipitation relationship (p-value=0.001). Increasing climate water deficit made it more likely that a city would not have a significant relationship (p-value=0.012). A city's climatic context, via the Köppen-Geiger classification, also mediated this relationship. Relative to cities in a temperate classification, cities in a cold classification (p=0.048) and tropical classification (p=0.002) had a greater probability of not having a significant NDVI-precipitation relationship.

LST-Precipitation varied between cities and reference sites, exhibiting the effect of urbanization on how precipitation cools the local environment. The highest correlation between LST and precipitation for both urban (pearson's r= -0.53, p-value<0.001) and

reference sites (pearson's r= -0.79, p-value<0.001) occurred at 8-months cumulative precipitation. The sensitivity of LST to precipitation was greater in reference sites than in cities, however, in both locations the greatest cooling from precipitation occurred in the most arid sites. In the most mesic environments LST cooling from precipitation was effectively zero in both cities and reference sites. Despite the greatest correlation between LST and precipitation occurring at 8-months cumulative precipitation, we assessed the urban and reference relationships at 2-months cumulative precipitation. The best relationship between LST-precipitation and precipitation occurred at 2 months of precipitation for both urban (pearson's r=0.40, p-value=0.003) and reference sites (pearson's r=0.61, p-value<0.001), which is what we used for analysis. Urban NDVI and LST precipitation sensitivity were therefore modified by gradients of aridity and weakened by urbanization, however, the variability of these relationships in arid compared to mesic cities suggests that climate may modify this urban to rural difference.

3.3 *The effect of urbanization is mediated by climate, landcover, and race*

The effect of urbanization on NDVI or LST can be indirectly assessed by treating the delta (▲) between urban and reference sites as a dependent variable (Fig. 4). The difference in NDVI between a city and its reference site was explained by landcover and the climate. NDVI was as high or higher than a reference site when urban NDVI was as high or higher than a reference site (p-value<0.001). In regions with high vapor pressure deficit, cities were more likely to have higher NDVI than a reference site (p-value<0.001); these two variables explained 76% of the continental-scale variability in the difference between urban and non-urban greenness. The difference in LST between a

city and its reference site was driven solely by the difference in NDVI. Cities which had higher NDVI than their reference site were cooler (p-value<0.001); the difference in NDVI explained 89% of the variability in the difference in LST. Vegetative cooling was greater in a city than its reference site in environments with a high climate water deficit (p-value=0.002) and in cities with a larger white population (p=0.018). Climate water deficit and race explained 22% of the variability in the difference in urban to reference vegetative cooling.

3.4 *Multidecadal trends in NDVI, LST, and Vegetative Cooling between 2000-2022*

The long-term trends in NDVI, LST, and vegetative cooling were highly variable at a continental scale (Fig. 5). Between 2000-2022 NDVI significantly decreased in six cities and significantly increased in 36 cities. A generalized linear model explained 59% of the variability in whether a city's NDVI trend was positive or negative. A higher mean VPD increased the likelihood of a decline in NDVI (p<0.001), while cities with a larger white population were more likely to have an increase in NDVI through time (p=0.015). On average, all cities increased NDVI at a rate of 0.001/year, half as fast as the increase in NDVI in reference sites of 0.002/year. However, variability was high for both cities and reference sites, as the standard deviation for either cities or reference sites was the mean of its rate of change. The rate of change in NDVI was different by biome (p<0.001) and by Köppen-Geiger classification (p<0.001), where cities in arid/desert environments had the lowest NDVI trends. Urban NDVI trends in the arid southwestern United States exhibited unusually similar trends (Fig. S1), where NDVI trends appeared to be more like other arid western cities than to the reference sites associated with those cities. NDVI is

an important component of urban ecosystems, and one which typically has a strong influence on LST.

Over the 22-year time series, 35 out of 52 cities (67%) got significantly hotter; no city had a significant cooling trend. Warming across all cities was 0.16 °C/year; cities warmed 45% faster than their reference sites, which warmed 0.11 °C/year. There was wide inter-urban variability in the LST trends (Fig. S2). Cities with a larger Hispanic population also experienced faster rates of warming at a rate of 0.025 °C/year per 10% increase in a city's Hispanic population ($p<0.001$). Multiple regression also identified latitude as a significant mediator of the warming trend despite latitude not being significant in univariate regression. For every 1 ° latitude movement north, urban warming increased by 0.006 °C/year (p-value=0.003). Testing with ANOVA identified differences in the warming trend by Köppen-Geiger classification ($p<0.001$), where a post-hoc Tukey HSD identified the warming trend in arid environments as being faster than cities anywhere else. Mean warming by Köppen-Geiger classification was 0.08 °C/year for tropical cities, 0.12 °C/year for temperate cities, 0.13 °C/year for cold cities, and 0.23 °C/year for arid cities.

Across all cities, vegetative cooling increased at a rate of 0.01 °C/year. The trend in vegetative cooling was nearly evenly split between cities which increased vegetative cooling and cities which decreased vegetative cooling. A generalized linear model explained 30% of the variance in whether vegetative cooling increased or decreased ($p=0.04$). Cities with a larger Hispanic population were more likely to have had vegetative cooling decrease through time (p-value=0.003). The trend was also regionally

specific, with cities in the West more likely to increase vegetative cooling (p-value=0.016). In multiple regression, the vegetative cooling trend was mediated by race and a city's mean vegetative cooling. For every 10% increase in the size of a city's Hispanic population, vegetative cooling declined an additional 0.041 °C/NDVI/year ($p<0.001$). Vegetative cooling was also more likely to decrease in cities which had the lowest average amount of vegetative cooling (p-value=0.001). Every 1 °C/NDVI decrease in a city's mean vegetative cooling was associated with a decline of vegetative cooling through time of 0.022 °C/NDVI/year. The widespread variability in the NDVI, LST, and vegetative cooling trajectories at the continental scale may have important equity implications for the ability of urban residents to mediate these trends.

3.5 *The Luxury Effect substantially declined at a continental, multidecadal scale*

At the continental scale, sociodemographic and climatic factors influenced the mean luxury effect (Fig. 6), which was assessed at 2000, 2010, and 2020. Across all cities, income had an average effect on NDVI of 0.03/$10,000 and an average effect on LST of -0.37 °C/$10,000. The effect of income on NDVI was moderated by sociodemographic variables alone. In cities with a stronger relationship between NDVI and home ownership ($p<0.001$) and with a larger population of white residents ($p<0.001$), income was more effective at increasing NDVI. We tested racial distributions of Hispanic, Asian, Black, and White communities, however, we found that only the size of the white population modified the NDVI-income relationship. When evaluating variability of the mean LST-income relationship, only NDVI-income emerged as a significant moderator. The effect of income on LST increased in conjunction with an increase in the effect of income on

NDVI, at a rate of -0.11 °C per 0.01 increase in the effect on NDVI ($p<0.001$). The variable dynamics between income, NDVI, and LST against sociodemographic gradients suggests that these relationships may not have been stable through time as income, NDVI, LST, and the urban sociodemographic distributions are known to have changed.

The luxury effect substantially declined at a multidecadal, continental scale (Fig. 7). Between 2000 and 2020 the effect of median household income on reducing LST declined in all but eight cities, and significantly so in 22 out of 52 cities. Across all cities, LST-income declined on average 0.015 °C/$10,000/year; income was weaker by 53% in 2020 compared to 2000 as a mediator of urban temperatures. Income as a mediator of urban greenness exhibited similar trends. Between 2000 and 2020 NDVI-income declined in all but six cities, and significantly so in 34 out of 52 cities. Across all cities, NDVI-income declined on average 0.0014 NDVI/$10,000/year, such that the ability for income to mediate urban greenness was 62% weaker in 2020 as it was in 2000. NDVI-income and LST-income did not become significantly stronger in any city. We sought to explain the variability in which cities did and did not have a significant decline in the luxury effect using a generalized linear model. We were able to explain 67% of the variability in whether NDVI-income significantly declined ($p<0.001$). Cities with a higher mean household income ($p=0.008$) and higher 6-month cumulative precipitation (p-value=0.02) were more likely to have a significantly weaker NDVI-income relationship through time. Biome was also a significant mediator, where cities in dry woodland biomes were more likely to not have a significant decline in NDVI-income compared to cities in temperate forest biomes ($p=0.003$). The relationships mediating a

significant decline in LST-income were similar. Biome and mean household income explained 52% of the variability in whether LST-income significantly declined ($p<0.001$). Cities with a higher mean household income were more likely to have a significant loss in LST-income ($p=0.002$). Compared to a temperate forest biome, cities in dry woodland ($p=0.002$) and savanna/grassland biomes ($p=0.01$) were more likely to not have a significant decline in LST-income.

The continental-scale decline in the luxury effect was highly variable. The change in the ability for income to mediate LST was mediated only by the trend in NDVI-income (p-value<0.001). Every decline in NDVI-income of 0.01/$10,000/year decreased LST-income 0.11 °C/$10,000/year. The change in the ability for income to mediate NDVI was itself only mediated by a city's average NDVI-income relationship. Every increase in the mean NDVI-income relationship of 0.05/$10,000 was associated with a decline in NDVI-income through time of 0.035/$10,000/year. The declining relationships between income-LST and income-NDVI was a consequence of evolving dynamics between sociodemographics and the urban biophysical environment and hints at increasing inequities in the provision of urban greenness and distribution of urban temperatures.

Between 2000 and 2020, in conjunction with the continental-scale decline in the luxury effect, the effect of sociodemographics as a mediator of urban greenness and temperature were also not stable through time. The relationship between income and home ownership declined 0.24% home ownership/$10,000/year. However, the relationship between home ownership and NDVI and LST increased, such that in 2020 compared to 2000 every 10% increase in home ownership was associated with 0.03 °C

additional cooling, and 0.008 additional increase in NDVI. The race-based relationships with NDVI and LST also exhibited non-stationarity. In 2020 and for every 10% increase in the race-based population, White census tracts experienced a weakened relationship with NDVI of 0.007 and 0.03 °C greater warming compared to 2000. Hispanic census tracts experienced a stronger relationship with NDVI of 0.01 and 0.21 °C less warming compared to 2000. Black census tracts experienced a stronger relationship with NDVI of 0.007 and less warming of 0.10 °C. Finally, Asian census tracts experienced a stronger relationship with NDVI of 0.02 and less warming of 0.02 °C compared to 2000. However, only a minority of cities experienced significant race-based changes through time; for each race regressed against either NDVI or LST, fewer than 20 cities had a significantly different relationship in 2020 compared to 2000.

Discussion

This study investigated the relationship between precipitation, urban greenness, and temperature in 52 cities and their non-urban reference sites over a multidecadal period from 2000 through 2022. We show that the effect of urbanization weakened urban biophysical relationships, with urban greenness being fully decoupled from precipitation in the most arid cities. This decoupling corroborates intra-urban decoupling of urban greenness from precipitation in Phoenix, an arid city (Buyantuyev and Wu 2012), at a continental inter-urban scale. The non-sensitivity of urban greenness to precipitation in the most arid environments is highly suggestive of irrigation leading to this decoupling, particularly since similar trends were not observed in the most arid reference sites. However, the effect of urbanization wasn't consistent across all cities; cities weren't all

hotter than or less green than their reference site, and the magnitude of that difference exhibited wide variability. Landcover, the climate, and race mediated this change, emphasizing how urban heat and greenness are modified. Over time, NDVI, LST, and vegetative cooling all changed. The change in these dynamics contributed to a substantial decline in the luxury effect at a continental level, suggesting possible declines in the equitable distribution of urban heat or greenness. The dynamic relationships among climatic conditions, land cover, and socioeconomics uncovered in this study offers a more comprehensive understanding of urban ecosystems, emphasizing the importance of considering how these changing dynamics impact environmental equity in urban planning and development.

A primary goal of this research was to assess the effect of urbanization on urban greenness, temperature, and vegetative cooling. Urbanization weakened the relationships between the climate and landcover and either NDVI or LST. Cities, as complex socio-ecological systems, may respond differently to landcover and the climate from reference sites due to the luxury effect and aggregations of wealth (Hope et al. 2003, Leong et al. 2018), legacies of ecological disinvestment in minority communities (Wilson 2020, Nardone et al. 2021), or differences in cultural preference for what to plant (Clarke et al. 2014). The role of irrigation as a mediator of urban biophysical relationships is suggested multiple times in our data. Cities in environments with the greatest climate water deficit were greener than and cooler than their reference site and had greater vegetative cooling, cities in environments with a high mean VPD were greener than their reference site, and cities with the lowest cumulative rainfall had no significant relationships between NDVI

and precipitation, despite no such observation for reference sites. Urban biophysical parameters were well explained by gradients of water availability and water demand, supporting our inter-urban water deficit hypothesis. Precipitation's role in shaping urban ecosystems underscores the importance of incorporating climate-related factors into urban ecological research.

The sensitivity of urban and reference site NDVI to precipitation peaked at intermediate levels of cumulative rainfall. This optimal range of precipitation was due to not enough water to influence NDVI in very arid climates, and too much water to influence NDVI, due to, for example, waterlogged soils, in very wet climates. The relationship between precipitation and LST was similar in that the urban relationship was much weaker than the non-urban relationship. However, in both cities and reference sites, the greatest cooling from precipitation occurred under conditions of greatest aridity. That the most arid cities experienced the greatest cooling from precipitation was likely due to low vegetation cover and high pervious cover in very arid cities. Due to less total vegetative cooling from less vegetation, temperature in these cities may be more directly influenced by evaporative cooling brought about by precipitation. Urbanization decreased the sensitivity of NDVI and LST to precipitation, however, understanding what causes the effect of urbanization itself would have important implications for urban land management.

The effect of urbanization, or the difference in NDVI, LST, and vegetative cooling between a city and its reference site, were driven by landcover, the climate, and race. Cities were not uniformly less green than or hotter than their reference ecosystem; cities

were greener when they had more tree canopy cover, and they were cooler when they had greater NDVI. These parameters are policy decisions (Hill et al. 2010, Mincey et al. 2013), but are also heavily informed by income (Schwarz et al. 2015) and race (Watkins and Gerrish 2018). The cities which achieved these benefits were not rural, thus, these results were not due to low impervious cover and spontaneous vegetation. Sacramento, CA, a city of over half a million residents and which is known as the City of Trees (McPherson and Luttinger 1998), has an urban forest 5.2% greater than Sacramento's hinterlands, and consequently experiences urban temperatures on average 3.5 °C cooler than the land outside of Sacramento. Increasing urban greenness via an increase in tree canopy cover is therefore an effective strategy to minimize the urban heat island (Rahman et al. 2020). Race also mediated the effect of urbanization, with greater vegetative cooling in cities with a larger white population. Minority populations are associated with increased temperature and decreased greenness independent of income (Harlan et al. 2006, Casey et al. 2017, Benz and Burney 2021), suggesting that cities with larger white populations may have more favorable conditions for vegetative cooling. Urbanization led to variability in mean NDVI, LST, and vegetative cooling, however, these dynamics exhibited long-term change.

Dynamics of urban NDVI, LST, and vegetative cooling exhibited wide variability between 2000-2022 at a continental scale. Most cities became greener, which may have been due to changing economics (e.g., an increase in vacant lots leading to unimpeded plant growth), implementation of green infrastructure such as green roofs and bioswales, and higher urban temperatures making growing conditions more favorable for plants

(Smith et al. 2019). An increase in urban greenness is consistent with global observations (Piao et al. 2019) and may be due to afforestation. The NDVI trend was highly context dependent, with the lowest trends in arid and desert environments. This may have been associated with the LST trend; arid cities warmed significantly faster than cities anywhere else. Urban plants in these regions may have become stressed with increasing temperature, decreasing growth (Winbourne et al. 2020). Conversely, cities in arid environments may have been more likely to engage in xeriscaping as a practice to conserve water (Ismaeil and Sobaih 2022), a practice known to raise urban temperatures (Meerow et al. 2021). As well, drought in this region may have weakened NDVI trends, as drought is known to decrease urban greenness (Allen et al. 2021, Kucera and Jenerette 2023) even when irrigation is unchanged (Quesnel et al. 2019). NDVI trends in this region were unique compared to the rest of the country; urban NDVI trends in the arid southwest exhibited unusual synchronicity, fluctuating in ways more like other southwestern cities than to the reference site those cities replaced. These cities were located in a region spanning tens of thousands of square kilometers, suggesting a climatic role mediating these trends. However, climate would have been expected to alter the reference site trends in similar ways, which was not observed. These findings merit further analysis, but may be due to urban homogenization (Groffman et al. 2014) leading to changes in NDVI among arid cities more similar to other arid cites than to their reference ecosystem. These results suggest two predictions that require quantitative analysis: first, that in southwestern cities urban NDVI trends are dissimilar from the trends for that city's reference site. Second, these findings suggest the prediction that the

trends for southwestern cities exhibit synchronicity and are like one another. Although the urban NDVI trend exhibited unique spatial clustering, the LST trend did not.

Urban warming increased the most in cities arid, Hispanic-dominated cities. Across all 52 cities LST increased on average 0.16 °C/year, 45% faster than the warming of reference sites of 0.11 °C/year. Our observed rate of urban warming compared to reference site warming was greater than the 29% faster urban warming observed at a global scale (Liu et al. 2022). However, prior studies have utilized MODIS to assess temperature trends. MODIS, with a 1-km^2 spatial resolution for the thermal bands, is significantly coarser than the ~100-m^2 spatial resolution for the Landsat thermal bands. We suspect the faster rate of urban warming identified in this study is due to the use of a higher spatial resolution dataset. Nevertheless, the fastest increases in temperature in Hispanic-dominated cities poses challenges for environmental equity, as the inter-urban distribution of urban heat is becoming increasingly racially inequitable.

We further assessed the long-term trend in vegetative cooling, which was modified by race and mean vegetative cooling. Vegetative cooling declined the fastest in cities with the largest Hispanic populations. This may have been a consequence of Hispanic-dominated cities warming the fastest, leading to stomatal closure if urban plants in these regions exhibited isohydric strategies. The trend in vegetative cooling was also associated with mean vegetative cooling, becoming stronger in cities which experienced the most vegetative cooling, and becoming weaker in cities which experienced the least vegetative cooling. This observation may be reflective of a feedback loop (Abram and Dyke 2018), where cities with conditions suitable for vegetative cooling are able to maintain those

conditions, while cities with less favorable conditions are losing the capacity for vegetative cooling. The spatially variable long-term dynamics of NDVI and LST suggests possible changes to the benefits, and equity implications of, maintaining greener and cooler cities.

The luxury effect, being the ability for income to mediate both an increase in greenness and decrease in temperature, was spatially variable at an inter-urban continental scale. The effectiveness of income on increasing NDVI was modified by sociodemographics, where cities with the strongest relationship between home ownership and NDVI as well as with the largest population of white residents also had the largest effect of income on increasing NDVI. In our dataset home ownership had a strong influence on increasing NDVI. We find that when the relationship between home ownership and NDVI became stronger, so did the relationship between income and NDVI. Home ownership is associated with other sociodemographic variables such as income and education (Fossa et al. 2023), providing the means to manage plant cover. Renters may have a reduced capacity to influence urban plants for numerous reasons, including high turnover, as planting typically is greatest in the first five years of home ownership (Summit and McPherson 1998), lack of financial resources, or lack of permission from the landowner (Riedman et al. 2022). Home ownership may influence plant cover via a desire to signal social status (Grove et al. 2014) or to match community norms (Ossola et al. 2019). Therefore, part of the inter-urban variability in NDVI-income is related to home ownership, and specifically to how engaged homeowners are in modifying their greenspace. NDVI-income was also modified by the proportion of a

city's population that was white. Racist legacies of redlining from the 1930s, where minority neighborhoods were more likely to be redlined, has led to inequities in greenness distributions where neighborhoods red lined in the 1930s have the lowest plant greenness in the 21st century (Nardone et al. 2021). The positive association between the size of a city's white population and the effectiveness of income on NDVI reinforces how past legacies of greenspace disinvestment in minority communities has led to the inequitable distribution of the luxury effect on NDVI at a continental scale. The increase in income-LST with an increase in income-NDVI suggests that where income has a greater effect on urban greenness vegetative cooling from transpiration and shading increases, subsequently enhancing LST-income. Wealthy cities and regions of cities have high tree canopy cover (Schwarz et al. 2015), producing a strong income-NDVI relationship and producing cooler temperatures. However, the variables modifying the inter-urban variability of the luxury effect are changing over time, not least due to climate change, suggesting that the luxury effect itself may exhibit non-stationarity.

The luxury effect declined at the continental scale in its ability to mediate both urban greenness and temperature, highlighting important shifts in environmental equity due to changes in demographics, the climate, and the amount of urban vegetation. The luxury effect has profound consequences for environmental equity, disproportionately affecting low-income and non-White populations due to higher temperatures and lower plant cover. A decline in the luxury effect has led to an increase in environmental equity as high-income cities became more like low-income cities in their reduced ability to manage urban greenness and temperature. The only variable which described the change in the

LST-income relationship through time was income-NDVI; income-LST declined linearly with a decline in NDVI-income, suggesting that the effect of income on LST is fundamentally driven by vegetative cooling. In contrast, the change in NDVI-income through time was driven by the average strength of the NDVI-income relationship, becoming weaker through time more quickly in cities in which income was a stronger mediator of NDVI. A weakening of the luxury effect in these cities indicates a more equitable greenspace distribution, which could be due to either a decrease in NDVI in wealthy regions, or an increase in NDVI in low-income communities. Policy, such as an increase in urban densification, could also have mediated this change. The observed decline in the luxury effect at the continental scale corroborates Kucera and Jenerette (2023), who found a multidecadal decline in the luxury effect for the Los Angeles urban region. This multidecadal decoupling of income from greenness and temperature underscores the need for continued research to understand the evolving relationship between socioeconomic factors and the temperature and greenness dynamics of urban ecosystems. Important urban ecological relationships should not be assumed to exhibit stationarity; assumptions about stationarity need to be explicitly tested.

This research contributes to the growing field of urban macroecology, providing valuable insights into the complex interplay of climate, landcover, and social factors among many urban ecosystems. In comparing urban to non-urban ecosystems across many cities this research supports an ecology *of* cities paradigm, which emphasizes the importance of comparative urban ecosystem studies for advancing the theory of urban ecosystems (McPhearson et al. 2016). Urban macroecology is uniquely suited to

understanding how urbanization affects urban ecosystems, providing a more holistic view of where and why urban ecosystems differ from their non-urban reference sites. Adopting an urban macroecological approach is essential for addressing the challenges posed by rapid urbanization, climate change, and changing sociodemographics. This research suggests two avenues for future research. First, there is a need to identify the cause(s) behind the synchronicity in urban NDVI in southwestern cities. The distance between the cities and their location in the arid southwest suggests that climate plays a role. However, understanding if and how urban greenness in arid western cities differs from how urban greenness varies in more mesic cities has important implications for the planning and equitable distribution of this urban ecosystem service. Second, the decline in the luxury effect at the continental scale poses significant challenges for building environmentally just cities if more equitable distributions of NDVI and LST are not associated with an improvement of conditions for low-income, minority neighborhoods. Future research should focus on if and what kind of green infrastructure interventions can mitigate this decline and whether the decline of the luxury effect may have been associated with socio-economic transformations such as an increase in income disparity.

Conclusion

To address uncertainties in urban vegetation and climate distributions among cities and their dynamics, we asked whether urban macroecological patterns are consistent with those in non-urban urban reference sites, and how the continental-scale dynamics of land surface temperature, greenness, and vegetative cooling have changed among 52 cities at a continental scale. This study contributes valuable insights to the field

of urban ecology, emphasizing the complex interactions between climate, socioeconomics, and landcover in shaping urban greenness, temperature, and vegetative cooling. As the luxury effect becomes increasingly less important through time as a factor increasing urban greenness and decreasing urban temperatures, policymakers and urban planners should be able to leverage the dynamics of urban ecosystems to plan urban ecological interventions more appropriately. Understanding how to manage urban ecosystems where income is less important is critical as cities at the continental scale have been rapidly warming at a rate of up to 0.3 °C/year and on average 45% faster than non-urban reference sites. This decline in the role of income on urban greening and cooling has likely led to intra-urban decreases in environmental justice along with unaddressed implications about reduced public health and delivery of ecosystem services. Urban land managers should consider the non-stationarity of urban dynamics when designing strategies for mitigating the urban heat island, enhancing urban green spaces, and promoting environmental equity across diverse urban populations.

References

Abatzoglou, J. T., S. Z. Dobrowski, S. A. Parks, and K. C. Hegewisch. 2018. TerraClimate, a high-resolution global dataset of monthly climate and climatic water balance from 1958-2015. Sci Data **5**:170191.

Abdelkader, M., M. Temimi, A. Colliander, M. H. Cosh, V. R. Kelly, T. Lakhankar, and A. Fares. 2022. Assessing the Spatiotemporal Variability of SMAP Soil Moisture Accuracy in a Deciduous Forest Region. Remote Sensing **14**.

Abram, J. J., and J. G. Dyke. 2018. Structural Loop Analysis of Complex Ecological Systems. Ecological Economics **154**:333-342.

Allen, M. A., D. A. Roberts, and J. P. McFadden. 2021. Reduced urban green cover and daytime cooling capacity during the 2012–2016 California drought. Urban Climate **36**.

Banskota, A., N. Kayastha, M. J. Falkowski, M. A. Wulder, R. E. Froese, and J. C. White. 2014. Forest Monitoring Using Landsat Time Series Data: A Review. Canadian Journal of Remote Sensing **40**:362-384.

Beck, H. E., T. R. McVicar, N. Vergopolan, A. Berg, N. J. Lutsko, A. Dufour, Z. Zeng, X. Jiang, A. I. J. M. van Dijk, and D. G. Miralles 2023. High-resolution (1 km) Köppen-Geiger maps for 1901–2099 based on constrained CMIP6 projections. Scientific Data **10**.

Benz, S. A., and J. A. Burney. 2021. Widespread Race and Class Disparities in Surface Urban Heat Extremes Across the United States. Earth's Future **9**.

Bostic, R. W., and B. J. Surette. 2001. Have the doors opened wider? Trends in homeownership rates by race and income. Journal of Real Estate Finance and Economics **23**:411-434.

Buyantuyev, A., and J. Wu. 2012. Urbanization diversifies land surface phenology in arid environments: Interactions among vegetation, climatic variation, and land use pattern in the Phoenix metropolitan region, USA. Landscape and Urban Planning **105**:149-159.

Casey, J. A., P. James, L. Cushing, B. M. Jesdale, and R. Morello-Frosch. 2017. Race, Ethnicity, Income Concentration and 10-Year Change in Urban Greenness in the United States. Int J Environ Res Public Health **14**.

Chai, R., J. Mao, H. Chen, Y. Wang, X. Shi, M. Jin, T. Zhao, F. M. Hoffman, D. M. Ricciuto, and S. D. Wullschleger. 2021. Human-caused long-term changes in global aridity. npj Climate and Atmospheric Science **4**.

Chamaillé-Jammes, S., and H. Fritz. 2009. Precipitation–NDVI relationships in eastern and southern African savannas vary along a precipitation gradient. International Journal of Remote Sensing **30**:3409-3422.

Cheng, M., Y. Liang, C. Zeng, Y. Pan, J. Zhu, and J. Wang. 2023a. Economic Growth Does Not Mitigate Its Decoupling Relationship with Urban Greenness in China. Land **12**.

Cheng, M., S. Wu, C. Zeng, X. Yu, and J. Wang. 2023b. Can economic growth and urban greenness achieve positive synergies during rapid urbanization in China? Ecological Indicators **150**.

Clarke, L. W., L. Li, G. D. Jenerette, and Z. Yu. 2014. Drivers of plant biodiversity and ecosystem service production in home gardens across the Beijing Municipality of China. Urban Ecosystems **17**:741-760.

Das, K., and A. Ramaswami. 2022. Who Gardens and How in Urban USA: Informing Social Equity in Urban Agriculture Action Plans. Frontiers in Sustainable Food Systems **6**.

Dwyer, J. L., D. P. Roy, B. Sauer, C. B. Jenkerson, H. K. Zhang, and L. Lymburner. 2018. Analysis Ready Data: Enabling Analysis of the Landsat Archive. Remote Sensing **10**.

Lymburner, Leo. 2018. Analysis Ready Data: Enabling Analysis of the Landsat Archive. Remote Sensing **10**.

Entekhabi, D., E. G. Njoku, P. E. O'Neill, K. H. Kellogg, W. T. Crow, W. N. Edelstein, J. K. Entin, S. D. Goodman, T. J. Jackson, J. Johnson, J. Kimball, J. R. Piepmeier, R. D. Koster, N. Martin, K. C. McDonald, M. Moghaddam, S. Moran, R. Reichle, J. C. Shi, M. W. Spencer, S. W. Thurman, L. Tsang, and J. Van Zyl. 2010. The Soil Moisture Active Passive (SMAP) Mission. Proceedings of the IEEE **98**:704-716.

Ermida, S. L., P. Soares, V. Mantas, F.-M. Göttsche, and I. F. Trigo. 2020. Google Earth Engine Open-Source Code for Land Surface Temperature Estimation from the Landsat Series. Remote Sensing **12**.

Estoque, R. C., Y. Murayama, and S. W. Myint. 2017. Effects of landscape composition and pattern on land surface temperature: An urban heat island study in the megacities of Southeast Asia. Sci Total Environ **577**:349-359.

Fan, C., S. Myint, S. Kaplan, A. Middel, B. Zheng, A. Rahman, H.-P. Huang, A. Brazel, and D. Blumberg. 2017. Understanding the Impact of Urbanization on Surface Urban Heat Islands—A Longitudinal Analysis of the Oasis Effect in Subtropical Desert Cities. Remote Sensing **9**.

Fossa, A. J., J. Zelner, R. Bergmans, K. Zivin, and S. D. Adar. 2023. Sociodemographic correlates of greenness within public parks in three U.S. cities. Wellbeing, Space and Society **5**.

Gong, C., J. Chen, and S. Yu. 2013. Biotic homogenization and differentiation of the flora in artificial and near-natural habitats across urban green spaces. Landscape and Urban Planning **120**:158-169.

Gorelick, N., M. Hancher, M. Dixon, S. Ilyushchenko, D. Thau, and R. Moore. 2017. Google Earth Engine: Planetary-scale geospatial analysis for everyone. Remote Sensing of Environment **202**:18-27.

Groffman, P. M., J. Cavender-Bares, N. D. Bettez, J. M. Grove, S. J. Hall, J. B. Heffernan, S. E. Hobbie, K. L. Larson, J. L. Morse, C. Neill, K. Nelson, J. O'Neil-Dunne, L. Ogden, D. E. Pataki, C. Polsky, R. R. Chowdhury, and M. K. Steele. 2014. Ecological homogenization of urban USA. Frontiers in Ecology and the Environment **12**:74-81.

Grove, J. M., D. H. Locke, and J. P. O'Neil-Dunne. 2014. An ecology of prestige in New York City: examining the relationships among population density, socio-economic status, group identity, and residential canopy cover. Environ Manage **54**:402-419.

Guo, L., L. Di, C. Zhang, L. Lin, F. Chen, and A. Molla. 2022. Evaluating contributions of urbanization and global climate change to urban land surface temperature change: a case study in Lagos, Nigeria. Sci Rep **12**:14168.

Gyourko, J., P. Linneman, and S. C. Wachter. 1999. Analyzing the relationships among race, wealth, and home ownership in America. Journal of Housing Economics **8**:63-89.

Harlan, S. L., A. J. Brazel, L. Prashad, W. L. Stefanov, and L. Larsen. 2006. Neighborhood microclimates and vulnerability to heat stress. Soc Sci Med **63**:2847-2863.

Hengl, T. 2018. Global Maps of Potential Natural Vegetation at 1 km resolution. Harvard Dataverse.

Hill, E., J. H. Dorfman, and E. Kramer. 2010. Evaluating the impact of government land use policies on tree canopy coverage. Land Use Policy **27**:407-414.

Hope, D., C. Gries, W. Zhu, W. F. Fagan, C. L. Redman, N. B. Grimm, A. L. Nelson, C. A. Martin, and A. Kinzig. 2003. Socioeconomics drive urban plant diversity. Proc Natl Acad Sci U S A **100**:8788-8792.

Huxman, T. E., M. D. Smith, P. A. Fay, A. K. Knapp, R. M. Shaw, M. E. Loik, S. D. Smith, D. T. Tissue, J. C. Zak, J. F. Weltzin, W. T. Pockman, O. E. Sala, B. M. Haddad, J. Harte, G. W. Koch, S. Schwinning, E. E. Small, and D. G. Williams. 2004. Convergence across biomes to a common rain-use efficiency. Nature **429**:651-654.

Ibsen, P. C., D. Borowy, T. Dell, H. Greydanus, N. Gupta, D. M. Hondula, T. Meixner, M. V. Santelmann, S. A. Shiflett, M. C. Sukop, C. M. Swan, M. L. Talal, M. Valencia, M. K. Wright, and G. D. Jenerette. 2021. Greater aridity increases the magnitude of urban nighttime vegetation-derived air cooling. Environmental Research Letters **16**.

Ismaeil, E. M. H., and A. E. E. Sobaih. 2022. Assessing Xeriscaping as a Retrofit Sustainable Water Consumption Approach for a Desert University Campus. Water **14**.

Jenerette, G. D., G. Miller, A. Buyantuev, D. E. Pataki, T. W. Gillespie, and S. Pincetl. 2013. Urban vegetation and income segregation in drylands: a synthesis of seven metropolitan regions in the southwestern United States. Environmental Research Letters **8**.

Jesdale, B. M., R. Morello-Frosch, and L. Cushing. 2013. The racial/ethnic distribution of heat risk-related land cover in relation to residential segregation. Environ Health Perspect **121**:811-817.

Kondratyeva, A., S. Knapp, W. Durka, I. Kühn, J. Vallet, N. Machon, G. Martin, E. Motard, P. Grandcolas, and S. Pavoine. 2020. Urbanization Effects on Biodiversity Revealed by a Two-Scale Analysis of Species Functional Uniqueness vs. Redundancy. Frontiers in Ecology and Evolution **8**.

Kucera, D., and G. D. Jenerette. 2023. Urban greenness and its cooling effects are influenced by changes in drought, physiography, and socio-demographics in Los Angeles, CA. Urban Climate **52**.

Kühn, I., and S. Klotz. 2006. Urbanization and homogenization – Comparing the floras of urban and rural areas in Germany. Biological Conservation **127**:292-300.

Lazzarini, M., A. Molini, P. R. Marpu, T. B. M. J. Ouarda, and H. Ghedira. 2015. Urban climate modifications in hot desert cities: The role of land cover, local climate, and seasonality. Geophysical Research Letters **42**:9980-9989.

Leong, M., R. R. Dunn, and M. D. Trautwein. 2018. Biodiversity and socioeconomics in the city: a review of the luxury effect. Biol Lett **14**.

Liu, Z., W. Zhan, B. Bechtel, J. Voogt, J. Lai, T. Chakraborty, Z.-H. Wang, M. Li, F. Huang, and X. Lee. 2022. Surface warming in global cities is substantially more rapid than in rural background areas. Communications Earth & Environment **3**.

Markham, B. L., J. C. Storey, D. L. Williams, and J. R. Irons. 2004. Landsat sensor performance: history and current status. IEEE Transactions on Geoscience and Remote Sensing **42**:2691-2694.

McCabe, B. J. 2018. Why Buy a Home? Race, Ethnicity, and Homeownership Preferences in the United States. Sociology of Race and Ethnicity **4**:452-472.

McKinney, M. L. 2006. Urbanization as a major cause of biotic homogenization. Biological Conservation **127**:247-260.

McPhearson, T., S. T. A. Pickett, N. B. Grimm, J. Niemelä, M. Alberti, T. Elmqvist, C. Weber, D. Haase, J. Breuste, and S. Qureshi. 2016. Advancing Urban Ecology toward a Science of Cities. BioScience **66**:198-212.

McPherson, E. G., and N. Luttinger. 1998. From nature to nurture: The history of Sacramento's urban forest. Journal of Arboriculture **24**:72-88.

Meerow, S., M. Natarajan, and D. Krantz. 2021. Green infrastructure performance in arid and semi-arid urban environments. Urban Water Journal **18**:275-285.

Mincey, S. K., M. Schmitt-Harsh, and R. Thurau. 2013. Zoning, land use, and urban tree canopy cover: The importance of scale. Urban Forestry & Urban Greening **12**:191-199.

Nardone, A., K. E. Rudolph, R. Morello-Frosch, and J. A. Casey. 2021. Redlines and Greenspace: The Relationship between Historical Redlining and 2010 Greenspace across the United States. Environ Health Perspect **129**:17006.

Nowak, D. J., and E. J. Greenfield. 2012. Tree and impervious cover change in U.S. cities. Urban Forestry & Urban Greening **11**:21-30.

Nowak, D. J., and E. J. Greenfield. 2018. Declining urban and community tree cover in the United States. Urban Forestry & Urban Greening **32**:32-55.

Ossola, A., D. Locke, B. Lin, and E. Minor. 2019. Greening in style: Urban form, architecture and the structure of front and backyard vegetation. Landscape and Urban Planning **185**:141-157.

Ossola, A., L. A. Schifman, D. L. Herrmann, A. S. Garmestani, K. Schwarz, and M. E. Hopton. 2018. The provision of urban ecosystem serices throughout the private-social-public domain: A conceptual framework. Cities and the Environment (CATE) **11**:1-15.

Pearse, W. D. C.-B., J., S. E. A. Hobbie, M. L., N. Bettez, R. R. Chowdhury, L. E. Darling, P. M. Groffman, J. Grove, S. J. Hall, J. B. Heffernan, J. Learned, C. Neill, K. C. Nelson, D. Pataki, B. Ruddell, M. K. Steele, and T. L. E. Trammell. 2018. Homogenization of plant diversity, composition, and structure in North American urban yards. Ecosphere **9**.

Pettorelli, N., S. Ryan, T. Mueller, N. Bunnefeld, B. Jedrzejewska, M. Lima, and K. Kausrud. 2011. The Normalized Difference Vegetation Index (NDVI): unforeseen successes in animal ecology. Climate Research **46**:15-27.

Piao, S., X. Wang, T. Park, C. Chen, X. Lian, Y. He, J. W. Bjerke, A. Chen, P. Ciais, H. Tømmervik, R. R. Nemani, and R. B. Myneni. 2019. Characteristics, drivers and feedbacks of global greening. Nature Reviews Earth & Environment **1**:14-27.

Polsky, C., J. M. Grove, C. Knudson, P. M. Groffman, N. Bettez, J. Cavender-Bares, S. J. Hall, J. B. Heffernan, S. E. Hobbie, K. L. Larson, J. L. Morse, C. Neill, K. C. Nelson, L. A. Ogden, J. O'Neil-Dunne, D. E. Pataki, R. R. Chowdhury, and M. K. Steele. 2014. Assessing the homogenization of urban land management with an application to US residential lawn care. Proc Natl Acad Sci U S A **111**:4432-4437.

Potchter, O., D. Goldman, D. Kadish, and D. Iluz. 2008. The oasis effect in an extremely hot and arid climate: The case of southern Israel. Journal of Arid Environments **72**:1721-1733.

Qiu, S., Y. Lin, R. Shang, J. Zhang, L. Ma, and Z. Zhu. 2018. Making Landsat Time Series Consistent: Evaluating and Improving Landsat Analysis Ready Data. Remote Sensing **11**.

Quesnel, K. J., N. Ajami, and A. Marx. 2019. Shifting landscapes: decoupled urban irrigation and greenness patterns during severe drought. Environmental Research Letters **14**.

Rahman, M. A., L. M. F. Stratopoulos, A. Moser-Reischl, T. Zölch, K.-H. Häberle, T. Rötzer, H. Pretzsch, and S. Pauleit. 2020. Traits of trees for cooling urban heat islands: A meta-analysis. Building and Environment **170**.

Reyes-Paecke, S., J. Gironás, O. Melo, S. Vicuña, and J. Herrera. 2019. Irrigation of green spaces and residential gardens in a Mediterranean metropolis: Gaps and opportunities for climate change adaptation. Landscape and Urban Planning **182**:34-43.

Riedman, E., L. A. Roman, H. Pearsall, M. Maslin, T. Ifill, and D. Dentice. 2022. Why don't people plant trees? Uncovering barriers to participation in urban tree planting initiatives. Urban Forestry & Urban Greening **73**.

Roy, D. P., V. Kovalskyy, H. K. Zhang, E. F. Vermote, L. Yan, S. S. Kumar, and A. Egorov. 2016. Characterization of Landsat-7 to Landsat-8 reflective wavelength and normalized difference vegetation index continuity. Remote Sensing of Environment **185**:57-70.

Roy, D. P., Z. Li, H. K. Zhang, and H. Huang. 2020. A conterminous United States analysis of the impact of Landsat 5 orbit drift on the temporal consistency of Landsat 5 Thematic Mapper data. Remote Sensing of Environment **240**.

Schwarz, K., M. Fragkias, C. G. Boone, W. Zhou, M. McHale, J. M. Grove, J. O'Neil-Dunne, J. P. McFadden, G. L. Buckley, D. Childers, L. Ogden, S. Pincetl, D. Pataki, A.
Whitmer, and M. L. Cadenasso. 2015. Trees grow on money: urban tree canopy cover and environmental justice. PLoS One **10**:e0122051.

Smith, I. A., V. K. Dearborn, and L. R. Hutyra. 2019. Live fast, die young: Accelerated growth, mortality, and turnover in street trees. PLoS One **14**:e0215846.

Summit, J., and E. G. McPherson. 1998. Residential tree planting and care: Study of attitudes and behavior in Sacramento, CA. Journal of Aboriculture **24**:89-97.

Sun, B., P. Groisman, F. Keimig, and R. Bradley. 2000. Temporal Changes in the Observed Relationship between Cloud Cover and Surface Air Temperature. Journal of Climate **13**:4341-4357.

Threlfall, C. G., L. D. Gunn, M. Davern, and D. Kendal. 2022. Beyond the luxury effect: Individual and structural drivers lead to 'urban forest inequity' in public street trees in Melbourne, Australia. Landscape and Urban Planning **218**.

Trenberth, K. E., and D. J. Shea. 2005. Relationships between precipitation and surface temperature. Geophysical Research Letters **32**

Watkins, S. L., and E. Gerrish. 2018. The relationship between urban forests and race: A meta-analysis. J Environ Manage **209**:152-168.

Wilson, B. 2020. Urban Heat Management and the Legacy of Redlining. Journal of the American Planning Association **86**:443-457.

Winbourne, J. B., T. S. Jones, S. M. Garvey, J. L. Harrison, L. Wang, D. Li, P. H. Templer, and L. R. Hutyra. 2020. Tree Transpiration and Urban Temperatures: Current Understanding, Implications, and Future Research Directions. BioScience **70**:576-588.

Wong, D. W., and M. Sun. 2013. Handling Data Quality Information of Survey Data in GIS: A Case of Using the American Community Survey Data. Spatial Demography **1**:3-16.

Yang, C., R. Li, and Z. Sha. 2020. Exploring the Dynamics of Urban Greenness Space and Their Driving Factors Using Geographically Weighted Regression: A Case Study in Wuhan Metropolis, China. Land **9**.

Yang, L., F. Qian, D.-X. Song, and K.-J. Zheng. 2016. Research on Urban Heat-Island Effect. Procedia Engineering **169**:11-18.

Yu, Z., S. Xu, Y. Zhang, G. Jorgensen, and H. Vejre. 2018. Strong contributions of local background climate to the cooling effect of urban green vegetation. Sci Rep **8**:6798.

Zhang, Y., C. Song, L. E. Band, G. Sun, and J. Li. 2017. Reanalysis of global terrestrial vegetation trends from MODIS products: Browning or greening? Remote Sensing of Environment **191**:145-155.

Zhao, L., X. Lee, and N. M. Schultz. 2017. A wedge strategy for mitigation of urban warming in future climate scenarios. Atmospheric Chemistry and Physics **17**:9067-9080.

Zhao, L., X. Lee, R. B. Smith, and K. Oleson. 2014. Strong contributions of local background climate to urban heat islands. Nature **511**:216-219.

Zhu, B., Y. Cheng, X. Hu, Y. Chai, W. R. Berghuijs, A. G. L. Borthwick, and L. Slater. 2023. Constrained tropical land temperature-precipitation sensitivity reveals decreasing evapotranspiration and faster vegetation greening in CMIP6 projections. npj Climate and Atmospheric Science **6**.

Zhu, Z. 2019. Science of Landsat Analysis Ready Data. Remote Sensing **11**.

Figures

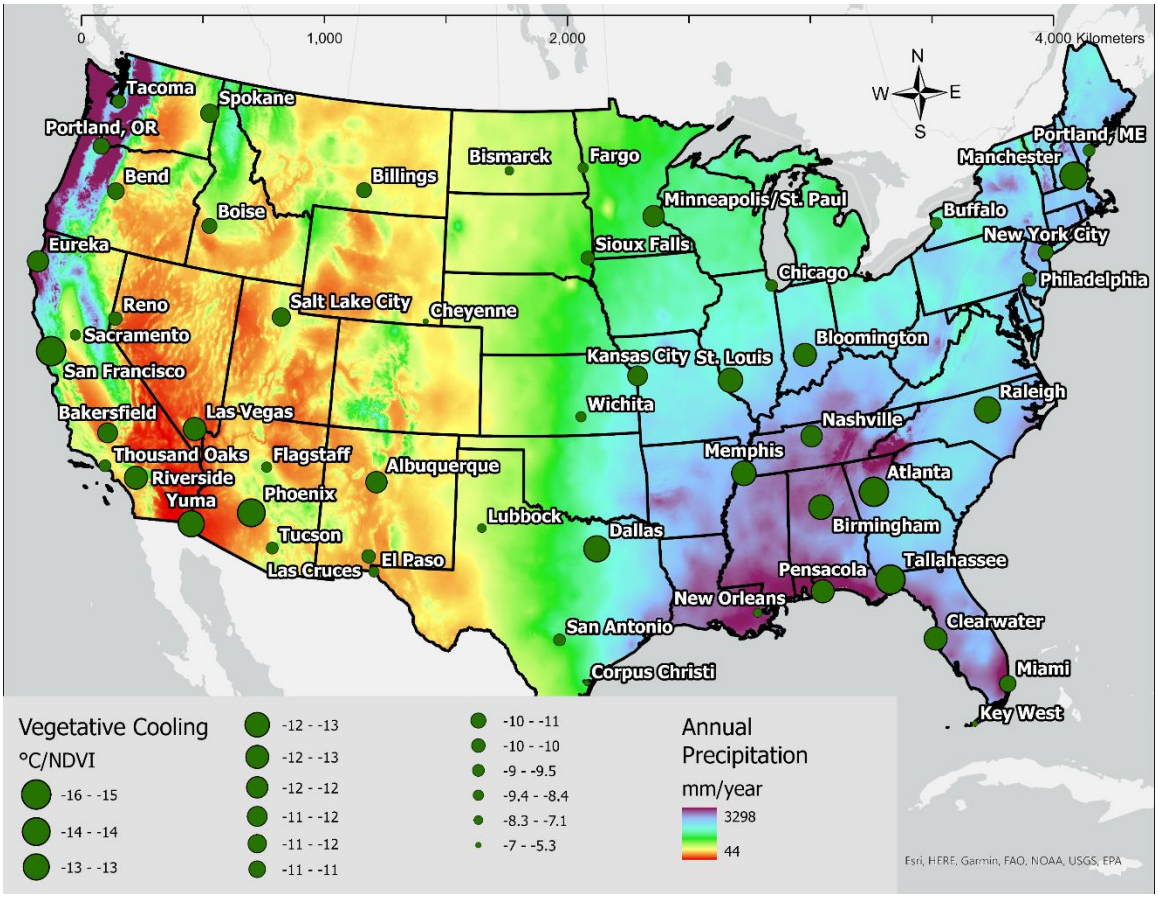

Figure 2.1 We assessed how vegetative cooling change at the continental scale for 52 cities in the conterminous United States, and the difference between cities and reference sites using the Landsat Analysis Ready Data dataset. Circles represent the cooling effectiveness of urban vegetation, with larger circles indicating greater vegetative cooling.

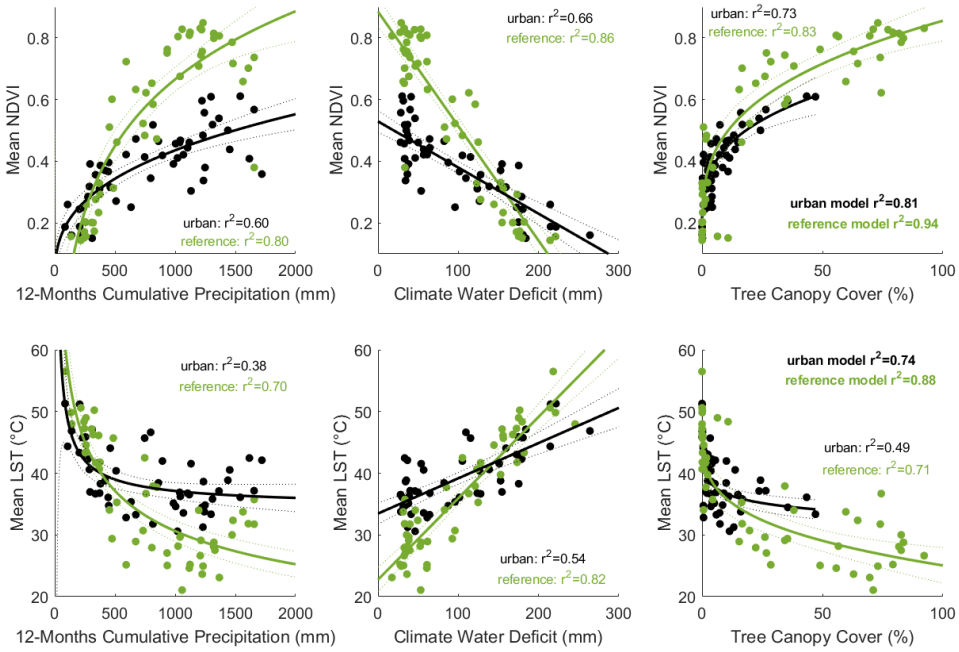

Figure 2.2 Urbanization decreased the sensitivity of NDVI and LST to annual precipitation at the continental scale, while the relationship of urban NDVI and LST with VPD was significantly different from that in reference sites. Similarly, tree canopy cover had a weaker relationship on the NDVI and LST of cities than in reference sites.

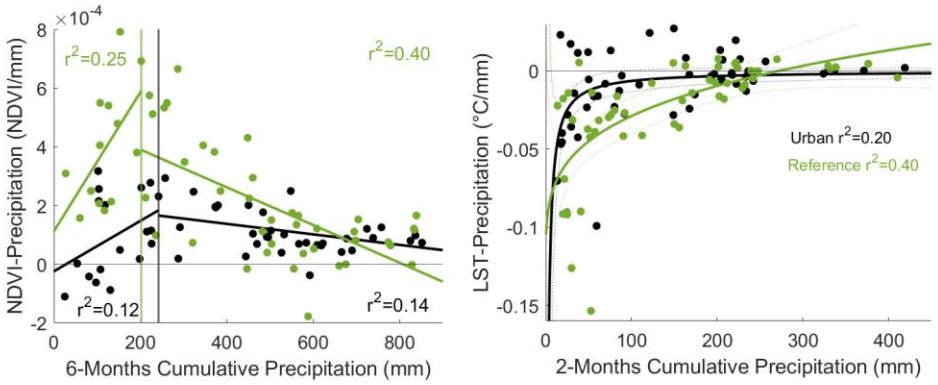

Figure 2.3 The sensitivity of NDVI to rain was driven by changes in the climate, with this response stronger in reference sites compared to urban sites. In both reference and urban sites, the sensitivity of NDVI to rain increased with low levels of rainfall up to a maximum at about 200 mm of 6-months cumulative rainfall, after which the sensitivity of NDVI to rain declined with increasing precipitation. At the lowest levels of precipitation there was no relationship (slope of 0 or negative) between urban NDVI and precipitation, suggesting the effect of irrigation in decoupling urban greenness from precipitation in the driest cities. The LST~Precipitation relationship was similar; LST decreased the most with rainfall in arid cities, whereas LST was not affected by rainfall in high-precipitation cities. In contrast to the NDVI relationship, where the reference site NDVI responded more strongly to rain than urban NDVI, urban LST was more sensitive to rain than reference site LST.

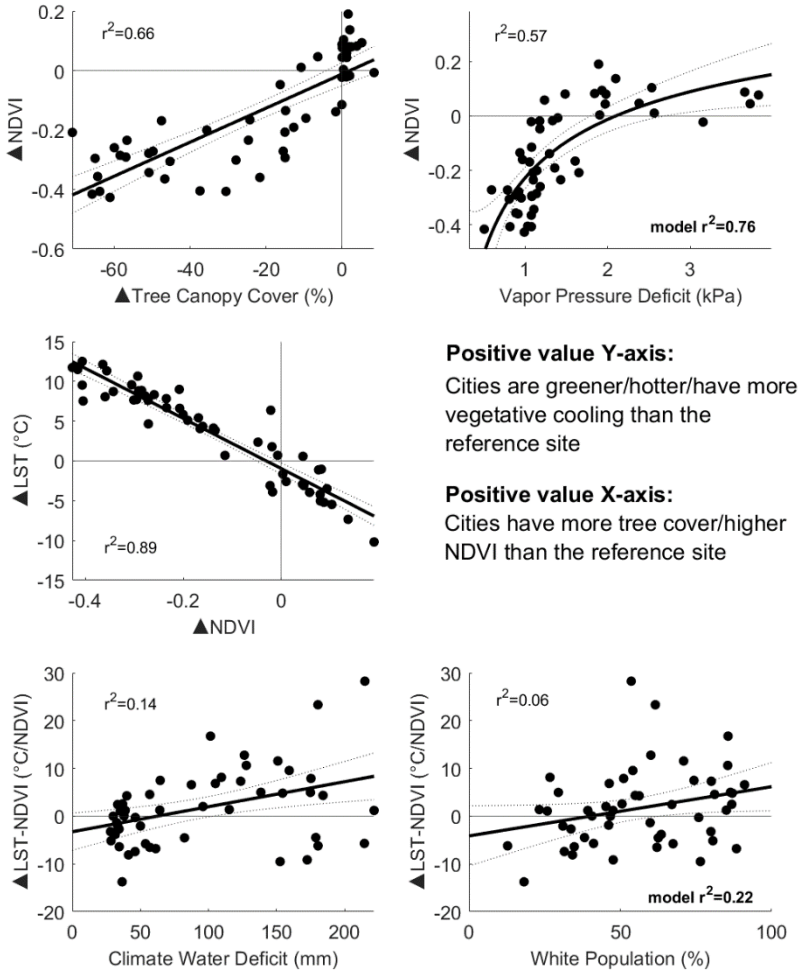

Figure 2.4 The difference in urban NDVI, LST, and vegetative cooling between a city and its non-urban reference site is predominantly driven by climate and landcover. NDVI was greater in cities when cities had more tree cover, while regions with high VPD favored higher NDVI in cities. The difference in LST between cities and reference sites was driven solely by the difference in NDVI; cities with higher NDVI than their reference site were cooler. Vegetative cooling was greater in cities in regions with a higher climate water deficit, while cities with a higher percentage of white residents were weakly associated with greater vegetative cooling compared to a non-urban reference site.

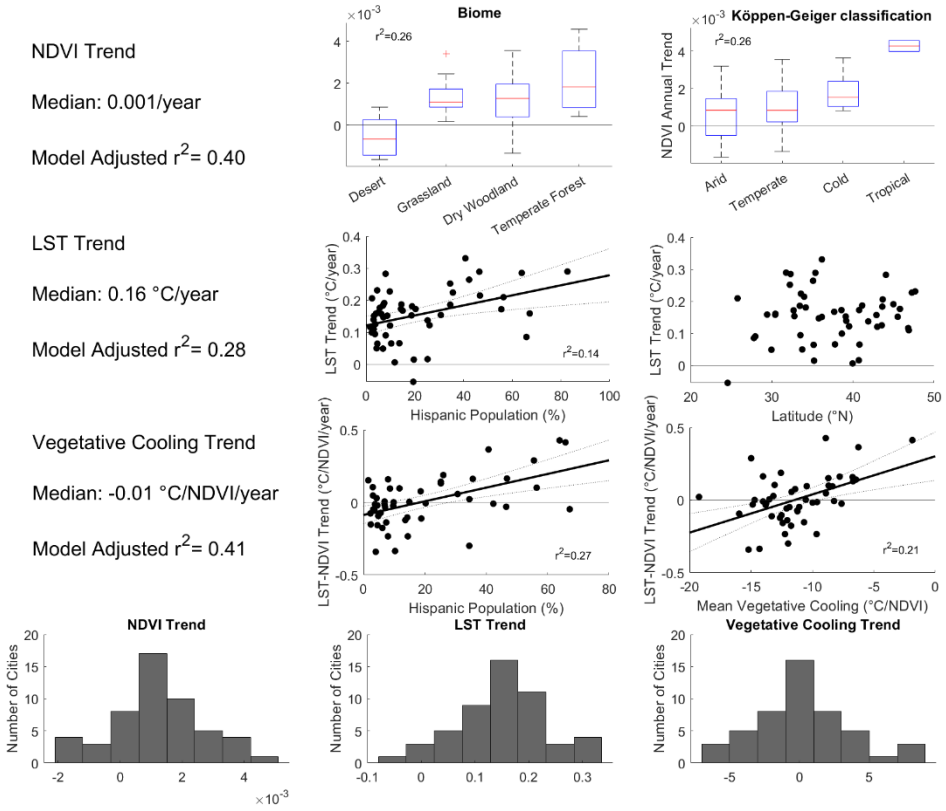

Figure 2.5 NDVI, LST, and vegetative cooling all changed through time at a continental, multidecadal scale. The change in NDVI was geographically dependent on biome or Köppen-Geiger classification. The LST trend was more rapid in cities with a larger Hispanic population, and in cities which were further north. The vegetative cooling trend was split among cities between an increase and a decrease; vegetative cooling was more likely to decrease through time in cities with a large Hispanic population and which had the lowest mean levels of vegetative cooling.

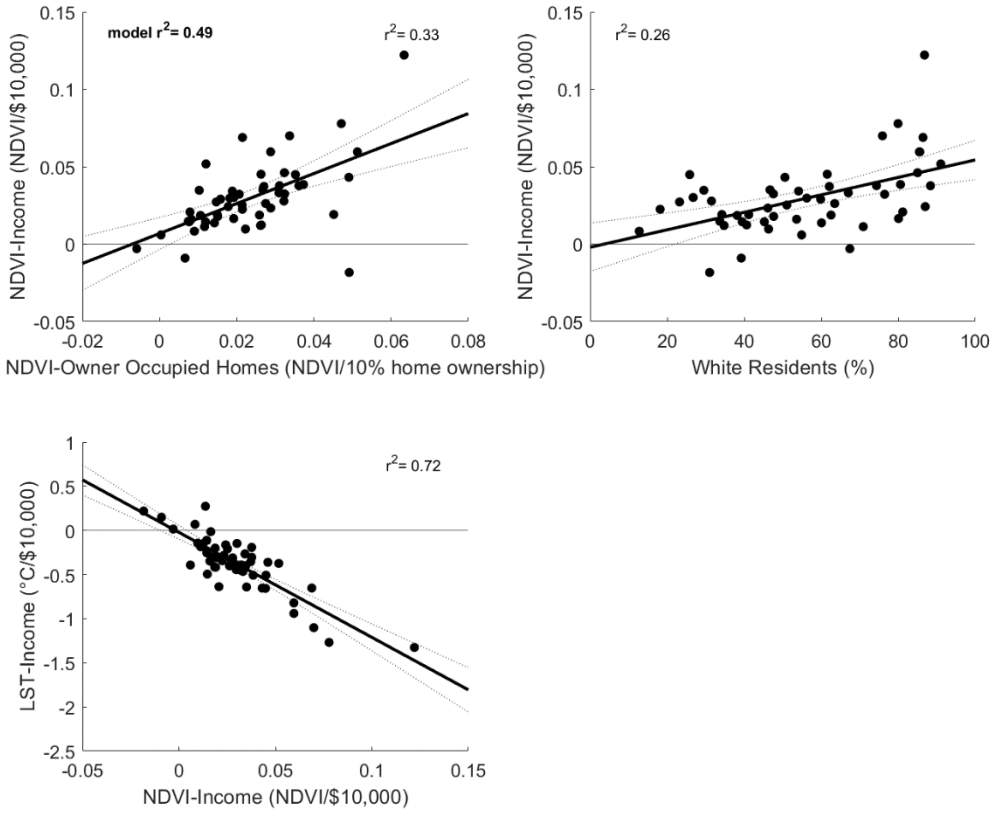

Figure 2.6 At the continental scale, the mean effect of income on NDVI was stronger in cooler cities and in those with a higher proportion of white residents. Mean income-LST was only explained by income-NDVI, where cities which had a stronger relationship between income and NDVI also had a stronger relationship between income and LST.

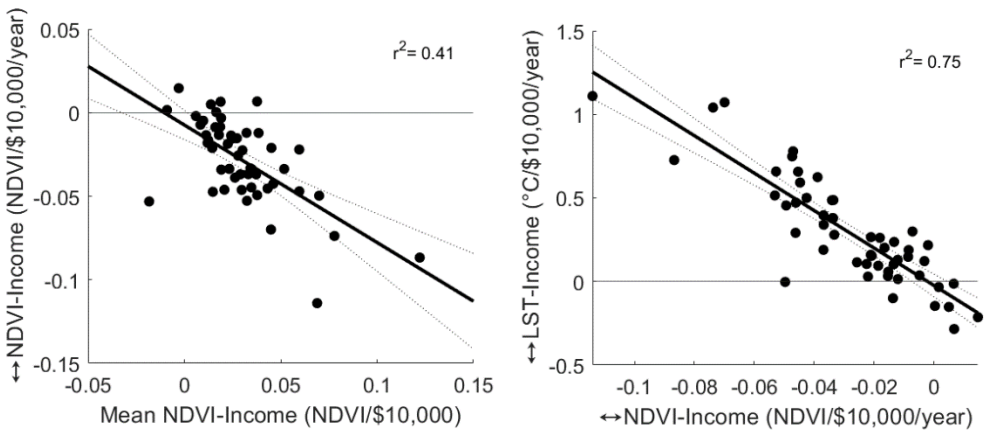

Figure 2.7 The luxury effect with regards to NDVI-income and LST-income declined 62% and 53% respectively between 2000 and 2020. The decline in the effect of income as a mediator of LST was greatest in cities which had the greatest declines in the effect of income as a mediator of NDVI. The decline in the effect of income as a mediator of NDVI declined the most in cities with a stronger mean relationship between income and NDVI.

Supplementary Figures

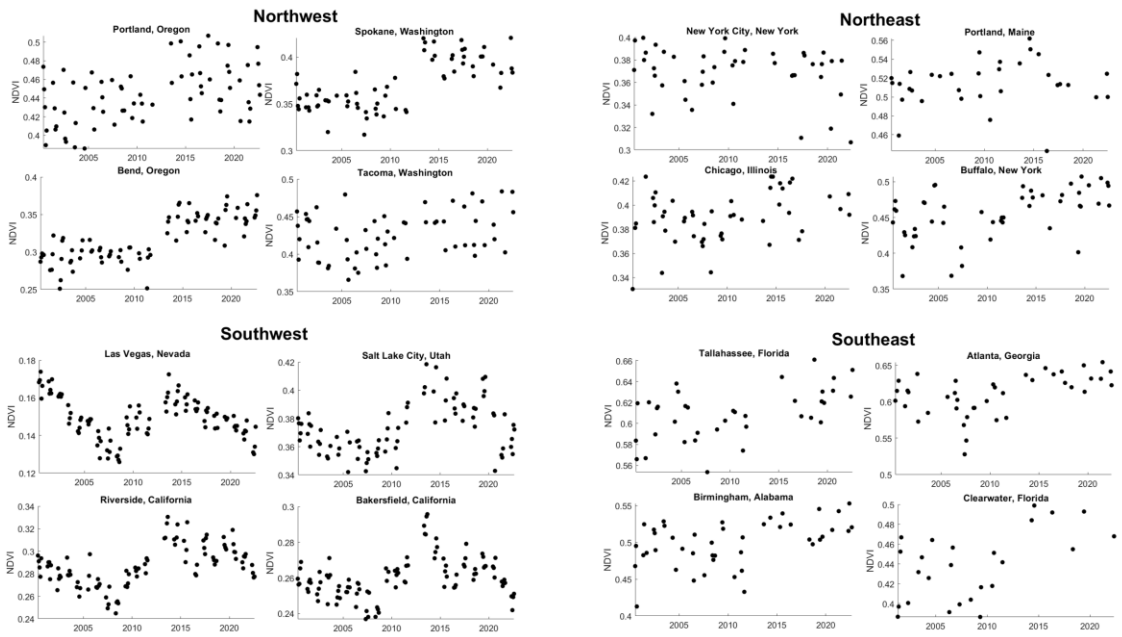

Figure 2.S1 Trends in urban NDVI were generally increasing at the continental scale between 2000 and 2022, however, cities in the arid southwest exhibited NDVI trends unusually similar to other cities within the same biome. Within this region urban NDVI trends were more similar to other arid cities than to the non-urban ecosystems those cities replaced.

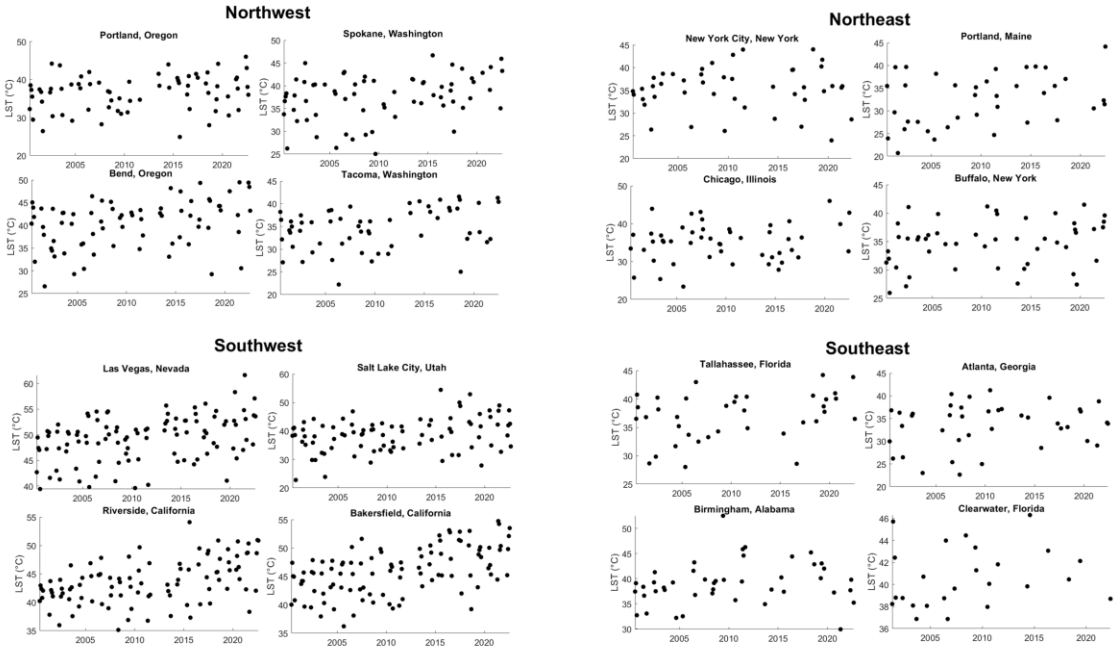

Figure 2.S2 At the continental scale cities warmed on average 0.16 °C/year between 2000 and 2022, however, cities in arid environments warmed most rapidly at a rate of 0.23 °C/year.

Chapter 3

Global-Scale Multidecadal Changes in Urban Greenness and Temperature Has Led to Declines in Vegetative Cooling

Abstract

The temporal evolution of urban microclimates, particularly under the influence of drought and ongoing climate change, profoundly affects the quality of life in cities. The dynamics of urban greenness and temperature change through time, yet our understanding of the temporal changes in these variables and their associated factors among cities at a global scale is poor. Here, we focus on a diverse set of 266 cities from across 82 countries, examining the changing dynamics and interactions among urban vegetation, and temperature, and associated changes in vegetative cooling, through the lens of Landsat-derived greenness and surface temperature data from 1995 through 2023. We hypothesize that intercity urban dynamics are primarily driven by inter-urban water availability and water demand, as well as being mediated by a city's developmental categorization either by continent or by being in the Global North, a BRICS nation, or a low-and-middle-income nation. Our findings indicate that urban surface temperatures increased by 0.14 °C/year, greenness increased by 7.01 x 10^{-4} per year, and vegetative cooling declined by 0.04 °C/NDVI/year. Global changes in urban dynamics were associated with a city's climatic context and geographic location, leading to global-scale changes that were highly variable. We find that cities in Europe greened the most while cities in Africa greened the least, cities in Europe and North America exhibited the fastest rates of warming, while low-and-middle-income countries experienced the fastest declines in vegetative cooling. These findings have implications for future urban planning

and climate change adaptation strategies, particularly in the importance of emphasizing a city's unique environmental and geographic context in fully appreciating urban environmental dynamics.

Introduction

Urban greenness and temperature are known to be spatially dependent, however, the global evolution of these dynamics at multidecadal scales, in the context of climate change and rapid urbanization, are not well understood. At multidecadal scales, urbanization is intensifying (Zhang 2016, Ren et al. 2022) altering the availability of greenspace (Richards et al. 2017), while precipitation has increased in select geographies (Adler et al. 2017), leading to altered relationships between landcover or precipitation and greenness and temperatures through time. Further, cities are warming more rapidly than their non-urban hinterlands (Liu et al. 2022), while ecosystems globally have been experiencing greening (Piao et al. 2019). The relationships between urban greenness and temperature may therefore not be temporally stable, leading to uncertain changes to urban vegetative cooling, particularly on a global scale. Thus, the relationships between urban greenness, temperature, and vegetative cooling are likely changing across cities over multidecadal periods, although many uncertainties remain as to how these relationships change through time or how this change is mediated.

The inter-urban relationship between urban greenness and temperature is known to be mediated by many variables, particularly the climate (Jenerette et al. 2016) and socio-economics (Schwarz et al. 2015). Socioeconomics are an important driver of the greenness-temperature relationship; the increase in greenness and decrease in temperature with income has been well-studied at intra-urban scales via assessment of the luxury effect (Jenerette et al. 2006, Buyantuyev and Wu 2009, Shih 2022). The luxury effect may lower urban temperatures via increased vegetative cooling. Vegetative cooling is

known to be climate dependent, with greater vegetative cooling with greater aridity (Ibsen et al. 2021) and during the summer months (Su et al. 2022). Precipitation can have a direct influence on vegetation greenness, and by extension vegetative cooling, by moderating the availability of water, which affects the growth and distribution of vegetation (Pettorelli et al. 2005). Conversely, at intra-urban scales the sensitivity of urban vegetation to precipitation has been shown to decline with aridity due to increasing irrigation (Buyantuyev and Wu 2012), although this may not be applicable at the global scale due to cities in the Low- and lower-middle-income countries (LMIC) lacking the necessary irrigation infrastructure (Dos Santos et al. 2017). A city's climatic and socio-economic context is therefore crucial to fully understanding that city's greenness and temperature relationship.

Changes in the climate, particularly changes in aridity, soil moisture, and drought conditions, modify the water available to urban plants. Other geographic and physiographic gradients also mediate urban water availability. Elevation may be associated with a decline in soil moisture (Pellet and Hauck 2017), while precipitation patterns favor tropical regions. Continental-scale differences in greenness and temperature may likewise be attributable to differences in water availability and water demand. At multidecadal scales a city's climatic context as well as its landcover and socioeconomics undergo change, suggesting the need for a multidecadal analysis to fully appreciate changing urban dynamics.

This multidecadal, global analysis takes a macrosystems approach (Heffernan et al. 2014) to understanding urban ecological dynamics, utilizing the Landsat suite of

satellites to both quantify changes over large spatial scales and long temporal spans. We seek to provide a holistic understanding of the interactions between urban greenness, temperature, and vegetative cooling to identify general patterns and processes that govern urban ecosystems, in an ecology "of" cities paradigm (Pickett et al. 2017). In doing so we assess the dynamics of urban greenness and temperature among 266 global cities at a multidecadal scale. In assessing the spatiotemporal distributions of urban biophysical dynamics, we ask: How does urban greenness, temperature, and vegetative cooling differ among cities at the global scale, and how have these variables changed over time?

In answering our research question, we employ advanced statistical techniques and leverage a large urban dataset, revealing the dynamic relationships between urban greenness, temperature, and vegetative cooling at a global, inter-urban scale. We test two hypotheses: first, an inter-urban water deficit hypothesis, which says that at a global scale urban greenness, temperature, and vegetative cooling dynamics will be related to climatic and topographic variables associated with water availability and demand. We also test an economic hypothesis, which says that dynamics in urban greenness, temperature, and vegetative cooling will be different by a city's developmental categorization, with cities in more affluent nations experiencing greater greening, less warming, and greater vegetative cooling. We predict that global greenness and temperature are dependent on a city's climatic and geographic context, with greenness and temperature increasing in more mesic and more arid environments, respectively. Greenness and land surface temperature are tightly associated at local scales, and we predict that this is also the case at the global scale, where greener cities are also cooler. However, dynamics of urban

greenness and temperature are likely not stable through time. We predict that through time greenness and temperature increased in response to afforestation and climate change. We test variability in urban surface temperature trends, predicting that a city's geographic and climatic context mediates these relationships. We predict that the long-term trend in vegetative cooling is related to landcover and the climate, decreasing with low tree canopy cover and increasing with high tree canopy cover, while decreasing with greater vapor pressure deficit. Our research highlights the role of a city's climatic and socio-economic context in shaping global inter-urban dynamics in greenness, temperature, and vegetative cooling, providing valuable insights for effective policymaking, resource allocation, and evidence-based strategies for sustainable urban development and climate change adaptation.

Methods

2.1 *Study Sites*

We selected 266 cities from 82 countries for a multidecadal analysis spanning the summer months from 1995 through 2023. City boundaries were manually delineated using average RGB Landsat imagery from 1990-1995, ensuring that changes in greenness or temperature over time were not due to land use transitions from non-urban or agricultural to urban areas. Most of the cities (86%) were in the Northern Hemisphere, reflecting a larger land area and population. To capture vegetative dynamics during periods when trees were not defoliated due to winter leaf fall, data for all cities were centered around each city's summer season. For cities in the Northern Hemisphere, data

were acquired for May through September, while for cities in the Southern Hemisphere, data were acquired from November through March.

City selection was guided by identifying cities within developmental categories of the Global North, BRICS nations (Brazil, Russia, India, China, South Africa), and the low-and-middle-income countries (LMIC). Within each development category, we selected a minimum of seven cities along gradients of temperature, aridity, and population. Cities with populations larger than 500,000 were considered large, while all others were considered small. The coldest cities (bottom 10%) had a summertime mean air temperature of 13.0 °C while the hottest cities (top 10%) had a summertime mean air temperature of 31.3 °C. The wettest cities received an average of 1,082.2 mm of rain per year, while the driest cities received 76.5 mm of rain per year. Cities from the United States constituted more than 20% of the cities in the dataset, reflecting this study's extension of prior work examining multi-decadal urban greenness, temperature, and vegetative cooling dynamics at a continental scale.

2.2 *Landsat NDVI, Temperature, and Google Earth Engine Data Acquisition*

To efficiently assess vegetative greenness and land surface temperature (LST) across large spatial and temporal scales, we utilized the Google Earth Engine (GEE) platform, a JavaScript-based petabyte-scale GIS housed in the cloud (Gorelick et al. 2017). GEE allows for rapid manipulation of vast quantities of geospatial imagery, both temporally and spatially. All dependent and independent variables for this analysis were collected and pre-processed in GEE. All greenness and temperature data came from the Landsat suite of satellites. Landsat, first launched in 1972, and maintained with the

launch of the most recent Landsat 9 in 2021, represents the longest continuous record of space-based Earth-observation imagery (Showstack 2022).

Using GEE, we analyzed the Normalized Difference Vegetation Index (NDVI) as an indicator of vegetative greenness. NDVI is a widely employed vegetation index that leverages the ratio between the visible and near-infrared parts of the electromagnetic spectrum to identify photosynthetically active vegetation (Carlson et al. 1994). Working with time series Landsat imagery within GEE presented challenges in terms of necessary inter-satellite calibrations. Analysis Ready Data (ARD), provided by the United States Geological Survey (USGS), largely addresses this issue through standardized atmospheric and radiometric calibration (Dwyer 2018). ARD ensures the Landsat satellites are comparable and suitable for time series analysis (Zhu 2019) yet is only available for the conterminous United States, Alaska, and Hawaii. To extend the length of our time series and maintain the flexibility of manipulating a dataset entirely available on GEE, we opted to manually harmonize the spectral bands of the Landsat satellites.

We harmonized NDVI using Landsat Collection-2 Level-2 Tier 1 imagery for Landsat 5 (LANDSAT/LT05/C02/T1_L2), Landsat 7 (LANDSAT/LE07/C02/T1_L2), Landsat 8 (LANDSAT/LC08/C02/T1_L2), and Landsat 9 (LANDSAT/LC09/C02/T1_L2) with scaling coefficients published in Roy et al. (2016). The scaling coefficients were derived by using ordinary least squares regression to linearly transform Landsat 8/OLI reflectance values, ensuring consistency with the reflectance values of Landsat 5/TM and Landsat 7/ETM+. We applied the same scaling coefficients for Landsat 8 to Landsat 9. The instrumentation on Landsat 9 is nearly

identical to that on Landsat 8 (Masek et al. 2020), leading to low disagreement of less than 0.2% for most spectral bands with uncertainty of up to 0.5-1% for the green band for certain vegetation (Gross et al. 2022). Harmonization of spectral bands and derivation of NDVI was completed in GEE.

In addition to NDVI we evaluated land surface temperature (LST), the thermal radiance from land due to solar radiation (Khan et al. 2021), which plays a crucial role in many ecologically significant phenomena (Li et al. 2013). To assess LST we used the Surface Temperature product bundled with the Landsat Collection-2 Level-2 imagery. We initially sought to harmonize the thermal bands among the Landsat satellites, however, doing so is more challenging as no straightforward methodology has been proposed due to high spatial and temporal variability in thermal emission (Cao et al. 2022) and stray light contamination. However, the Surface Temperature product is radiometrically calibrated, making it suitable for inter-satellite time series analysis (Wang et al. 2023). Many urban studies utilize MODIS to assess urban temperatures (Shen and Leptoukh 2011, Peng et al. 2012, Zhou et al. 2015, Zhao and Wentz 2016, Liu et al. 2022), however, MODIS thermal imagery is provided at 1 km^2 resolution. Between Landsat 5 and 9, thermal imagery is captured at between 60 and 120 m^2 resolution, much finer than MODIS and which we felt would provide novel insights into global-scale urban thermal dynamics.

After acquiring our NDVI and LST datasets we then cloud masked and clipped them to the city extents within GEE. We used all available 1995-2023 Landsat imagery from Landsat 5, 8, and 9 and Landsat 7 through May 31st, 2003, due to the failure of that

satellite's scan line corrector (SLC). The SLC failure resulted wedges of missing pixels, increasing from zero missing pixels in the image center up to 14 missing pixels on the image periphery (Petrovskaia et al. 2022). In GEE we employed a strict filtering process to ensure the return of only the highest-quality imagery. This included setting filtering IMAGE_QUALITY_OLI and IMAGE_QUALITY_TIRS to 9, representing the best image quality. Following cloud and water masking we removed any individual image in which at least 5% of the pixels within a city's boundary were masked out. We removed any cities which had less than 15 valid, remaining images from across the time series. Many of the removed cities were from the tropics, including the Amazon, equatorial Africa, and the Malay Archipelago. Persistent cloud cover in these regions poses clear challenges to using visible spectrum satellite remote sensing to improve our understanding of the urban ecology of tropical cities (Ling et al. 2021).

After acquiring NDVI and LST from GEE, we uploaded the data to Matlab r2023b for analysis. We primarily employed gradient boosted machines (GBMs) to assess variability in our dependent variables. GBMs, while more sophisticated than other statistical tools such as multiple regression, are a powerful machine learning technique known for their effectiveness. GBMs are particularly adept at handling non-linear relationships and multicollinearity in a way similar to random forests. However, they often outperform random forests in predictive accuracy, especially in scenarios where the underlying data structure is complex (Friedman 2001). This advantage is largely due to the method's iterative approach, where each new tree is built to correct the errors of the previous ones. Additionally, GBMs provide a framework for estimating variable

importance, which offers valuable insight into the most influential predictors on the dependent variable. To increase our confidence of the GBM's selection of top predictors, we additionally implemented 5-fold cross validation, hyperparameter optimization via Bayesian optimization, the use of training and holdout datasets, and calculated permutation importance scores on multiple runs of the optimized model. The output from the GBM are partial dependence plots, which visualize adjusted values of the independent variable on the dependent variable considering the effects of all other variables in the model. In modelling the spatial dependencies of NDVI, LST, and vegetative cooling, we did not include variables of landcover as the relationship between, for instance, temperature and impervious surfaces is well understood. We defined our top predictors as those with a permuted importance score at least 1.5 standard deviations above the mean.

2.3 *Climate, Social, and Landcover Predictor Variables*

We assessed changes of NDVI and LST in response to select social, climatic, and landcover variables. We accessed climate variables using GEE from the TerraClimate (IDAHO_EPSCOR/TERRACLIMATE) dataset. TerraClimate is a global climate dataset valid from January 1958 through December 2021 (Abatzoglou et al. 2018), collected at a monthly scale and a ~4 km^2 resolution. From TerraClimate, we accessed climate water deficit, precipitation, potential evapotranspiration, solar radiation, minimum and maximum temperature, and vapor pressure deficit. We further modified the precipitation variable to create new variables representing 1-12 months of cumulative precipitation. We supplemented climate data with 2-meter air temperature from ERA5, a monthly

dataset at 0.25° resolution (Hersbach et al. 2023). From the Global Land Data Assimilation System (GLDAS) 2.2, a monthly dataset at 0.25° resolution, we acquired plant canopy surface water, evapotranspiration, and terrestrial water storage (Li et al. 2019, Li et al. 2020a). We were also interested in characterizing climatological drought in the region of each city. We did so with the Standardized Precipitation Evapotranspiration Index (SPEI; CSIC/SPEI/2_8). The standardization of this index allows for direct comparison through time and across space (Beguería et al. 2023).

Other variables we utilized included an elevation dataset from the Shuttle Radar Topography Mission digital elevation map (USGS/SRTMGL1_00) provided at 1-arc second resolution (Farr et al. 2007). We utilized a global map of biomes from (OpenLandMap/PNV/PNV_BIOME-TYPE_BIOME00K_C/v01) providing a global distribution of potential biomes at 1 km^2 resolution (Hengl 2018) and complemented this dataset with the Köppen-Geiger classification map for 1991-2020 (Beck et al. 2023). We did not utilize the "tundra" biome as none of our cities were present in this region. To facilitate analysis, we aggregated the remaining 16 biome classifications into five classes: tropical forest, temperate and cold forest, dry woodlands and scrub, savanna and grassland, and desert. We aggregated the 21 Köppen-Geiger classifications into classes of tropical, arid, Mediterranean, temperate, and cold. We assigned each city to a specific biome or Köppen-Geiger classification based on the mode of biome or climate classification pixels within the city's boundary. We used each city's latitude in absolute value as an independent variable and created new categorical variables denoting a city's geographic location on a given continent or whether it was in the Global North, a BRICS

nation, or in an LMIC. Finally, we utilized SMAP (NASA_USDA/HSL/SMAP10KM_soil_moisture) to assess global-scale variability in surface and sub-surface soil moisture (Sazib et al. 2018).

For a global study, sub-national socioeconomic data was unavailable for many countries, particularly LMIC. We used data from the World Bank (data.worldbank.org) to characterize a city's socio-economic status using national-scale data, acquiring variables representing national income and education. We took the mean of the annual-scale World Bank data that coincided with the length of our time series. From GEE we further acquired data on population size (CIESIN/GPWv411/GPW_Population_Count) and population density (CIESIN/GPWv411/GPW_UNWPP-Adjusted_Population_Density) at 30-arc second resolution between 2000 and 2020 (Center for International Earth Science Information Network - CIESIN - Columbia University 2018a, b). We complemented this dataset with the Global Human Settlement Layers, Built-Up Volume Grid (JRC/GHSL/P2023A/GHS_BUILT_V), from which we acquired the above-ground volume of the built urban infrastructure at 100 m^2 resolution (Pesaresi and Politis 2023).

Lastly, we obtained landcover data from the Dynamic World V1 dataset (GOOGLE/DYNAMICWORLD/V1). Dynamic World is a global landcover dataset provided at approximately 3 days temporal frequency and 10 m^2 spatial resolution (Brown et al. 2022). Achieved using deep learning, Dynamic World is unique in its high global spatial and temporal resolution. A value for a Dynamic World pixel represents the probability that the given pixel is entirely covered by the land cover of interest. From Dynamic World we acquired data on tree cover, grass cover, bare cover, and built

(impervious) cover. We characterized each city's landcover as the mean value of all landcover imagery from 2015 through 2023.

Results

3.1 *Long-term Trends in NDVI, LST, and Vegetative Cooling*

At a global scale, greenness and temperature were correlated, corroborating known intra-urban dynamics on an inter-urban scale (pearson's r=-0.65, p-value<0.001). The slope of the regression between NDVI and LST, termed vegetative cooling, provides a standardized indicator for how much cooling is derived per unit of NDVI (Fig. 1). NDVI and LST significantly changed in most cities between 1995 and 2023, leading to an overall reduction in vegetative cooling through time (Fig. 2). On average, NDVI increased among all cities at 7.0652×10^{-4}/year, where 126, or 47% of cities had a significant greening trend and 47, or 18%, of cities became significantly less green. The remaining 94 cities experienced no change in greenness. In a generalized linear model which explained 45% of the variability in whether the greenness trend for a city was positive or negative, cities with high mean NDVI (p-value<0.001), high surface soil moisture (p-value<0.001), and high maximum air temperature (p=0.024) were all significantly associated with a decline in greenness through time. The high spatial variability in the NDVI trend was also observed with the LST trend. Across all cities LST increased 0.14 °C/year with a standard deviation of 0.09 °C/year, while the 172 cities with a significant warming trend warmed at 0.17 °C/year. No city became significantly cooler. The long-term trends in NDVI and LST led to an evolving relationship between

NDVI and LST which had the consequence of a global decline in urban vegetative cooling.

Summertime vegetative cooling declined across all cities at a rate of 0.043 °C/NDVI/year. The trend in vegetative cooling was significantly different in 149 cities, decreasing in 129 and increasing in 20. We sought to explain these differences in trends by using a generalized linear model which allowed us to explain 53% of the variability in whether urban vegetative cooling increased or decreased. Only in cities where the bare soil surface temperature increased was vegetative cooling also more likely to increase ($p<0.001$). Vegetative cooling was likely to decrease in cities with high potential evapotranspiration ($p<0.001$), high impervious cover ($p<0.001$), and which had larger increases in land surface temperature ($p<0.001$). We sought to explain the long-term variability in urban NDVI, LST, and vegetative cooling by using gradient-boosted machines.

NDVI increased the most through time in cities which had the lowest mean NDVI (Fig. 3). Cities with high NDVI above approximately 0.4 had a higher probability of experiencing a decrease in NDVI through time. Although not identified as a top predictor via machine learning, raw greening trends were different by biome following ($p<0.001$) and Köppen-Geiger classification ($p<0.001$) from ANOVA. Tropical and temperate forests had NDVI trends significantly lower than dry woodlands, savanna, or desert biomes. The results were similar by Köppen-Geiger classification, where cities in tropical classifications had a significantly lower NDVI trend than any other classification while

cities which became the greenest were in arid or Mediterranean classifications. Trends in urban surface temperatures were also dependent on geographic context.

The trend in urban surface warming was associated with a city's geographic context and water availability (Fig. 4). Gradient boosted machines (GBM) identified the trend in mean annual precipitation as a top predictor, where cities which became the hottest were also the ones which had the largest decreases in precipitation. Cities near the equator warmed the least, while cities closer to the poles warmed faster. Geographic context also influenced the LST trend by continent, where the highest adjusted LST trends were in North America and Europe. These differences in warming trends by continent were corroborated by ANOVA (p-value<0.001). Results from a post-hoc Tukey HSD showed that the raw warming trends were more rapid in Europe compared to Oceania at a rate of 0.008 °C/year (p-value=0.022), were more rapid in North America compared to Oceania at a rate of 0.1030 °C/year (p-value=0.002) and were more rapid in North America compared to Asia at a rate of 0.0501 °C/year (p-value=0.004). The mean rate of warming was greatest in North America (0.16 °C/year), followed by Europe (0.15 °C/year), Africa (0.13 °C/year), South America (0.12 °C/year), and Asia (0.11 °C/year), with the lowest mean warming occurring in cities in Oceania (0.06 °C/year). The rate of warming was also different by biome (p=0.003); cities in tropical forest biomes warmed more slowly than cities in any other biome. The evolving relationship between urban greenness and temperature led to a global-scale reduction in urban vegetative cooling.

A GBM identified a city's developmental categorization as being the most important predictor influencing the vegetative cooling trend (Fig. 5). This result was

corroborated with ANOVA, which found a significant difference in the vegetative cooling trend for cities between the Global North, BRICS nations, and LMIC (p-value<0.001). Follow up testing with a post-hoc Tukey HSD found that cities in LMIC had a greater rate of loss in vegetative cooling than for cities in either the Global North (p-value<0.001) or in BRICS nations (p-value=0.015), but the trend in BRICS nations and the Global North was not different from one another. As well, the slowest declines in vegetative cooling occurred in cities that had higher tree canopy cover and which had lower average surface temperatures.

3.2 *Spatial Dependencies of NDVI, LST, and Vegetative Cooling*

Greenness exhibited high inter-urban variability (Fig. S1). Machine learning identified a city's developmental categorization being either in the Global North, a BRICS nation, or LMIC as the top predictor of urban greenness. This result was corroborated with ANOVA, which found significant differences in mean urban NDVI by developmental categorization (p-value<0.001). Follow-up testing with a post-hoc Tukey HSD found urban NDVI in the Global North 0.12 higher than in LMIC/Global South (p<0.001) and 0.032 higher than in BRICS nations (p-value<0.001). Urban NDVI in BRICS nations was 0.021 higher than in LMIC (p-value=0.004). NDVI was also higher in cities which had a lower climate water deficit. Although not identified as a top predictor in our gradient boosted model, ANOVA identified mean urban NDVI as being different by biome (p<0.001) and Köppen-Geiger classification (p<0.001). The highest mean NDVI was in cities in the temperate forest biome, while desert cities had lower NDVI than any other biome. By Köppen-Geiger classification, mean NDVI was greatest

in temperate and cold cities, with arid cities having lower NDVI than any other classification. In a similar way, global mean LST was associated with the climate and geographic context.

Mean LST also exhibited context-dependence, where latitude and vapor pressure deficit strongly determined a city's temperature (Fig. S2). Latitude was the primary determinant of urban temperatures even after accounting for urban NDVI, landcover, and socioeconomics. Urban temperatures began to decrease with latitude beyond approximately 30 °N or 30 °S. Cities with the highest mean vapor pressure deficit were also the hottest. The relationship between LST and NDVI led to variability in mean vegetative cooling.

Mean vegetative cooling exhibited high spatial heterogeneity (Fig. S3). Across all cities, vegetation provided an average cooling benefit of 7.73 °C/NDVI with a standard deviation of 3.05 °C/NDVI. Out of the 266-city dataset, five cities had an LST~NDVI relationship that was greater than zero, indicating an increase in land surface temperature with an increase in vegetation. We were unable to explain why these cities had a positive relationship, but these cities were Aden, Yemen, Agadez, Niger, Bhuj, India, Bikaner, India, and Timbuktu, Mali. However, all these cities are in arid environments with a mean VPD 1.81 standard deviations greater than the global mean in our data set. A GBM identified tree canopy cover as the top predictor of the inter-urban variability in mean vegetative cooling. Vegetative cooling was greatest in the cities with the largest urban forests.

Discussion

This study highlights the interactions between vegetation greenness (NDVI), land surface temperature (LST), and their interrelationship (LST~NDVI) among 266 global cities in 82 countries, spanning various climatic conditions and socioeconomic contexts across 28 years. Across all cities, urban greenness and land surface temperatures increased, but vegetative cooling declined. Changes in these dynamics were associated with a city's climatic context and geographic location. Drivers of change in urban greenness and temperature were multifactorial and often non-linear, making machine learning a valuable tool to assess global variability. The importance of climate as a mediator of these dynamics supports our inter-urban water deficit hypothesis. Cities in Europe greened the most, cities in North America and Europe warmed the most, but cities in low-and-lower-middle-income countries experienced the largest declines in vegetative cooling. Yet, intra-urban dependencies of surface temperature on vegetation (Maimaitiyiming et al. 2014) were observed among cities at a global inter-urban scale, aiding our understanding of plant physiology, particularly on the cooling effects of plants in urban contexts. Urban biophysical relationships are not stable through time at a global scale. The consequence of these changing relationships was the decline in vegetative cooling, suggesting greater challenges in actualizing urban resistance and resilience to global change.

Between 1995 and 2023 increases in LST and variable changes in NDVI led to an overall reduction in vegetative cooling. Global urban greening is consistent with other studies (Yang et al. 2014) and may be due to afforestation (Piao et al. 2019). Notably, we

observed urban temperature trends that were substantially more rapid than what has been observed previously (Liu et al. 2022). We suspect that this was due to our use of Landsat, which provides thermal imagery at approximately 100 m^2 spatial resolution, rather than MODIS, which provides thermal imagery at 1 km^2 native resolution. Other studies utilizing Landsat for assessing urban thermal trends found similar results: low-intensity development in Atlanta warmed 0.15 °C/year between 1985 and 2018 (Xian et al. 2022), nearly identical to our observed warming in Atlanta of 0.14 °C/year between 1995 and 2023. These results emphasize the importance of considering scale in urban environments. In heterogenous landscapes such as cities, coarse-resolution imagery such as MODIS may be inappropriate if temperature variability is greater than the pixel size. The NDVI and LST trends exhibited high inter-urban variability; we used machine learning to explain this variation.

An intriguing pattern that emerged from our data was the largest increase in urban greenness in low-NDVI cities, which occurred most frequently in arid and Mediterranean environments. This phenomenon contradicts general expectations of reduced vegetation cover and enhanced warming in arid cities, thereby hinting at possible interventions such as improved irrigation practices or increased urban tree planting (Gill et al. 2007, Locke et al. 2010), which would be consistent with our observed increase in global urban greenness. This increase in greenness in cities with low greenness may be suggestive of land use change, such as low-income or abandoned properties increasing greenness through time (Ryznar and Wagner 2001), or easy-to-build low-vegetation areas being developed (Gallardo and Martínez-Vega 2016). Cities with moderate greenness exhibited

more stable long-term greenness trends, while the greenest cities tended to lose greenness. Green cities may have become less green through time due to changing precipitation patterns leading to less available water (Güneralp et al. 2015, Franceschi et al. 2023). Globally the greenest cities were in temperate and cold climate categories, with the highest overall greenness in cities in the Global North. The lowest mean NDVI was consistently in cities in arid, desert environments; these results emphasize the importance of a city's climatic and developmental context on the dynamics of urban ecosystems. Enhanced greenness in cities of the Global North may be due to unique urban morphology. For instance, peri-urban (suburban) communities in Africa and Asia are characterized by gated communities (Hutchings et al. 2022). Public-facing vegetation is maintained differently than private vegetation (Locke et al. 2018) for reasons that may include an ecology of prestige (Grove et al. 2014), leading to possible fundamental differences in how urban vegetation is maintained in the Global North compared to elsewhere. Variability in LST trends was also climatically and geographically dependent.

The LST trend was mediated by geographic context and water availability. Globally, mean urban LST was primarily associated with a city's latitude and aridity, highlighting how a city's geographic and climatic context fundamentally shapes the urban thermal environment. The rate of warming was also geographically and climatically dependent, emphasizing how urban relationships are, on a global scale, sensitive to local conditions. The more rapid increase in temperature in North American and European cities was unlikely due to population growth (Manoli et al. 2019) or socio-economic development (Li et al. 2020b), both variables known to mediate urban

temperatures but which were controlled for in our model. Further, the most rapidly growing cities in population and economic development over our time series were outside the Global North (Sun et al. 2020). These results emphasize the importance of geographic and climatic context in shaping urban microclimates (Jacobs et al. 2020, Tan et al. 2021). The changing dynamics of NDVI and LST through time had the consequence of a global-scale decline in urban vegetative cooling.

Urban vegetative cooling exhibited summertime declines in most cities, with declines in this important ecosystem service being significantly greater in LMIC. On average, mean vegetative cooling was greater in cities with more tree cover, suggesting that urban trees become more effective at cooling when located in a denser urban forest. In Madison, Wisconsin, urban tree cover above 40% was more effective at cooling (Ziter et al. 2019), while urban forests in Munich, Germany were most effective at cooling when they were between 70-80% cover (Alavipanah et al. 2017). However, at a global scale vegetative cooling declined through time. Vulnerability of cities in LMIC is therefore greater in response to warming from climate change, as the ability to mitigate warming with vegetative cooling is becoming substantially weaker over time. The greater decline in vegetative cooling in LMIC cities may be due to unique urban morphology, economics, or socio-demographic distributions which alter the availability of and function of urban vegetation. The decline in vegetative cooling was also greatest in cities with a higher mean surface temperature. Increased urban heat and inadequate available water for transpiration may have surpassed the physiological limits of some trees leading to stomatal closure (Litvak et al. 2017). Isohydric strategies are commonly found in urban

trees such as Acer, Platanus, and Malus (Caplan et al. 2019); further, urban trees across species have been shown to exhibit convergence of transpiration with transpiration declining similar amounts with VPD (Chen et al. 2012), further suggesting that urban trees exhibit isohydric strategies. Planning for future urban forests therefore requires thoughtful selection of vegetation types in urban greening strategies, favoring species that can withstand temperature-induced evaporative demand yet provide sustained cooling benefits. The increasing inequity in global vegetative cooling underscores the challenges of incorporating urban vegetation into urban greening and heat reduction strategies.

This study's findings offer important implications for sustainable urban planning and development but highlight increasing inequity in the global distribution of urban vegetative cooling. First, the dynamic and changing relationships between NDVI, LST, and vegetative cooling can be leveraged in urban planning and design to improve urban resilience to a changing climate (Zhang et al. 2019), with a focus on cities in LMIC which are becoming less able to use vegetation to mitigate urban heat. Second, our findings demonstrate that urban greenness and temperature dynamics are mediated by the climate and geographic context often in complex, non-linear interactions. Support for our inter-urban water deficit hypothesis suggests that an integrated and multi-dimensional approach is needed to address urban water management (Marlow et al. 2013), particularly during drought conditions. Policymakers need to go beyond supply-demand management of water resources to consider aspects such as evapotranspiration, climate water deficit, and the resistance of urban greenness and temperature to changes in the water balance. The non-stationarity of urban biophysical relationships will likely alter urban resistance

and resilience to global change, underscoring how past conditions may be a poor guide to understand future conditions (Lenton et al. 2008, Bueno de Mesquita et al. 2021). Through time cities are becoming warmer and greener but vegetative cooling is declining. Understanding why these dynamics are changing can inform necessary interventions to mitigate adverse impacts from climate change and ensure the resilience and sustainability of urban environments (Pickett et al. 2011, McPhearson et al. 2016).

Conclusion

In an era where urban ecosystems worldwide are navigating a new normal characterized by hotter temperatures and changing precipitation patterns, this global analysis highlighted urban dynamics that can guide future urban planning. This global-scale inter-urban study unveiled the complex, sometimes non-linear relationships among urban greenness, temperature, and vegetative cooling. This study showed examples of urban adaptation and resilience; cities around the world are warming, vegetative cooling is changing dynamically, yet urban greenness is on average increasing. Climate and geographic context are critical to consider to fully understand a city's biophysical environment. While we observed global-scale trends, we also identified examples of regional-scale variability in these trends. These results emphasize that stationarity in urban ecosystems should not be assumed; socio-biophysical relationships change through time and need to be explicitly tested. Our conclusions show the changing dynamics of urban ecosystems in response through time; maintaining benefits of urban ecosystems such as vegetative cooling and lower temperatures will require a concerted effort to focus resources on low-and-lower-middle income nations.

References

Abatzoglou, J. T., S. Z. Dobrowski, S. A. Parks, and K. C. Hegewisch. 2018. TerraClimate, a high-resolution global dataset of monthly climate and climatic water balance from 1958-2015. Sci Data **5**:170191.

Adler, R. F., G. Gu, M. Sapiano, J.-J. Wang, and G. J. Huffman. 2017. Global Precipitation: Means, Variations and Trends During the Satellite Era (1979–2014). Surveys in Geophysics **38**:679-699.

Alavipanah, S., D. Haase, T. Lakes, and S. Qureshi. 2017. Integrating the third dimension into the concept of urban ecosystem services: A review. Ecological Indicators **72**:374-398.

Beck, H. E., T. R. McVicar, N. Vergopolan, A. Berg, N. J. Lutsko, A. Dufour, Z. Zeng, X. Jiang, A. I. J. M. van Dijk, and D. G. Miralles 2023. High-resolution (1 km) Köppen-Geiger maps for 1901–2099 based on constrained CMIP6 projections. Scientific Data **10**.

Beguería, S., S. M. V. Serrano, F. Reig-Gracia, and B. L. Garcés. 2023. SPEIbase v.2.8 [Dataset].

Brown, C. F., S. P. Brumby, B. Guzder-Williams, T. Birch, S. B. Hyde, J. Mazzariello, W. Czerwinski, V. J. Pasquarella, R. Haertel, S. Ilyushchenko, K. Schwehr, M. Weisse, F. Stolle, C. Hanson, O. Guinan, R. Moore, and A. M. Tait. 2022. Dynamic World, Near real-time global 10 m land use land cover mapping. Scientific Data **9**.

Bueno de Mesquita, C. P., C. T. White, E. C. Farrer, L. M. Hallett, K. N. Suding, and G. Battipaglia. 2021. Taking climate change into account: Non-stationarity in climate drivers of ecological response. Journal of Ecology **109**:1491-1500.

Buyantuyev, A., and J. Wu. 2009. Urbanization alters spatiotemporal patterns of ecosystem primary production: A case study of the Phoenix metropolitan region, USA. Journal of Arid Environments **73**:512-520.

Buyantuyev, A., and J. Wu. 2012. Urbanization diversifies land surface phenology in arid environments: Interactions among vegetation, climatic variation, and land use pattern in the Phoenix metropolitan region, USA. Landscape and Urban Planning **105**:149-159.

Cao, H., L. Han, and L. Li. 2022. Harmonizing surface reflectance between Landsat-7 ETM + , Landsat-8 OLI, and Sentinel-2 MSI over China. Environ Sci Pollut Res Int **29**:70882-70898.

Carlson, T. N., R. R. Gillies, and E. M. Perry. 1994. A method to make use of thermal infrared temperature and NDVI measurements to infer surface soil water content and fractional vegetation cover. Remote Sensing Reviews **9**:161-173.

Center for International Earth Science Information Network - CIESIN - Columbia University. 2018a. Gridded Population of the World, Version 4 (GPWv4): Population Count Adjusted to Match 2015 Revision of UN WPP Country Totals, Revision 11. NASA Socioeconomic Data and Applications Center (SEDAC), Palisades, New York.

Center for International Earth Science Information Network - CIESIN - Columbia University. 2018b. Gridded Population of the World, Version 4 (GPWv4): Population Density Adjusted to Match 2015 Revision UN WPP Country Totals, Revision 11. NASA Socioeconomic Data and Applications Center (SEDAC), Palisades, New York.

Dos Santos, S., E. A. Adams, G. Neville, Y. Wada, A. de Sherbinin, E. Mullin Bernhardt, and S. B. Adamo. 2017. Urban growth and water access in sub-Saharan Africa: Progress, challenges, and emerging research directions. Sci Total Environ **607-608**:497-508.

Dwyer, J. L., D. P. Roy, B. Sauer, C. B. Jenkerson, H. K. Zhang, and L. Lymburner. 2018. Analysis Ready Data: Enabling Analysis of the Landsat Archive. Remote Sensing **10**.

Lymburner, Leo. 2018. Analysis Ready Data: Enabling Analysis of the Landsat Archive. Remote Sensing **10**.

Farr, T. G., P. A. Rosen, E. Caro, R. Crippen, R. Duren, S. Hensley, M. Kobrick, M. Paller, E. Rodriguez, L. Roth, D. Seal, S. Shaffer, J. Shimada, J. Umland, M. Werner, M. Oskin, D. Burbank, and D. Alsdorf. 2007. The Shuttle Radar Topography Mission. Reviews of Geophysics **45**.

Franceschi, E., A. Moser-Reischl, M. Honold, M. A. Rahman, H. Pretzsch, S. Pauleit, and T. Rötzer. 2023. Urban environment, drought events and climate change strongly affect the growth of common urban tree species in a temperate city. Urban Forestry & Urban Greening **88**.

Friedman, J. H. 2001. Greedy Function Approximation: A Gradient Boosting Machine. The Annals of Statistics **29**:1189-1232.

Gallardo, M., and J. Martínez-Vega. 2016. Three decades of land-use changes in the region of Madrid and how they relate to territorial planning. European Planning Studies **24**:1016-1033.

Gill, S. E., J. F. Handley, A. R. Ennos, and S. Pauleit. 2007. Adapting Cities for Climate Change: The Role of the Green Infrastructure. Built Environment **33**:115-133.

Gorelick, N., M. Hancher, M. Dixon, S. Ilyushchenko, D. Thau, and R. Moore. 2017. Google Earth Engine: Planetary-scale geospatial analysis for everyone. Remote Sensing of Environment **202**:18-27.

Gross, G., D. Helder, C. Begeman, L. Leigh, M. Kaewmanee, and R. Shah. 2022. Initial Cross-Calibration of Landsat 8 and Landsat 9 Using the Simultaneous Underfly Event. Remote Sensing **14**.

Grove, J. M., D. H. Locke, and J. P. O'Neil-Dunne. 2014. An ecology of prestige in New York City: examining the relationships among population density, socio-economic status, group identity, and residential canopy cover. Environ Manage **54**:402-419.

Güneralp, B., İ. Güneralp, and Y. Liu. 2015. Changing global patterns of urban exposure to flood and drought hazards. Global Environmental Change **31**:217-225.

Heffernan, J. B., P. A. Soranno, M. J. Angilletta, L. B. Buckley, D. S. Gruner, T. H. Keitt, J. R. Kellner, J. S. Kominoski, A. V. Rocha, J. Xiao, T. K. Harms, S. J. Goring, L. E. Koenig, W. H. McDowell, H. Powell, A. D. Richardson, C. A. Stow, R. Vargas, and K. C. Weathers. 2014. Macrosystems ecology: understanding ecological patterns and processes at continental scales. Frontiers in Ecology and the Environment **12**:5-14.

Hengl, T. 2018. Global Maps of Potential Natural Vegetation at 1 km resolution. Harvard Dataverse.

Hersbach, H., B. Bell, P. Berrisford, G. Biavati, A. Horányi, J. Muñoz Sabater, J. Nicolas, C. Peubey, R. Radu, I. Rozum, D. Schepers, A. Simmons, C. Soci, D. Dee, and J.-N. Thépaut. 2023. ERA5 monthly averaged data on single levels from 1940 to present.*in* C. C. C. S. C. S. C. D. S. (CDS), editor.

Hutchings, P., S. Willcock, K. Lynch, D. Bundhoo, T. Brewer, S. Cooper, D. Keech, S. Mekala, P. P. Mishra, A. Parker, C. M. Shackleton, K. Venkatesh, D. R. Vicario, and I. Welivita. 2022. Understanding rural–urban transitions in the Global South through peri-urban turbulence. Nature Sustainability **5**:924-930.

Ibsen, P. C., D. Borowy, T. Dell, H. Greydanus, N. Gupta, D. M. Hondula, T. Meixner, M. V. Santelmann, S. A. Shiflett, M. C. Sukop, C. M. Swan, M. L. Talal, M. Valencia, M. K. Wright, and G. D. Jenerette. 2021. Greater aridity increases the magnitude of urban nighttime vegetation-derived air cooling. Environmental Research Letters **16**.

Jacobs, C., L. Klok, M. Bruse, J. Cortesão, S. Lenzholzer, and J. Kluck. 2020. Are urban water bodies really cooling? Urban Climate **32**.

Jenerette, G. D., L. W. Clarke, M. Avolio, D. Pataki, T. Gillespie, S. Pincetl, D. Nowak, L. R. Hutyra, M. McHale, J. P. McFadden, and M. Alonzo. 2016. Climate Tolerances and Trait choices shape continental patterns of urban tree biodiversity. Global Ecology and Biogeography **25**:1367-1376.

Jenerette, G. D., S. L. Harlan, A. Brazel, N. Jones, L. Larsen, and W. L. Stefanov. 2006. Regional relationships between surface temperature, vegetation, and human settlement in a rapidly urbanizing ecosystem. Landscape Ecology **22**:353-365.

Khan, A., S. Chatterjee, and Y. Weng. 2021. Characterizing thermal fields and evaluating UHI effects. Pages 37-67 Urban Heat Island Modeling for Tropical Climates.

Lenton, T. M., H. Held, E. Kriegler, J. W. Hall, W. Lucht, S. Rahmstorf, and H. J. Schellnhuber. 2008. Tipping elements in the Earth's climate system. Proc Natl Acad Sci U S A **105**:1786-1793.

Li, B., H. Beaudoing, and M. Rodell. 2020a. GLDAS Catchment Land Surface Model L4 daily 0.25 x 0.25 degree GRACE-DA1 V2.2.*in* NASA/GSFC/HSL, editor. Goddard Earth Sciences Data and Information Services Center (GES DISC), Greenbelt, Maryland, USA.

Li, B., M. Rodell, S. Kumar, H. K. Beaudoing, A. Getirana, B. F. Zaitchik, L. G. de Goncalves, C. Cossetin, S. Bhanja, A. Mukherjee, S. Tian, N. Tangdamrongsub, D. Long, J. Nanteza, J. Lee, F. Policelli, I. B. Goni, D. Daira, M. Bila, G. de Lannoy, D. Mocko, S. C. Steele-Dunne, H. Save, and S. Bettadpur. 2019. Global GRACE Data Assimilation for Groundwater and Drought Monitoring: Advances and Challenges. Water Resources Research **55**:7564-7586.

Li, X., W. Zhou, and Z. Ouyang. 2013. Relationship between land surface temperature and spatial pattern of greenspace: What are the effects of spatial resolution? Landscape and Urban Planning **114**:1-8.

Li, Y., Y. Sun, J. Li, and C. Gao. 2020b. Socioeconomic drivers of urban heat island effect: Empirical evidence from major Chinese cities. Sustainable Cities and Society **63**.

Ling, J., H. Zhang, and Y. Lin. 2021. Improving Urban Land Cover Classification in Cloud-Prone Areas with Polarimetric SAR Images. Remote Sensing **13**.

Liu, Z., W. Zhan, B. Bechtel, J. Voogt, J. Lai, T. Chakraborty, Z.-H. Wang, M. Li, F. Huang, and X. Lee. 2022. Surface warming in global cities is substantially more rapid than in rural background areas. Communications Earth & Environment **3**.

Locke, D. H., M. Avolio, T. L. E. Trammell, R. Roy Chowdhury, J. Morgan Grove, J. Rogan, D. G. Martin, N. Bettez, J. Cavender-Bares, P. M. Groffman, S. J. Hall, J. B. Heffernan, S. E. Hobbie, K. L. Larson, J. L. Morse, C. Neill, L. A. Ogden, J. P. M. O'Neil-Dunne, D. Pataki, W. D. Pearse, C. Polsky, and M. M. Wheeler. 2018. A multi-city comparison of front and backyard differences in plant species diversity and nitrogen cycling in residential landscapes. Landscape and Urban Planning **178**:102-111.

Locke, D. H., J. M. Grove, J. W. T. Lu, A. Troy, and J. P. M. O'Neil-Dunne. 2010. Prioritizing preferable locations for increasing urban tree canopy in New York City. Cities and the Environment (CATE) **3**.

Maimaitiyiming, M., A. Ghulam, T. Tiyip, F. Pla, P. Latorre-Carmona, Ü. Halik, M. Sawut, and M. Caetano. 2014. Effects of green space spatial pattern on land surface temperature: Implications for sustainable urban planning and climate change adaptation. ISPRS Journal of Photogrammetry and Remote Sensing **89**:59-66.

Manoli, G., S. Fatichi, M. Schlapfer, K. Yu, T. W. Crowther, N. Meili, P. Burlando, G. G. Katul, and E. Bou-Zeid. 2019. Magnitude of urban heat islands largely explained by climate and population. Nature **573**:55-60.

Marlow, D. R., M. Moglia, S. Cook, and D. J. Beale. 2013. Towards sustainable urban water management: a critical reassessment. Water Res **47**:7150-7161.

Masek, J. G., M. A. Wulder, B. Markham, J. McCorkel, C. J. Crawford, J. Storey, and D. T. Jenstrom. 2020. Landsat 9: Empowering open science and applications through continuity. Remote Sensing of Environment **248**.

McPhearson, T., S. T. A. Pickett, N. B. Grimm, J. Niemelä, M. Alberti, T. Elmqvist, C. Weber, D. Haase, J. Breuste, and S. Qureshi. 2016. Advancing Urban Ecology toward a Science of Cities. BioScience **66**:198-212.

Pellet, C., and C. Hauck. 2017. Monitoring soil moisture from middle to high elevation in Switzerland: set-up and first results from the SOMOMOUNT network. Hydrology and Earth System Sciences **21**:3199-3220.

Peng, S., S. Piao, P. Ciais, P. Friedlingstein, C. Ottle, F. M. Breon, H. Nan, L. Zhou, and R. B. Myneni. 2012. Surface urban heat island across 419 global big cities. Environ Sci Technol **46**:696-703.

Pesaresi, M., and P. Politis. 2023. GHS-BUILT-V R2023A - GHS built-up volume grids derived from joint assessment of Sentinel2, Landsat, and global DEM data, multitemporal (1975-2030).*in* E. Commission, editor. Joint Research Centre (JRC).

Petrovskaia, A., R. Jana, and I. Oseledets. 2022. A Single Image Deep Learning Approach to Restoration of Corrupted Landsat-7 Satellite Images. Sensors (Basel) **22**.

Pettorelli, N., J. O. Vik, A. Mysterud, J. M. Gaillard, C. J. Tucker, and N. C. Stenseth. 2005. Using the satellite-derived NDVI to assess ecological responses to environmental change. Trends Ecol Evol **20**:503-510.

Piao, S., X. Wang, T. Park, C. Chen, X. Lian, Y. He, J. W. Bjerke, A. Chen, P. Ciais, H. Tømmervik, R. R. Nemani, and R. B. Myneni. 2019. Characteristics, drivers and feedbacks of global greening. Nature Reviews Earth & Environment **1**:14-27.

Pickett, S. T., M. L. Cadenasso, J. M. Grove, C. G. Boone, P. M. Groffman, E. Irwin, S. S. Kaushal, V. Marshall, B. P. McGrath, C. H. Nilon, R. V. Pouyat, K. Szlavecz, A. Troy, and P. Warren. 2011. Urban ecological systems: scientific foundations and a decade of progress. J Environ Manage **92**:331-362.

Pickett, S. T. A., M. L. Cadenasso, D. L. Childers, M. J. McDonnell, and W. Zhou. 2017. Evolution and future of urban ecological science: ecology in, of, and for the city. Ecosystem Health and Sustainability **2**.

Ren, Z., Y. Fu, Y. Dong, P. Zhang, and X. He. 2022. Rapid urbanization and climate change significantly contribute to worsening urban human thermal comfort: A national 183-city, 26-year study in China. Urban Climate **43**.

Richards, D. R., P. Passy, and R. R. Y. Oh. 2017. Impacts of population density and wealth on the quantity and structure of urban green space in tropical Southeast Asia. Landscape and Urban Planning **157**:553-560.

Roy, D. P., V. Kovalskyy, H. K. Zhang, E. F. Vermote, L. Yan, S. S. Kumar, and A. Egorov. 2016. Characterization of Landsat-7 to Landsat-8 reflective wavelength and normalized difference vegetation index continuity. Remote Sensing of Environment **185**:57-70.

Ryznar, R. M., and T. W. Wagner. 2001. Using remotely sensed imagery to detect urban change: Viewing Detroit from space. Journal of the American Planning Association **37**:327-336.

Sazib, N., I. Mladenova, and J. Bolten. 2018. Leveraging the Google Earth Engine for Drought Assessment Using Global Soil Moisture Data. Remote Sensing **10**:1265.

Schwarz, K., M. Fragkias, C. G. Boone, W. Zhou, M. McHale, J. M. Grove, J. O'Neil-Dunne, J. P. McFadden, G. L. Buckley, D. Childers, L. Ogden, S. Pincetl, D. Pataki, A. Whitmer, and M. L. Cadenasso. 2015. Trees grow on money: urban tree canopy cover and environmental justice. PLoS One **10**:e0122051.

Shen, S., and G. G. Leptoukh. 2011. Estimation of surface air temperature over central and eastern Eurasia from MODIS land surface temperature. Environmental Research Letters **6**.

Shih, W.-Y. 2022. Socio-ecological inequality in heat: The role of green infrastructure in a subtropical city context. Landscape and Urban Planning **226**.

Showstack, R. 2022. Landsat 9 Satellite Continues Half-Century of Earth Observations. BioScience **72**:226-232.

Su, Y., J. Wu, C. Zhang, X. Wu, Q. Li, L. Liu, C. Bi, H. Zhang, R. Lafortezza, and X. Chen. 2022. Estimating the cooling effect magnitude of urban vegetation in different climate zones using multi-source remote sensing. Urban Climate **43**.

Sun, L., J. Chen, Q. Li, and D. Huang. 2020. Dramatic uneven urbanization of large cities throughout the world in recent decades. Nat Commun **11**:5366.

Tan, X., X. Sun, C. Huang, Y. Yuan, and D. Hou. 2021. Comparison of cooling effect between green space and water body. Sustainable Cities and Society **67**.

Wang, M., C. He, Z. Zhang, T. Hu, S.-B. Duan, K. Mallick, H. Li, and X. Liu. 2023. Evaluation of Three Land Surface Temperature Products From Landsat Series Using in Situ Measurements. IEEE Transactions on Geoscience and Remote Sensing **61**:1-19.

Xian, G., H. Shi, Q. Zhou, R. Auch, K. Gallo, Z. Wu, and M. Kolian. 2022. Monitoring and characterizing multi-decadal variations of urban thermal condition using time-series thermal remote sensing and dynamic land cover data. Remote Sensing of Environment **269**.

Yang, J., C. Huang, Z. Zhang, and L. Wang. 2014. The temporal trend of urban green coverage in major Chinese cities between 1990 and 2010. Urban Forestry & Urban Greening **13**:19-27.

Zhang, X., N. Chen, H. Sheng, C. Ip, L. Yang, Y. Chen, Z. Sang, T. Tadesse, T. P. Y. Lim, A. Rajabifard, C. Bueti, L. Zeng, B. Wardlow, S. Wang, S. Tang, Z. Xiong,

D. Li, and D. Niyogi. 2019. Urban drought challenge to 2030 sustainable development goals. Sci Total Environ **693**:133536.

Zhang, X. Q. 2016. The trends, promises and challenges of urbanisation in the world. Habitat International **54**:241-252.

Zhao, Q., and E. Wentz. 2016. A MODIS/ASTER Airborne Simulator (MASTER) Imagery for Urban Heat Island Research. Data **1**.

Zhou, D., S. Zhao, L. Zhang, G. Sun, and Y. Liu. 2015. The footprint of urban heat island effect in China. Sci Rep **5**:11160.

Zhu, Z. 2019. Science of Landsat Analysis Ready Data. Remote Sensing **11**.

Ziter, C. D., E. J. Pedersen, C. J. Kucharik, and M. G. Turner. 2019. Scale-dependent interactions between tree canopy cover and impervious surfaces reduce daytime urban heat during summer. Proc Natl Acad Sci U S A **116**:7575-7580.

Figures

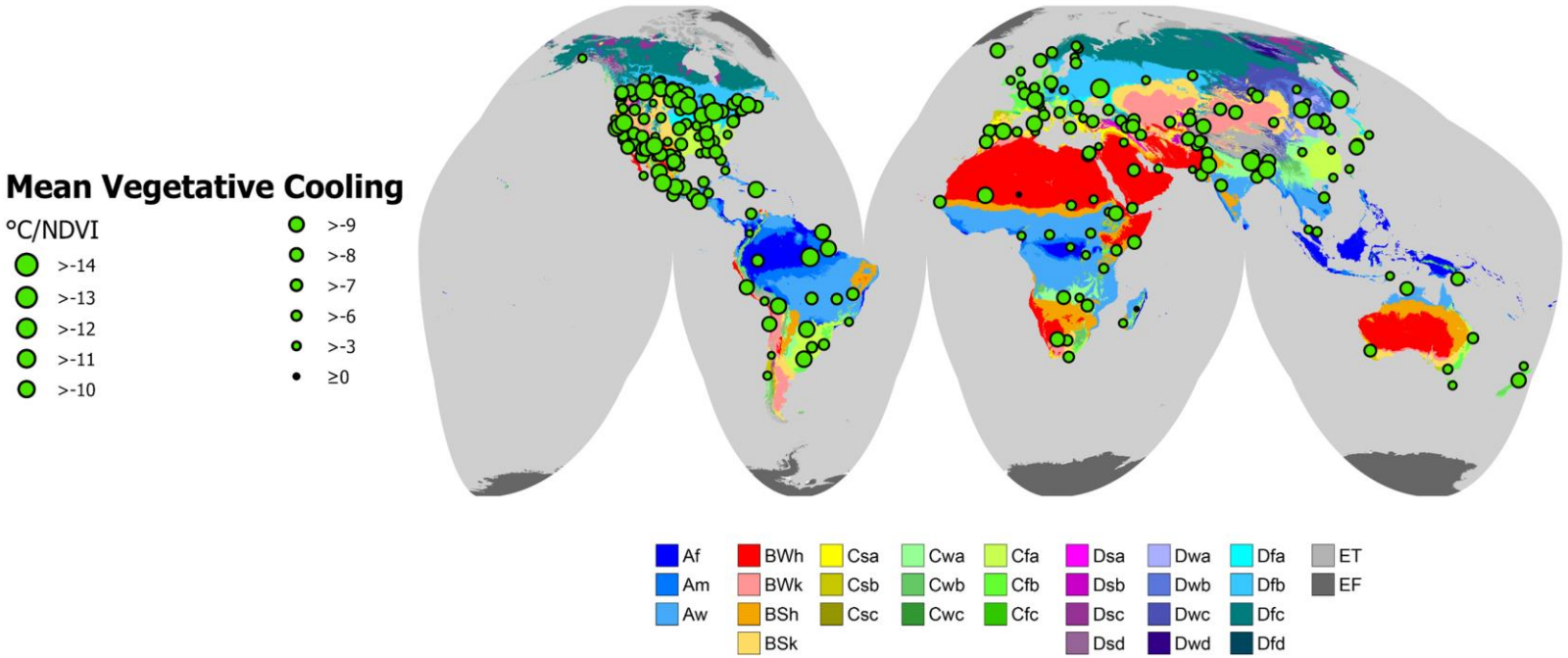

Figure 3.1 The 266 cities in this analysis represent a global subset of cities from 82 countries. The circles represent mean urban vegetative cooling, which is the slope of the relationship between NDVI and land surface temperature. Green circles indicate land surface temperatures decrease with greenness, with larger circles indicating more cooling for the same amount of greenness. Black circles indicate the six cities where the relationship is positive. The land area displays the Köppen-Geiger classification map for 1991-2020.

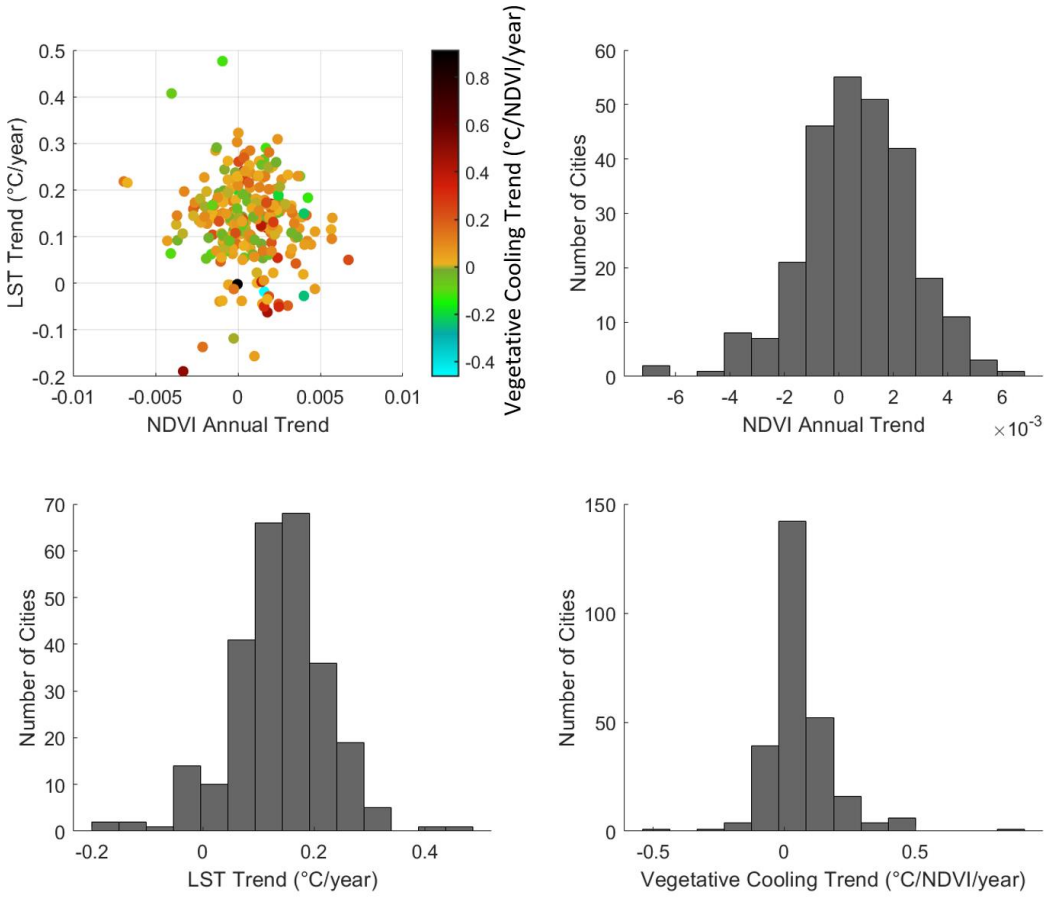

Figure 3.2 Between 1995 and 2023 the global subset of cities experienced significant changes in the relationship between urban greenness and temperature, leading to observed significant declines in vegetative cooling in 149 of the 266 cities. LST increased on average 0.14 °C/year, NDVI increased 7.006 x10^{-4}/year, and vegetative cooling decreased 0.043 °C/year. No city became significantly cooler.

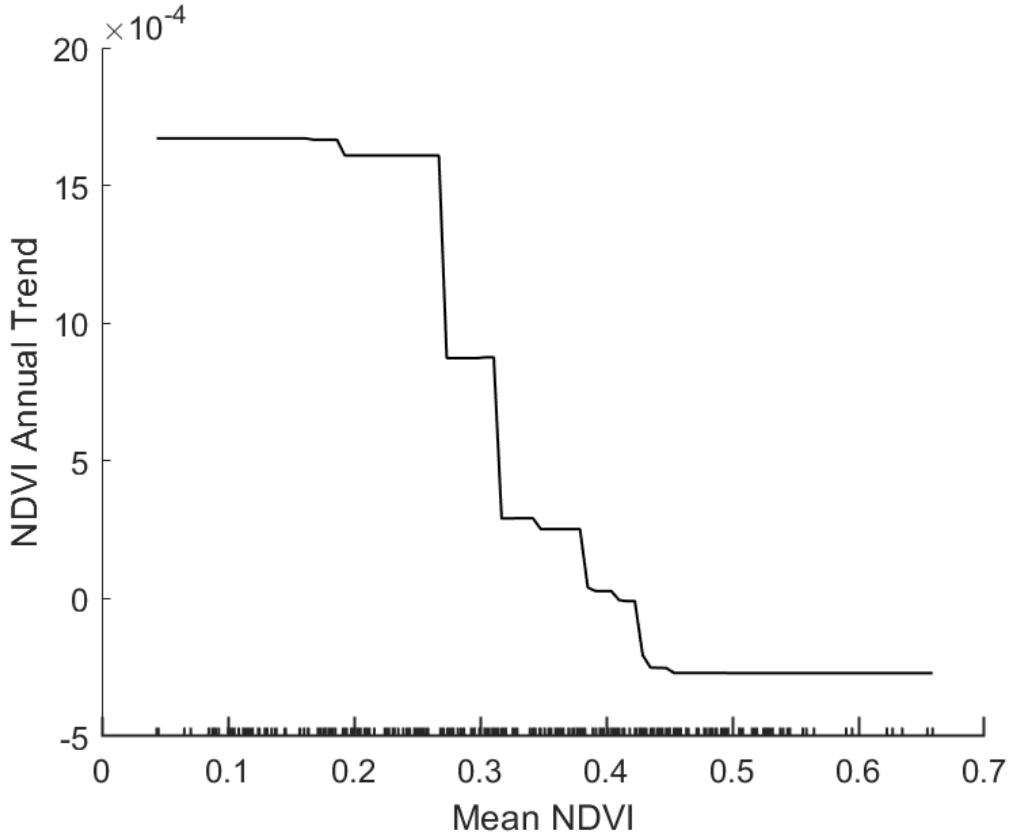

Figure 3.3 Between 1995 and 2023, cities which increased the most in greenness were those which were least green. Afforestation may be associated with an increase in greenness in cities with low green cover, while changing precipitation patterns may be associated with a decline in greenness in cities with high green cover.

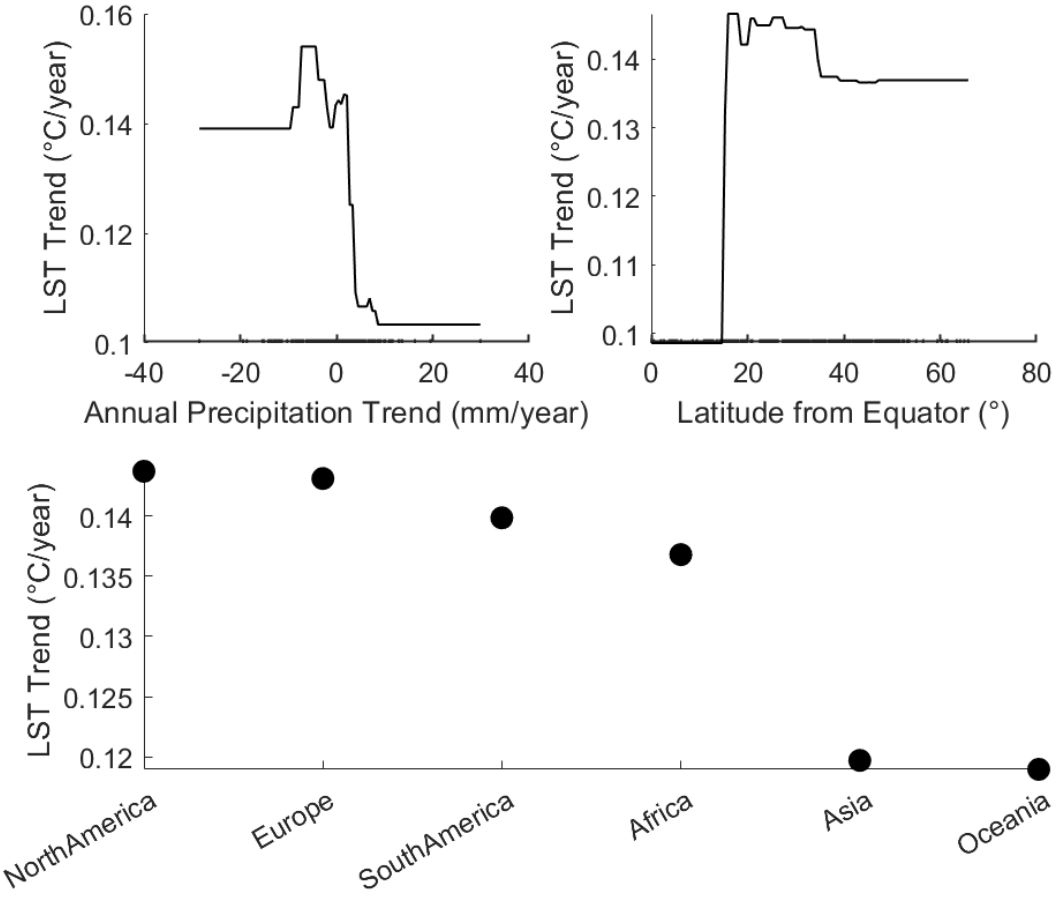

Figure. 3.4 All cities warmed on average 0.14 °C/year, where no city became significantly cooler. Cities which warmed the fastest were those which had a trend of decreasing mean annual precipitation. As well, cities closer to the poles warmed faster than cities near the equator. Geographic context further played a role in the warming trend on a continental scale, where cities in North America and Europe warmed the fastest.

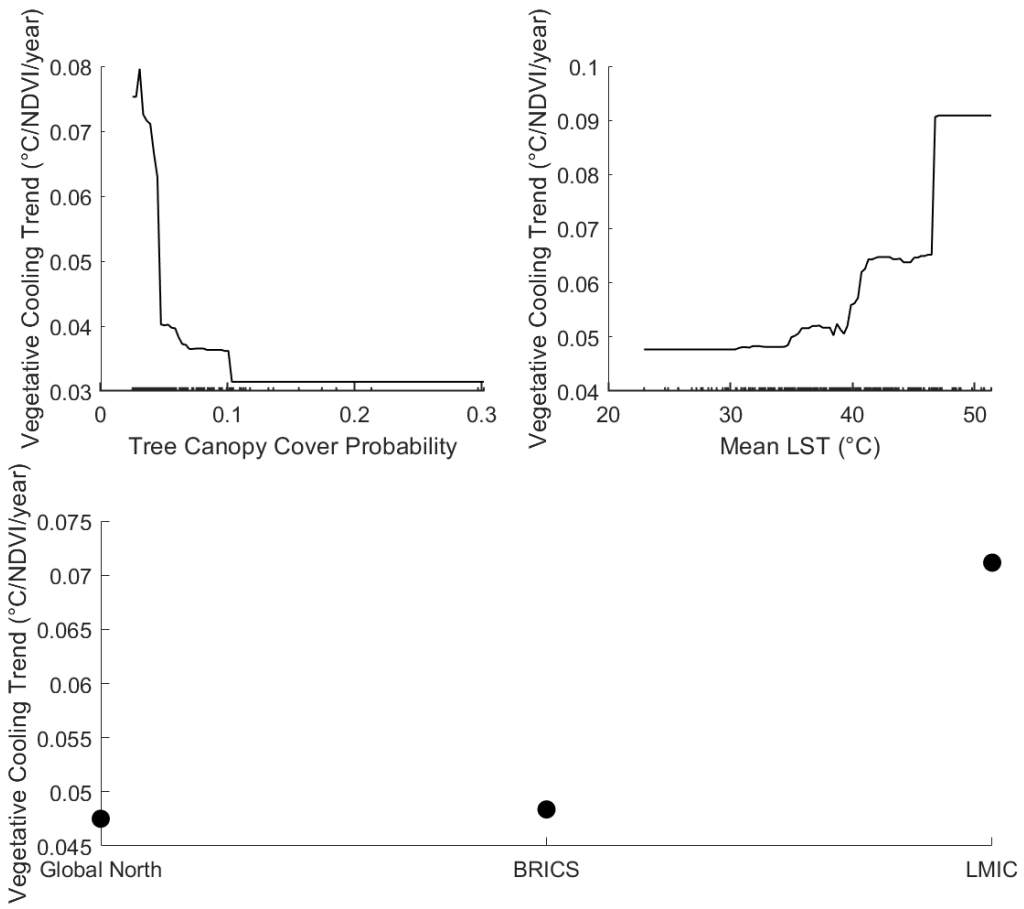

Figure. 3.5 Global summertime vegetative cooling declined, on average, 0.043 °C/NDVI/year. Vegetative cooling decreased more in cities that were less likely to have tree cover and which had, on average, the highest surface temperatures. The vegetative cooling trend was also different by a city's developmental categorization, where cities in low-and-middle-income countries lost vegetative cooling at a rate faster than cities in either the Global North or a BRICS nation.

Supplementary Figures

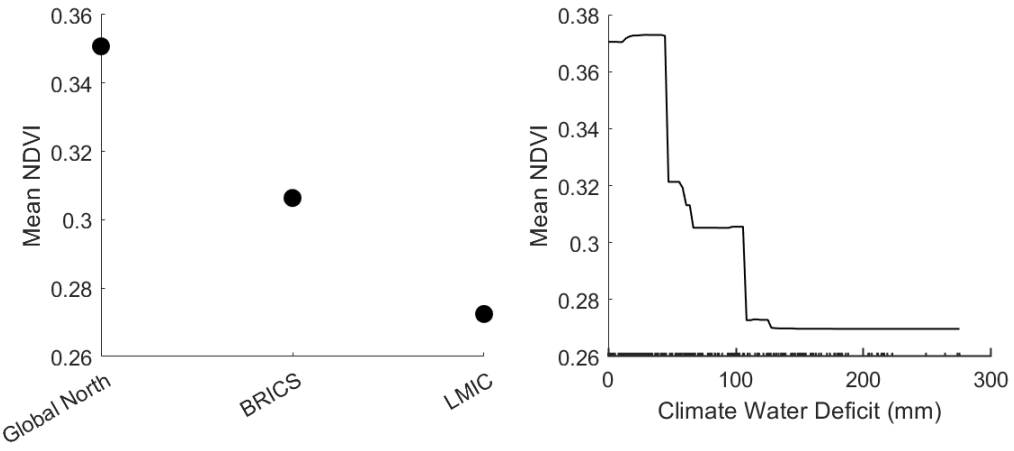

Figure 3.S1 The global variability in mean urban NDVI was heavily influenced by a city's socioeconomic context, where adjusted mean NDVI was greatest in the Global North and lowest in low-and-middle-income countries. A city's climatic context also mediated mean NDVI, where the most arid cities were the ones with the lowest NDVI.

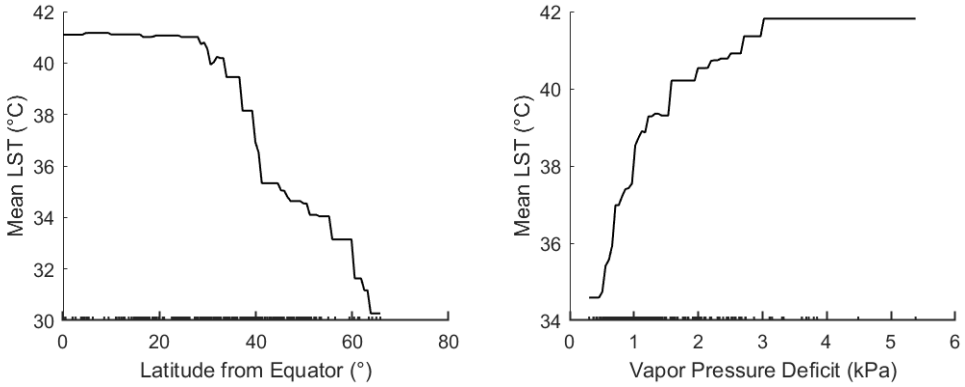

Figure. 3.S2 Mean urban surface temperatures were predominately driven by a city's latitude and mean vapor pressure deficit (VPD). Urban temperatures began to decline beyond approximately 30 °N or 30 °S, emphasizing how a city's geographic context informed its thermal environment. Cities with a higher VPD were also the hottest.

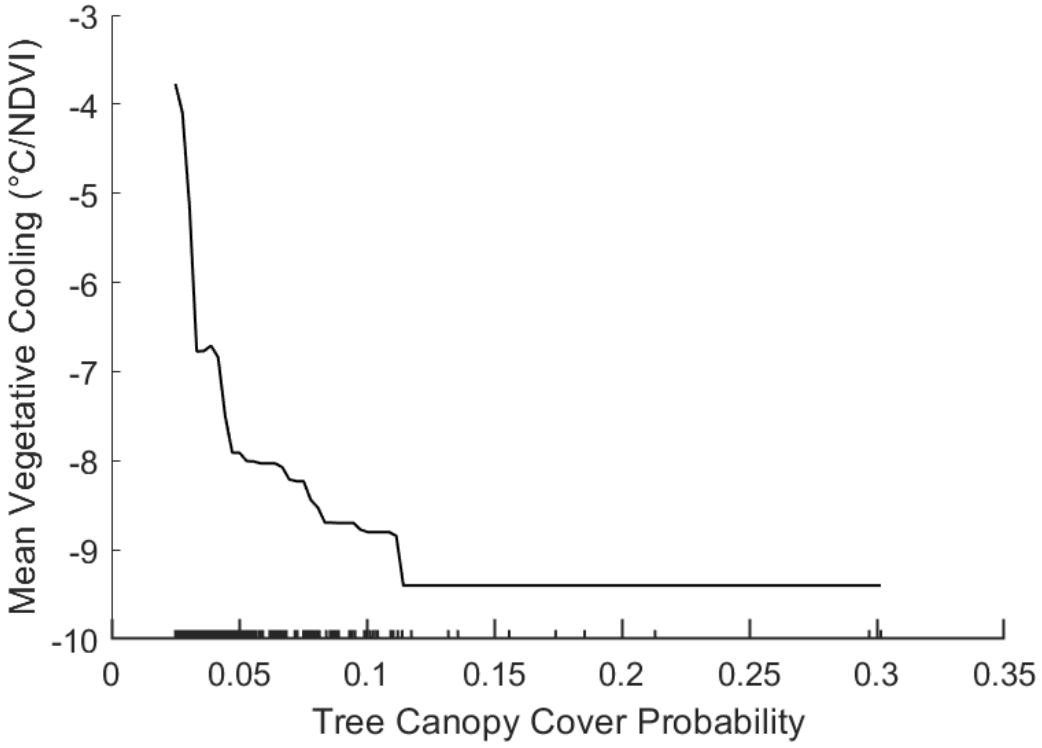

Figure 3.S3 Mean vegetative cooling was primarily influenced by the inter-urban variability in tree canopy cover, increasing in more canopy-dense cities. As vegetative cooling is standardized, the increase in cooling with tree cover suggests an increase in cooling efficiency with more trees.

Conclusion

Synthesis and Contributions to Theory

This dissertation focused on the dynamics of urban greenness, temperature, and vegetative cooling, and sought to understand how these dynamics vary across space and time at three distinct spatial scales. At the city scale, using the Los Angeles urban region as a case study (chapter 1), I found spatially variable relationships between urban greenness and temperature that are modified by drought, socio-demographics, and the climate. The shifting relationships between these variables through time had various consequences, one being that vegetative cooling increased, partially offsetting urban warming of 0.13 °C/year. While past research has suggested that vegetative cooling has increased in biomes globally partially in response to rising temperatures (Piao et al. 2019), this was the first time vegetative cooling had been shown to increase in an urban setting at a multidecadal scale. Non-stationarity of the relationship between greenness and temperature also led to changes in the distribution of environmental equity. I showed, for the first time, that the luxury effect, being the relationship between income and either urban greenness or temperature, has substantially declined through time.

At the national scale (chapter 2), I corroborated the findings from Los Angeles and found that the luxury effect on greenness and temperature substantially declined at the continental scale over a multidecadal period. The finding that the effectiveness of income as a mediator of urban greenness and temperature is declining highlights how an important relationship in urban ecosystems- the luxury effect- is not stable through time. I also described the effect of urbanization as being dependent on landcover, race, and the

climate. Tree cover is a major determinant of the difference in greenness and temperature between cities and non-urban reference sites; even in large cities with a high amount of impervious cover, if a city has a similar amount or more tree cover as its reference site, it tends to be as cool if not cooler than its reference. It is not inevitable that cities have significantly hotter temperatures than their surroundings; the magnitude of this temperature difference is in large part a policy decision.

At the global scale (chapter 3), I explained global trends in urban greenness, temperature, and vegetative cooling, where cities warmed 0.14 °C/year but vegetative cooling declined 0.04 °C/NDVI/year. I showed that changes in the trajectories of greenness and temperature altered the relationship between these variables, with the consequence of a global decline in the cooling effectiveness of urban vegetation. Variability in the NDVI, LST, and vegetative cooling trends were associated with a city's climatic and geographic context. This global-scale, multi-decadal analysis of how dynamics in urban ecosystems have changed through time contributes to our understanding of the ecology of cities as such in its assessment of general patterns and processes governing urban ecosystems.

Together, my findings underscore how urban dynamics may not exhibit stationarity, and that assumptions about stationarity need to be tested. Overall, the work in this dissertation supports my hypotheses about the spatial and temporal variability of urban greenness and temperature being associated with water availability, either directly through precipitation, or indirectly via sociodemographic variables of race or income. My studies highlight the importance of climate on urban greenness and temperature

dynamics, where drought led to large changes in greenness and temperature in the Los Angeles urban region and where precipitation influenced greenness even in irrigated cities. However, sociodemographics are strong drivers of urban greenness and temperature; in the Los Angeles urban region the spatial distribution of urban temperature and greenness were solely explained by landcover and income. These studies answer uncertainties about how urban greenness and temperature dynamics have changed at multidecadal scales, of drivers influencing the effect of urbanization, and in possible consequences for equity as a result of changing dynamics.

This research also helps to build a theory of cities, supporting the ecology "of" cities framework (Pickett et al. 2017). Broadly, ecology "in" cities applies ecological concepts and techniques from non-urban ecosystems to urban environments, such as for the study of urban parks (Nielsen et al. 2013), water bodies (Hassall 2014), or ethology (Magle et al. 2012). Ecology "for" cities is an applied urban ecology (Breuste et al. 2013, Felson et al. 2013, Wu 2014) where the science of how urban ecosystems operate is applied towards sustainable development. Ecology "of" cities, then, is the science of urban ecosystems as such. The ecology of cities treats the entire city as a cohesive and complex urban ecosystem (Zhang et al. 2006), considering the interactions between social, ecological, and technological systems (SETS) that define a city (Sharifi 2023). The ecology of cities is interested in how cities, as their own urban ecosystems, function and in how they are distinct from non-urban ecosystems. In assessing this, comparisons among multiple cities, as well as comparisons between urban and non-urban reference sites, are crucial towards building this "integrated ecology of cities" (McPhearson et al.

2016). This dissertation research, which assessed over 250 distinct cities over multidecadal time periods spanning up to 36 years, and which compared urban to non-urban reference sites, made important contributions towards our understanding of urban ecosystems and how they have changed through time.

Future Directions

While this dissertation assesses changes in urban dynamics over multidecadal periods and from the scale of a single city up through a planet-wide distribution of cities, this research suggests important avenues for future research. In the Los Angeles urban region, vegetative cooling increased, however, on a global scale, vegetative cooling declined, suggesting that the urban ecology of the Los Angeles urban region is unique compared to the global average. The decline in global vegetative cooling demands a more thorough assessment of cites, such as the Los Angeles urban region, in which vegetative cooling increased, and whether properties of these urban ecosystems can be transferred more broadly. However, the benefit of increased vegetative cooling in the minority of global cities where this was observed will not increase indefinitely with increasing temperature-induced evaporative demand, likely the driver of the observed increase in urban vegetative cooling (Manzoni et al. 2013, Will et al. 2013, Sadok et al. 2021, Yang et al. 2022). Plants are physiologically limited to a maximum transpiration rate, E_{max} (Manzoni et al. 2013), beyond which transpiration will not increase with temperature. Future temperature increases brought about by climate change may non-linearly accelerate the arrival to E_{max}; under hot, dry conditions trees may be forced into a positive feedback loop where reduced soil moisture increases sensible heat flux, increasing VPD

and transpiration, which further reduces soil moisture to the point of tree mortality (Breshears et al. 2013). If urban vegetative cooling is constrained by E_{max} then urban temperatures can be expected to rise more rapidly once E_{max} is surpassed. To maintain appropriate thermal conditions for urban residents, future research is needed to identify where E_{max} is for different common urban plants as well as to weigh the costs and benefits of using limited water resources for vegetative cooling.

Further, the resolution of the spectral bands used for this dissertation, from the Landsat suite of satellites, was 30 m^2, while the thermal bands ranged in resolution from 60-120 m^2. While this resolution is suitable for inter- and intra-urban analyses, the spatial distribution and configuration of greenness and temperature in global cities may be sufficiently different from that observed in the United States that the full variability of greenness/temperature dynamics are not being captured at 30 m^2. In the United States, sub-meter National Agriculture Imagery Program (NAIP) would be a valuable resource to corroborate whether the findings from Landsat are consistent at a substantially finer spatial resolution; in chapter 3 we identified important differences in results between MODIS and Landsat imagery on urban surface warming trends. In chapter 2 the data suggest that aridity decouples greenness from precipitation at the parcel scale; the use of NAIP imagery, which has the spatial resolution to identify individual trees, could assess whether this is true. At a global scale, the use of Sentinel-2 imagery, which provides spectral imagery at 10 m^2, may be better suited to non-Western configurations of urban greenness and temperature. ASTER, an instrument aboard the Terra satellite, may also be appropriate. ASTER collects spectral imagery at 15 m^2 resolution and has been collecting

data since 2000 while Sentinel-2 is available from 2015. While utilization of these satellites would trade temporal reach for spatial fidelity, doing so would provide valuable insight into the dynamics of non-Western cities which may be very context dependent and atypical from what has been described in high-income countries (Guerrieri 2020, Myers 2021, Shackleton et al. 2021).

Finally, a significant finding from this dissertation is the multidecadal decline in the luxury effect on both temperature and greenness at both the city and continental scales. Since it was first described by Hope et al. (2003), the luxury effect has been considered a fundamental characteristic of cities: wealthy regions of cities and wealthier cities are cooler and greener. The decoupling of the relationship between income and both greenness and temperature merits significant further research. Foremost, more research is needed to understand how the multidecadal decline in the luxury effect was mediated by changes in macroeconomics, such as by the Great Recession or the COVID lockdowns. Large observed declines in the effectiveness of income in mediating temperature and greenness suggests that the delivery of urban ecosystem services may be similarly shifting in response to the possible changing cost for these service benefits.

It would be prudent to understand whether the observed decline in the relationship between income and greenness and temperature at the continental scale is consistent with the other luxury effects, and if so, what factors are driving the decline. A luxury effect has been identified for many properties of urban ecosystems, where higher income has been associated with greater arthropod diversity, woody plant diversity, bird diversity, lizard diversity, presence of native bird species (Leong et al. 2018), ornamental species

richness, floral height, and functional trait diversity (Philpott et al. 2023), among other properties. The multidecadal decline in the effectiveness of income on mediating greenness and temperature poses challenges in improving environmental conditions for poor and minority neighborhoods and of cities that rank lower socio-economically. There is the possibility that this decline in the mediating effect of income on temperature and greenness may lead to a poverty trap for disadvantaged communities, as framed in the theory on panarchy, leading to increasing difficulty for these regions to improve their environmental conditions (Tidball et al. 2016). Increasing inequity and difficulty in building resistance and resilience to global change in disadvantaged communities is also suggested at the global scale with the decline in vegetative cooling greatest in cities located in low-and-middle-income countries. As income has been shown to be an important mediator of urban greenness and temperature for two decades, the decoupling of these relationships requires future research detailing the causes, consequences, and challenges to equity posed by this decoupling.

References

Breshears, D. D., H. D. Adams, D. Eamus, N. G. McDowell, D. J. Law, R. E. Will, A. P. Williams, and C. B. Zou. 2013. The critical amplifying role of increasing atmospheric moisture demand on tree mortality and associated regional die-off. Front Plant Sci **4**:266.

Breuste, J., S. Qureshi, and J. Li. 2013. Applied urban ecology for sustainable urban environment. Urban Ecosystems **16**:675-680.

Felson, A., M. Pavao-Zuckerman, T. Carter, F. Montalto, B. Shuster, N. Springer, E. K. Stander, and O. Starry. 2013. Mapping the Design Process for Urban Ecology Researchers. BioScience **63**:854-865.

Guerrieri, P. M. 2020. Migration, translation, and transformation of western urban planning models. City, Territory and Architecture **7**.

Hassall, C. 2014. The ecology and biodiversity of urban ponds. Wiley Interdisciplinary Reviews: Water **1**:187-206.

Hope, D., C. Gries, W. Zhu, W. F. Fagan, C. L. Redman, N. B. Grimm, A. L. Nelson, C. A. Martin, and A. Kinzig. 2003. Socioeconomics drive urban plant diversity. Proc Natl Acad Sci U S A **100**:8788-8792.

Leong, M., R. R. Dunn, and M. D. Trautwein. 2018. Biodiversity and socioeconomics in the city: a review of the luxury effect. Biol Lett **14**.

Magle, S. B., V. M. Hunt, M. Vernon, and K. R. Crooks. 2012. Urban wildlife research: Past, present, and future. Biological Conservation **155**:23-32.

Manzoni, S., G. Vico, G. Katul, S. Palmroth, R. B. Jackson, and A. Porporato. 2013. Hydraulic limits on maximum plant transpiration and the emergence of the safety-efficiency trade-off. New Phytol **198**:169-178.

McPhearson, T., S. T. A. Pickett, N. B. Grimm, J. Niemelä, M. Alberti, T. Elmqvist, C. Weber, D. Haase, J. Breuste, and S. Qureshi. 2016. Advancing Urban Ecology toward a Science of Cities. BioScience **66**:198-212.

Myers, G. 2021. Urbanisation in the Global South. Pages 27-20 Urban Ecology in the Global South. Springer.

Nielsen, A. B., M. van den Bosch, S. Maruthaveeran, and C. K. van den Bosch. 2013. Species richness in urban parks and its drivers: A review of empirical evidence. Urban Ecosystems **17**:305-327.

Philpott, S. M., P. Bichier, G. Perez, S. Jha, H. Liere, and B. B. Lin. 2023. Land tenure security and luxury support plant species and trait diversity in urban community gardens. Frontiers in Sustainable Food Systems **7**.

Piao, S., X. Wang, T. Park, C. Chen, X. Lian, Y. He, J. W. Bjerke, A. Chen, P. Ciais, H. Tømmervik, R. R. Nemani, and R. B. Myneni. 2019. Characteristics, drivers and feedbacks of global greening. Nature Reviews Earth & Environment **1**:14-27.

Pickett, S. T. A., M. L. Cadenasso, D. L. Childers, M. J. McDonnell, and W. Zhou. 2017. Evolution and future of urban ecological science: ecology in, of, and for the city. Ecosystem Health and Sustainability **2**.

Sadok, W., J. R. Lopez, and K. P. Smith. 2021. Transpiration increases under high-temperature stress: Potential mechanisms, trade-offs and prospects for crop resilience in a warming world. Plant Cell Environ **44**:2102-2116.

Shackleton, C. M., S. S. Cilliers, M. Du Toit, and E. Davoren. 2021. The need for an urban ecology of the global south. Pages 1-26 Urban Ecology in the Global South. Springer.

Sharifi, A. 2023. Resilience of urban social-ecological-technological systems (SETS): A review. Sustainable Cities and Society **99**.

Tidball, K., N. Frantzeskaki, and T. Elmqvist. 2016. Traps! An introduction to expanding thinking on persistent maladaptive states in pursuit of resilience. Sustainability Science **11**:861-866.

Will, R. E., S. M. Wilson, C. B. Zou, and T. C. Hennessey. 2013. Increased vapor pressure deficit due to higher temperature leads to greater transpiration and faster mortality during drought for tree seedlings common to the forest-grassland ecotone. New Phytol **200**:366-374.

Wu, J. 2014. Urban ecology and sustainability: The state-of-the-science and future directions. Landscape and Urban Planning **125**:209-221.

Yang, Q., X. Huang, X. Tong, C. Xiao, J. Yang, Y. Liu, and Y. Cao. 2022. Global assessment of urban trees' cooling efficiency based on satellite observations. Environmental Research Letters **17**.

Zhang, Y., Z. Yang, and X. Yu. 2006. Measurement and evaluation of interactions in complex urban ecosystem. Ecological Modelling **196**:77-89.